

https://dspace.org/

Numerical solution of unsteady turbulent free convection over a vertical flat plate

Remar, Jaroslav

2015

http://hdl.handle.net/10539/19197

Downloaded from a DSpace repository. https://dspace.org/

N U M E R I C A L S O L U T I O N
O F U N S T E A D Y T U R B U L E N T
F R E E C O N V E C T I O N
O V E R A V E R T I C A L F L A T P L A T E

Jaroslav Remar

A Dissertation Submitted to the Faculty of Engineering,
University of the Witwatersrand, Johannesburg
for the Degree of Master of Science
in Engineering

Johannesburg, October 1975

ABSTRACT

A theoretical treatment of the problem of unsteady turbulent free convection over a vertical flat plate is presented in this dissertation. An exhaustive review of the relevant publications revealed, that at the present time no solution of this problem has been given.

The development of a method, by which the abovementioned problem could be tackled, is a substantial part of the dissertation. The equations of conservation of mass, momentum, and energy, written in a general form, were the starting point of the derivation. Various assumptions, simplifying the partial differential equations, were introduced. In the end, boundary layer equations were obtained.

Turbulence was simulated by a phenomenological model, consisting of an algebraic law of the wall and a partial differential rate equation. The turbulence model is based on the concept of effective viscosity. Also, a constant turbulent Prandtl number was employed.

The problem of an isothermal plate in a stagnant non-stratified fluid was treated, and appropriate initial and boundary conditions were formulated.

The system of equations was solved by an explicit finite-difference method. The numerical stability criteria were established. A computer programme, based on the numerical scheme, was developed and employed for calculations.

The calculations were carried out for dry air, water, and mercury, representing gases, liquids, and liquid metals, respectively. In this way, a broad range of Prandtl numbers was covered.

Temperature, velocity, and effective viscosity profiles are presented here together with some other results of the calculations. An important observation is that the overall heat transfer coefficient goes through a temporary minimum before attaining its steady state value. The transient, which is extremely fast, can be divided into three characteristic stages: the initial conduction regime, an intermediate stage, and the steady state.

Our results were verified by comparison with data available from other independent sources. Due to the lack of data covering

the whole transient, only the first and third stages were considered. The initial conduction regime was compared with an analytical solution and the final steady state results with experimental data of various authors, respectively. The agreement is good and no serious discrepancies were discovered.

Although the present method produces reliable results, it cannot be widely employed, because the computing times are almost prohibitive with the present-day computers.

ADDENDUM

1. Page 94; After line '(dis)-turbance. Anyway, the agreement is quite reasonable.' insert the following:

The formulae of Siegel /83/ and Nanbu /64/ were derived for laminar flow, and therefore complete agreement with the results for turbulent flow, obtained in the present work, cannot be expected. The flow along the lower part of the plate is laminar, and the agreement should be fairly good only here. However, the singular point at the leading edge, with which an infinite heat transfer coefficient is theoretically associated, causes a higher speed of the wavefront propagation along the lower part of the plate. This phenomenon results from the numerical discretization and cannot be eliminated. The flow along the upper part of the plate is turbulent, and as mentioned above, complete agreement should not be expected.

It must also be remembered, that both Siegel /83/ and Nanbu /64/ made considerable simplifications in derivation of their equations, and the disagreements between their results are at least of the same order of magnitude as the differences between their curves and our results.

2. Page 105; After line 'certainly adequate.' insert the following:

The correlations of both Coutanceau /8/ and Fujii et al. /23/ are empirical and were obtained by approximation of experimental results. As can be seen from figures given in their articles, an exact agreement cannot be expected, and the deviations of our results from the approximating curves are in most cases of a similar size as the deviations of their own experimental points from the curves.

The only major discrepancies can be observed at the outer edge of the boundary layer, and there seem to be two reasons for them. The first one results from the replacement of the asymptotic boundary conditions at infinity by a finite distance from the wall. However, this is the only possible approach in a finite-difference method. The second reason results from the Jones-Kovasznay turbulence model employed in our calculations. Kovasznay states on p. 99 of his article /137/: 'The solutions in the region where viscosity

plays a dominant role of course cannot be accurate.' This problem is solved at the inner boundary of the field by using a law of the wall, but no similar procedure is available for the outer boundary.

The discrepancies at the outer edge of the boundary layer could probably be diminished by increasing the distance, which simulates the boundary condition at infinity, and by employing a more sophisticated turbulence model. However, the resulting increase of computer time would hardly be compensated by the increased accuracy.

3. Page 105; Delete lines 'However, as in the case of temperature profiles, the two parts linear in semi-logarithmic coordinates are hardly displayed by our results.' and insert in place of these:

The nondimensional velocity profile, according to Coutanceau /8/, should exhibit two linear parts, if semi-logarithmic coordinates are used for the graph (see Fig. 48). However, as in the case of temperature profiles, such 'linear' parts cannot be recognised in our results.

ACKNOWLEDGEMENTS

I would like to take this opportunity to express my gratitude for all the assistance given to me by my supervisor, Mr. R. R. Horsley, lecturer in the School of Mechanical Engineering.

I thank also Professor B. W. Skews for his sincere interest in my work.

DECLARATION

I, Jaroslav Remar, declare hereby that this Dissertation is my own unaided work, and has not been submitted for the degree of Master of Science in Engineering at any other University.

J. Remar

CONTENTS

Abstract	ii
Acknowledgements	iv
Declaration	v
Contents	vi
Nomenclature	ix
List of Tables	xii
List of Figures	xiii
1. INTRODUCTION	1
2. LITERATURE REVIEW	4
2.1 Steady Laminar Free Convection	4
2.2 Unsteady Laminar Free Convection	7
2.3 Instability and Transition from Laminar to Turbulent Flow	9
2.4 Steady Turbulent Free Convection	10
2.5 Unsteady Turbulent Free Convection	13
3. MATHEMATICAL FORMULATION	15
3.1 Definition of the Problem	15
3.2 Conservation Principles and the Fundamental Equations	15
3.3 Simplification of the Fundamental Equations	17
3.4 Introduction of Turbulence	19
3.5 Smoothing of the Turbulent Equations	21
3.6 The Problem of Closure	22
3.7 Boundary Layer Approximation	23
3.8 Initial and Boundary Conditions	24
4. TURBULENCE MODEL	26
4.1 Phenomenological Models of Turbulence	26
4.2 The Turbulence Model of Nee & Kovasznay	27
4.3 Law of the Wall	29
4.4 Turbulent Prandtl Number	30
4.5 Empirical Constants	31
4.6 Complete Mathematical Formulation of the Problem	31

5. NUMERICAL METHOD	33
5.1 Finite Differences	33
5.2 System of Equations to be Solved	35
5.3 Errors Associated with the Method	37
5.4 Stability and Convergence	38
5.5 Calculation of Wall Gradients and Nusselt Numbers	42
5.6 Computer Programme	44
6. RESULTS OF CALCULATIONS	45
6.1 Common Features of the Calculations	45
6.2 Dry Air	47
6.3 Water	57
6.4 Mercury	74
7. COMPARISON WITH PUBLISHED DATA	92
7.1 Duration of the Transient	92
7.2 Propagation of the Leading-Edge Effect	93
7.3 Pure Conduction Regime	94
7.4 Temperature Profiles	102
7.5 Velocity Profiles	105
7.6 Heat Transfer Coefficients	108
8. CONCLUSIONS	117
8.1 Evaluation of the Present Work	117
8.2 Suggestions for Further Work	118
Appendix A. COMPUTER PROGRAMME	121
A.1 Programme Description	121
A.2 Symbols Used in the Programme	122
A.3 Programme Listing	122
Appendix B. COMPUTER PRINTOUT	139
B.1 Dry Air	139
B.2 Water	156
B.3 Mercury	173

Appendix C. APPROXIMATION OF AIR AND WATER PHYSICAL PROPERTIES 190

C.1 Dry Air 190

C.2 Water 195

BIBLIOGRAPHY 201

Free Convection 201

Fluid Mechanics and Heat Transfer 207

Applied Mathematics and Computer Programming 211

NOMENCLATURE

The physical system of units (cm-g-s) is used throughout this work.

Latin Symbols

a	- a coefficient
b	- a coefficient; an exponent
c	- specific heat; a coefficient
d	- a coefficient
g	- gravitational acceleration
h	- heat transfer coefficient
k	- thermal conductivity
ℓ	- mixing length; characteristic length
n	- limit; an empirical constant
p	- pressure
q_w	- wall heat flux
t	- time
u	- velocity component ir x-direction
$u^+ = \frac{u}{\sqrt{\tau_w/\rho}}$	- nondimensional velocity
v	- velocity component in y-direction
w	- velocity component in z-direction
x	- distance along the wall; general coordinate
y	- perpendicular distance from the wall
$y^+ = \frac{y\sqrt{\tau_w/\rho}}{\nu}$	- nondimensional distance from the wall
z	- cartesian coordinate perpendicular to x and y
A	- an empirical constant
B	- an empirical constant
D	- dissipation term, eq. (45)
F	- body-force acceleration
G	- generation term, eq. (41)
$Gr = \frac{\beta \Delta T q_w x^3}{\nu^2 k}$	- Grashof number
$K_1 = \nu\left(\frac{1}{Pr} - \frac{1}{Pr_t}\right)$	- a constant
$K_2 = \frac{1}{Pr_t}$	- a constant
L	- wall height
$Nu = \frac{h x}{k}$	- Nusselt number
$O[\ ]$	- truncation error
$Pr = \frac{\nu}{\alpha}$	- Prandtl number

$Pr_t = \frac{\varepsilon_M}{\varepsilon_H}$ - turbulent Prandtl number
Q - volumetric heat source
$Ra = Pr\,Gr$ - Rayleigh number
T - temperature
V - general velocity

Greek Symbols

$\alpha = \frac{k}{c_p \varrho}$ - molecular thermal diffusivity
β - volumetric thermal expansion coefficient
$\delta = \int_0^\infty \frac{u}{u_{max}} dy$ - displacement thickness
Δt - time step
$\Delta T = T_w - T_f$ - temperature drop
Δx - grid spacing in x-direction
Δy - grid spacing in y-direction
ε - eddy diffusivity
$\zeta = \frac{y}{x} Nu_x$ - nondimensional distance from the wall
$\vartheta = t \sqrt{\frac{g \beta \Delta T}{x}}$ - nondimensional time
$\vartheta = \frac{T - T_f}{T_w - T_f}$ - nondimensional temperature
μ - dynamic viscosity
ν - kinematic viscosity
ξ - a coefficient
$\pi = 3,14159\ldots$ - Ludolf's number
ϱ - fluid density
τ_w - wall friction
ϕ - dummy function
$\omega = \nu + \varepsilon_M$ - effective viscosity
$\omega^+ = \frac{\omega}{\nu}$ - nondimensional effective viscosity

Subscripts

dyn - dynamic
f - fluid
i - tensor index; grid index in x-direction
j - grid index in y-direction
k - tensor index; an index
lim - boundary between inner and outer region
max - maximum
mez - field boundary
p - constant pressure
t - turbulent

w	- wall
x	- local value
H	- heat
L	- overall value
M	- momentum

Superscripts

$\rightarrow$	- vector
$\overline{\quad}$	- mean value
$'$	- fluctuating component
$+$	- nondimensional
N	- next time level

LIST OF TABLES

1. Pure conduction in air 99
2. Pure conduction in water 100
3. Pure conduction in mercury 101
4. Overall Nusselt numbers in air and water 110
5. Overall Nusselt numbers in mercury 115
A-1. Computer programme symbols 122

LIST OF FIGURES

1. Free convection heat transfer over a vertical flat plate 16
2. Finite differences 34
3. Temperature profiles in air at x/L=0,50 48
4. Velocity profiles in air at x/L=0,50 49
5. Effective viscosity profiles in air at x/L=0,50 50
6. Temperature profiles in air at x/L=0,75 51
7. Velocity profiles in air at x/L=0,75 52
8. Effective viscosity profiles in air at x/L=0,75 53
9. Temperature profiles in air at x/L=1,00 54
10. Velocity profiles in air at x/L=1,00 55
11. Effective viscosity profiles in air at x/L=1,00 56
12. Temperature profiles in air at x/L=1,00 (control calculation) 58
13. Velocity profiles in air at x/L=1,00 (control calculation) 59
14. Overall Nusselt number in air versus time 60
15. Steady state local heat transfer in air 61
16. Temperature profiles in water at x/L=0,50 63
17. Velocity profiles in water at x/L=0,50 64
18. Effective viscosity profiles in water at x/L=0,50 65
19. Temperature profiles in water at x/L=0,75 66
20. Velocity profiles in water at x/L=0,75 67
21. Effective viscosity profiles in water at x/L=0,75 68
22. Temperature profiles in water at x/L=1,00 69
23. Velocity profiles in water at x/L=1,00 70
24. Effective viscosity profiles in water at x/L=1,00 71
25. Temperature profiles in water at x/L=1,00 (control calculation) 72
26. Velocity profiles in water at x/L=1,00 (control calculation) 73
27. Overall Nusselt number in water versus time 75
28. Steady state local heat transfer in water 76
29. Temperature profiles in mercury at x/L=0,50 78
30. Velocity profiles in mercury at x/L=0,50 79

LIST OF FIGURES

1. Free convection heat transfer over a vertical flat plate 16
2. Finite differences 34
3. Temperature profiles in air at x/L=0,50 48
4. Velocity profiles in air at x/L=0,50 49
5. Effective viscosity profiles in air at x/L=0,50 50
6. Temperature profiles in air at x/L=0,75 51
7. Velocity profiles in air at x/L=0,75 52
8. Effective viscosity profiles in air at x/L=0,75 53
9. Temperature profiles in air at x/L=1,00 54
10. Velocity profiles in air at x/L=1,00 55
11. Effective viscosity profiles in air at x/L=1,00 56
12. Temperature profiles in air at x/L=1,00 (control calculation) 58
13. Velocity profiles in air at x/L=1,00 (control calculation) 59
14. Overall Nusselt number in air versus time 60
15. Steady state local heat transfer in air 61
16. Temperature profiles in water at x/L=0,50 63
17. Velocity profiles in water at x/L=0,50 64
18. Effective viscosity profiles in water at x/L=0,50 65
19. Temperature profiles in water at x/L=0,75 66
20. Velocity profiles in water at x/L=0,75 67
21. Effective viscosity profiles in water at x/L=0,75 68
22. Temperature profiles in water at x/L=1,00 69
23. Velocity profiles in water at x/L=1,00 70
24. Effective viscosity profiles in water at x/L=1,00 71
25. Temperature profiles in water at x/L=1,00 (control calculation) 72
26. Velocity profiles in water at x/L=1,00 (control calculation) 73
27. Overall Nusselt number in water versus time 75
28. Steady state local heat transfer in water 76
29. Temperature profiles in mercury at x/L=0,50 78
30. Velocity profiles in mercury at x/L=0,50 79

31. Effective viscosity profiles in mercury at x/L=0,50 80
32. Temperature profiles in mercury at x/L=0,75 81
33. Velocity profiles in mercury at x/L=0,75 82
34. Effective viscosity profiles in mercury at x/L=0,75 83
35. Temperature profiles in mercury at x/L=1,00 84
36. Velocity profiles in mercury at x/L=1,00 85
37. Effective viscosity profiles in mercury at x/L=1,00 86
38. Temperature profiles in mercury at x/L=1,00 (control calculation) 87
39. Velocity profiles in mercury at x/L=1,00 (control calculation) 88
40. Overall Nusselt number in mercury versus time 89
41. Steady state local heat transfer in mercury 90
42. Propagation of the leading-edge disturbance in air 95
43. Propagation of the leading-edge disturbance in water 96
44. Propagation of the leading-edge disturbance in mercury 97
45. Temperature profile in air compared with Coutanceau /8/ 103
46. Temperature profile in air compared with Fujii et al. /23/ 104
47. Temperature profile in water compared with Fujii et al. /23/ 106
48. Velocity profile in air compared with Coutanceau /8/ 107
49. Velocity profile in water compared with Vliet & Liu /92/ 109
50. Nondimensional transient heat transfer in air and water 113

1. INTRODUCTION

The science of heat transfer, which originated as a branch of physics, is today one of the most important pillars of engineering design. However, heat transfer processes are not to be found exclusively in technological equipment, and heat transfer problems from bioengineering, geophysics, ecology and many other fields of scientific endeavour are increasingly being investigated in the recent years.

The fundamental ideas about heat transfer were formulated by a number of prominent physicists in the XIXth century, and the basic modes of heat transfer were classified as conduction, convection, and radiation.

It soon became apparent, that it is usually much easier to formulate a heat transfer problem mathematically, than to solve the equations. An exception is conduction heat transfer, which is amenable, at least in simple geometries, to rigorous analytical treatment. On the other hand, the fundamental equations of convective heat transfer are much more complicated, and this part of thermomechanics became to a great extent an empirical science.

This situation was changed rapidly with the advent of powerful digital computers and the development of the associated numerical techniques. These tools enable us today to solve many heat transfer problems which could be hitherto investigated by experimental means only.

Although such computations are sometimes also quite expensive, they are usually much cheaper than the corresponding experimental investigations. Therefore, the experimental methods are being relegated to their proper place, which is the verification of theoretical predictions. In this way, the status of convective heat transfer is approaching the standard of other more advanced physical sciences.

The convective heat transfer is further classified as forced or free, respectively. In the case of forced convection, fluid motion arises by the action of external means, such as pumps or fans, or by a propelled movement of an object through a fluid. The vast majority of technological applications comes into this category.

On the other hand, in the case of free convection fluid motion is driven by body forces in the fluid itself. The local density in a fluid depends on the temperature and/or composition (e.g. moisture in the atmosphere or salinity in the oceans) at the location. The differences in the local values of density create a buoyancy effect, which was, in a somewhat different connection, discovered already by Archimedes. It is understood, of course, that there is an acceleration (usually gravitational) field, as otherwise no buoyancy effect arises, in spite of possible density differences.

Although free convection is very important in the nature (hence the often used term natural convection), there are only a few applications in technology. The cooling of transformers and other electrical equipment or an internal cooling of gas turbine blades come on mind as possible examples. The reason for the prevailing use of forced convection is easy to explain: forced convection achieves much higher heat transfer rates than free convection.

However, there are also some technically important cases of unsteady free convection heat transfer. The situation occurs, if electric current is suddenly switched on in the case of an electrical equipment, or if control rods are suddenly withdrawn from the core of a nuclear reactor in the case of reactor fuel elements. Electric current or nuclear fission, respectively, generate heat immediately, while the cooling of the heated elements, at least in the initial stage, is due to free convection only.

It is not well known, whether the heat transfer coefficient decreases monotonously under such circumstances, or whether it goes through a minimum. In the first case, steady-state formula may be used for calculations of heat transfer coefficients, but in the second case, there is an 'overshoot' in the element surface temperature and a safety margin must be included.

The heated elements would start generating heat throughout their volume. Instead of a complicated formulation corresponding to such a case, we shall consider the classical problem of a half-infinite vertical flat plate, with the surface temperature suddenly raised to and kept at a value higher than the temperature of the surrounding fluid. An exact definition of this problem, as being investigated in the present work, is given in the Section 3.1.

The next Chapter enables the reader to get acquainted with the relevant literature. Publications concerning both experimental and theoretical investigations are covered in the survey.

In Chapter 3, the mathematical formulation of the problem is presented. The starting point is a very general form of the conservation equations. Suitable assumptions are introduced and the equations are, step by step, simplified. In the end, boundary layer equations are obtained. The relevant boundary and initial conditions are also formulated.

Chapter 4 describes the turbulence model used for evaluation of the effective viscosity introduced in the preceding Chapter.

The resulting system of partial differential equations is very complicated and can be solved by a numerical method only. The method of finite differences was employed for this purpose, as described in Chapter 5.

Calculations were made for three different fluids, namely air, water, and mercury. The results are presented in Chapter 6.

Although no similar results covering the whole transient exist, the initial stage can be compared with an analytical solution and the steady state results with experimental data of other authors. This is done in Chapter 7, together with a discussion of the results.

Chapter 8 contains conclusions from the present work and also some suggestions for further investigations.

A description of the computer programme and its listing are given in the Appendix A.

Computer printouts of the examples described in Chapter 6 are presented in the Appendix B.

The last Appendix C contains approximations of the physical properties of air and water.

In the end, an extensive bibliography of the relevant literature is included.

2. LITERATURE REVIEW

The first step in any scientific work is usually a search for relevant publications in the specialist literature. In this Chapter, the results of such a survey are presented.

It is well known, that almost all heat-transfer textbooks give only a very concise treatment of natural convection heat transfer. One of the few laudable exceptions is the relatively recent textbook written by Gebhart /120/@) , which can serve as a suitable introduction into this field.

Moreover, a number of review articles appeared, such as Levy /52/ in 1955, Schmidt /81/ in 1962, and especially Ede /13/ in 1967 and Gebhart /29/ in 1969. All these articles are recommended to the interested reader. Unfortunately, they are all quite obsolete now, as they had been compiled before the majority of turbulent free convection studies appeared. In fact, this Chapter seems to be the only up-to-date review of publications concerning free convection heat transfer over a vertical flat plate.

Thus far, no solution of the problem treated in this dissertation, i.e. unsteady turbulent free convection, has been presented in the open literature, at least to the author's knowledge.

However, there are many published papers concerning steady laminar, unsteady laminar, and steady turbulent free convection over a (usually semi-infinite) vertical flat plate, and they will be described under appropriate headings in the subsequent Sections. Moreover, some papers about instability and transition from laminar to turbulent flow regime, although not falling directly into the scope of the present treatise, will be also mentioned.

In each Section, the references are given in chronological order.

2.1 Steady Laminar Free Convection

L. Lorenz /58/ in 1881 was the first one to reveal the complex nature of the heat transfer coefficient for natural convection. In his treatment he simplified considerably the basic equations, but quite surprisingly his formula for the overall heat transfer

@) See the Bibliography.

coefficient is very close to modern experimental data.

After almost half a century, Nusselt & Jürges /66/ in 1928 succeeded in improving the theory of Lorenz. They measured the temperature field with thermocouples.

The classical paper of Schmidt & Beckmann /82/ appeared only two years later. They measured both temperature and velocity fields around a heated vertical plate in air and came to the conclusion, that the Prandtl's boundary-layer concept could be applied also to this problem. They formulated the boundary layer equations and solved them in cooperation with Pohlhausen, who found suitable substitutions and reduced the partial differential equations to two ordinary differential equations.

H.H. Lorenz /57/ investigated in 1934 experimentally free convection in oil. As expected, the velocity boundary layer was thicker ($Pr \gg 1$) than the temperature boundary layer.

Ostrach /67/ concluded the study of the Schmidt & Beckmann equations in 1952 by solving the system of two ordinary differential equations numerically by means of a computer. He obtained solutions for eight values of Prandtl number, which is a parameter in the equations.

Some other authors, e.g. Sugawara & Michiyoshi /86/ , used quite successfully the integral method for the solution of this classical problem (see Ede /13/).

Schechter & Isbin /76/ investigated free convection in a region of maximum fluid density. Their measurements were made in water around 4 degC and the equations were solved by means of an analogue computer.

Sparrow & Gregg /84/ investigated the influence of variable fluid properties.

Fujii /16,18/ used a modified integral method for a nonisothermal surface and measured heat transfer from a vertical cylinder in ethyleneglycol and water.

Braun & Heighway /3/ applied the integral method to free convection at very high and very low Prandtl numbers.

Eichhorn /14/ measured velocity profiles in air by a special technique of particle-trajectories visualization.

Acrivos /1/ obtained an expression for the rate of heat and mass transfer by piecing together two exact asymptotic solutions.

Scherberg /77,78/ investigated the situation in the neighborhood of different types of thermal leading edges on a semi-infinite vertical wall.

Yang & Jerger /95/ presented a perturbation analysis, with the classical boundary layer solution as the zeroth-order approximation.

Hayday et al. /40/ solved a nonsimilar free convection problem with step discontinuities in surface temperature by a numerical method.

Brodowicz /4/ discussed the reasons for discrepancies between theoretical and experimental results.

Sparrow & Guinle /85/ analysed deviations from the classical theory at low Prandtl numbers.

Zinnes /97/ investigated the coupling of conduction in and free convection from a vertical plate with arbitrary surface heating.

Kelleher /47/ calculated free convection from a plate with a step discontinuity in the wall temperature, using asymptotic series.

Gryzagoridis /38/ measured heat transfer coefficients in the low Grashof number range.

Dale & Emery /10/ used finite differences for calculations of free convection in some non-Newtonian 'pseudoplastic' fluids.

Gryzagoridis /39/ investigated experimentally the leading edge effect.

Fujii et al. /21/ employed a finite- difference method for natural convection from an isothermal plate to a non-Newtonian Sutterby fluid and made also some measurements.

Lock & Ko /55/ solved numerically the problem of heat conduction coupling between free convection boundary layers on two opposite sides of a plate.

Lienhard /53/ discussed the commonality of equations for natural convection from immersed bodies of different shapes.

Hieber /43/ investigated theoretically higher-order boundary layer effects.

Fujii et al. /22/ applied the previously published numerical method /21/ to free convection from a vertical surface of uniform heat flux to a Sutterby fluid, and produced also some experimental results.

Na & Habib /62/ employed the so-called method of parameter differentiation for solution of the boundary layer equations.

Erdmann & Merzkirch /15/ measured the temperature field along an isothermal vertical cylinder in air by an optical interferometric method.

Wiles & Welty /94/ presented measurements of the temperature field along a vertical cylinder with uniform wall heat flux, immersed in mercury.

Although this Section does not cover all published papers concerning steady laminar free convection, the many aspects of this problem and the advanced state of their treatment can be clearly seen from the references assembled here.

2.2 Unsteady Laminar Free Convection

The first analysis of unsteady free convection was apparently made by Illingworth /44/ in 1950. He assumed that the velocity profiles are the same for all stations along the wall, and obtained an analytical solution in terms of exponential and error functions. However, this solution is valid for only a short period during the initial stage of the transient.

A similar analysis for a semi-infinite plate was published also by Sugawara & Michiyoshi /87/ in 1951.

A big step in the treatment of this problem was the paper of Siegel /83/ , published in 1958. The method of characteristics was employed for the solution of time-dependent boundary layer equations in the integral formulation. Both the uniform temperature and the uniform heat flux cases were analysed for time step changes. Three stages of the transient were defined: the initial conduction regime, an intermediate stage, and the last stage, in which steady state is established. The time boundaries between these three stages are given by particular characteristics. In this way, formulae for the time when the conductive regime ends and for the time when the steady state is established are obtained. Heat transfer coefficients were calculated for the first stage, and at its end they were lower than the steady state value. It was concluded therefrom, that the heat transfer coefficient goes through a temporary minimum, corresponding to an 'overshoot' in the surface temperature.

Goldstein & Eckert /36/ measured with a Zehnder-Mach interferometer the transient response of a very thin electrically heated foil in air and water subjected to a step increase in the electrical energy input. The three stages described by Siegel /83/ were also observed. The heat transfer coefficients indicated only a very slight minimum.

Gebhart /24/ published in 1961 the first one of his many articles concerning free convection. He presented an integral method of analysis, which accounted for the thermal capacity effect of the plate. The transient was initiated by a step in heat flux at the surface. The calculated results did not show any substantial overshoot of the average surface temperature.

Chung & Anderson /7/ considered the Grashof number to be time-dependent through either the uniform wall temperature or the acceleration field. They derived a set of parameters, which allow solutions of the differential equations to be expressed in series form. The first few terms of perturbation equations were numerically integrated.

Lurie & Johnson /59/ investigated experimentally transient free convection from a vertical surface submerged in water and undergoing a step in heat generation. Most results concern cases which lead to boiling on the surface, but also some nonboiling heat transfer results were reported. A surface temperature overshoot was observed only in the case of subcooled boiling.

Schetz & Eichhorn /79/ obtained exact solutions for unsteady free convection near a doubly infinite vertical plate by means of Laplace transforms. The surface temperature or heat flux could be an arbitrary function of time. Unfortunately, due to the sweeping assumption of double infinity, the solution applies only to the initial flow development near a semi-infinite plate.

The first direct solution of the field equations describing the problem of unsteady laminar free convection is due to Hellums & Churchill /41,42/ . The boundary layer partial differential equations were transformed into a dimensionless form, approximated by explicit finite-difference equations, and solved by means of a digital computer. The complete development of temperature and velocity profiles was calculated. The results confirmed the existence of a temporary minimum in the heat transfer coefficient. This was apparently the first solution of a complete free convection transient.

Gebhart /25/ presented further results of calculations, using his previously published method /24/ . In a companion paper, Gebhart & Adams /31/ published results of experimental measurements in air and water. The surface temperature of a foil was measured by an infrared technique. There was a very good agreement with the results predicted by the integral analysis.

Gebhart /26/ discussed also the importance of realistic assumptions about boundary conditions for natural convection transients. Moreover, the same author published another article /27/ , in which he applied his 'double integral' method to calculations of cooling transients.

Goldstein & Briggs /35/ gave solutions for transients from vertical plates and cylinders for the initial one-dimensional stage. The length of time for which this regime applies was also calculated. This time is identical with the propagation of a leading-edge effect.

Gebhart et al. /33/ continued his series of articles. This time, the measurements of the response to a step in the energy input to a foil were done by a Mach-Zehnder interferometer in nitrogen. The results are again in agreement with Gebhart's theory /24/ . No surface temperature overshoot was observed. Gebhart & Dring /32/ used the same interferometer also for measurements of the leading-edge effect propagation.

Nanbu /64/ derived an analytical formula for the end of the pure conduction regime. He confirmed strictly for the first time the existence of an 'overshoot'. Its relative magnitude is decreasing with increasing Prandtl number.

Kleppe & Marner /48/ employed an explicit finite-difference method for calculations of transient free convection in a Bingham plastic. A temporal minimum in the mean Nusselt number was obtained.

Brown & Riley /5/ presented mathematical analysis of the three phases of a natural convection transient.

Yang et al. /96/ applied a finite-difference method to the problem of a vertical plate with periodically changing surface temperature.

It can be seen from this Section, that our present knowledge of unsteady laminar free convection is quite satisfactory, although naturally to a lesser degree, than in the case of the steady state.

2.3 Instability and Transition from Laminar to Turbulent Flow

The first study of laminar-turbulent transition in natural convection flows seems to be published by Eckert & Soehnghen /12/ in 1951. The transition process in air was experimentally investigated by means of a Mach-Zehnder interferometer. The conclusion from the study was that turbulence originated by amplification

of initially small disturbances.

Fujii /17/ observed the development of a vortex street in the free convection boundary layer along a vertical cylinder submerged in ethyleneglycol and water. He also attempted to analyse the observed phenomena.

Szewczyk /88/ investigated the problem of stability and transition both theoretically and experimentally. The measurements were done in water and the dye technique was employed for visualization of the flow patterns. A double-row vortex system was observed. For stability calculations, a small-perturbation theory was used.

Klyachko /49/ derived in a simple way the magnitude of Grashof number, for which the transition from laminar to turbulent regime takes place.

Nachtsheim /63/ calculated neutral stability curves, taking into account temperature disturbance coupling.

Polymeropoulos & Gebhart /72/ studied the behaviour of disturbances over a foil in nitrogen with a Mach-Zehnder interferometer.

Knowles & Gebhart /50/ presented a study of thermal coupling and other effects on the neutral stability.

Gebhart /28/ summarized in 1969 the advances achieved in this field and gave a detailed picture of the state-of-the-art at that time. Another review article was published by the same author /30/ in 1973.

In the last year (i.e. 1974), Godaux & Gebhart /34/ presented results of transition measurements in water. A similar investigation was also published by Jaluria & Gebhart /45/.

J.-M. Piau /70/ investigated, besides the influence of variable physical properties and thermal stratification of the fluid, also the transition to the turbulent regime. His measurements were done also in water.

In this Section, only a few references were included, as we are not directly concerned with the problem of instability and transition in the present work. However, the last three or four references can be consulted, should more information be desired.

2.4 Steady Turbulent Free Convection

The first investigator of steady turbulent free convection seems to be Nusselt himself. He predicted /65/ in 1915, that the nondimensional number, which today bears his name, must be

directly proportional to one-third power of Grashof number in the case of turbulent free convection.

Griffiths & Davis /37/ presented in 1922 the results of their experimental investigations. They measured local heat transfer rates and both velocity and temperature profiles near a vertical plate in air.

The first attempt at a quantitative analysis of turbulent free convection was made by Colburn & Hougen (see Ede /13/) in 1930. In spite of considerable simplifications, they obtained a formula which is in good agreement with modern results.

Saunders /74,75/ obtained experimentally heat transfer coefficients in air and water.

Touloukian et al. /90/ measured heat transfer coefficients along a vertical cylinder in fluids of Prandtl numbers between 2,4 and 118.

The first solution of the turbulent free convection boundary layer equations was presented by Eckert & Jackson /11/ in 1950. They used the integral method, for which they adopted the temperature and velocity profiles measured by Griffiths & Davis /37/ . The expressions for shear stress and heat flux at the wall were taken from forced convection work. A basic assumption was equal thickness of energy and momentum boundary layers. They obtained two ordinary differential equations, which were solved, after a substitution, by separation of variables. Correlations for local and overall Nusselt numbers were obtained as the final result of the analysis.

Bayley /2/ employed in his work a method similar to von Kármán's analysis of forced convection. He divided the boundary layer into a laminar sublayer and an outer turbulent region. An eddy diffusivity, calculated by means of Prandtl's mixing-length theory, was introduced. The integral equations were simplified then to ordinary differential equations, which could be solved analytically. Again, correlations for local and overall Nusselt numbers were obtained.

Fujii /19/ made measurements of heat transfer coefficients and temperature profiles along a vertical cylinder submerged in ethyleneglycol and water. Correlations for Nusselt numbers were also given.

The first modern study of turbulent free convection in air was published by Cheesewright /6/ in 1968. He measured local heat

transfer coefficients and both temperature and velocity profiles. These measurements were done mostly in the region of very high Grashof numbers and therefore completely developed turbulence.

Warner & Arpaci /93/ also measured heat transfer coefficients and temperature profiles in air.

Lock & Trotter /56/ made their measurements in water. Besides the mean values, they investigated mainly the turbulent features, such as the scale, intensity and intermittency of turbulent fluctuations.

Kato et al. /46/ treated free convection as a special type of forced convection. Although the integral equations were also employed, the use of prescribed profiles was avoided. They made a number of simplifying assumptions, based on forced convection methods, and wrote differential equations for shear stress and heat flux. Eddy viscosity, which appeared in these equations, was taken from a forced convection formula. The equations were solved numerically by trial and error. Heat transfer coefficients and velocity and temperature profiles were obtained.

Coutanceau /8/ measured heat flux and shear stress at the surface and also temperature and velocity profiles. The measurements were made in air. He derived dimensionless similarity criteria and evaluated his experimental results in the form of correlations for local Nusselt numbers, wall shear stress, and temperature and velocity profiles. Some aspects of this paper were criticised by Fujii et al. /20/ , and these comments were answered by Coutanceau /9/.

Measurements in water over a vertical plate with constant heat flux were reported by Vliet & Liu /92/. Heat transfer coefficients, temperature and velocity profiles and some turbulence characteristics were measured. A hydrogen bubble method was utilized for flow visualization.

A voluminous study was presented by Fujii et al. /23/. They investigated experimentally free convection from a vertical cylinder submerged in water, spindle oil and Mobiltherm oil. Heat transfer coefficients and both mean temperatures and temperature fluctuations were measured. However, velocity profiles were not investigated. Nondimensional correlations for Nusselt numbers and mean temperature profiles were suggested.

Pirovano et al. /71/ presented an experimental study of heat transfer coefficients and temperature and velocity profiles in air up to very high Grashof numbers. A criterion for transition from

laminar to turbulent flow was proposed. Simultaneous fluctuations of the surface heat flux and the adjacent fluid temperature were discovered.

Kutateladze et al. /51/ measured both mean velocities and velocity fluctuations in ethylalcohol. Aluminium particles were used for visualization of the flow.

Lloyd et al. /54/ presented an experimental investigation of natural convection mass transfer from vertical and inclined plates. Local mass transfer rates and their fluctuations were measured by an electrochemical technique.

Papailiou & Lykoudis /68/ measured mean temperatures, temperature fluctuations and their spectra in mercury. In a companion article /69/, they presented the results of similar investigations, but under the influence of a uniform magnetic field.

Raithy & Hollands /73/ proposed an analytical method, based on the similarity between the growth of a liquid condensate film and the inner part of a natural convection boundary layer.

The first direct solution of the partial differential equations describing turbulent free convection boundary layer was presented quite recently (in November 1974) by Mason & Seban /60/. For this purpose they modified the numerical method of Patankar & Spalding /150/. For the calculation of turbulence, the boundary layer was divided into two parts. In the inner part, mixing length was calculated according to van Driest's law of the wall /116/. In the outer part, a partial differential equation for turbulent kinetic energy was employed. Calculations for air, water, and oils were presented.

This Section is quite exhaustive and to the author's knowledge, all relevant papers published in the open literature were included. However, many articles described here are based on doctoral theses, and in such cases only the published articles were mentioned.

2.5 Unsteady Turbulent Free Convection

The only publication, which could possibly come under this heading, is the experimental investigation by Mollendorf & Gebhart /61/. Mach-Zehnder interferometer was utilized for measurement of transient thermal response of a foil submerged in nitrogen and subjected to a step increase in electrical current. These experiments were conducted in a region of relatively high Grashof numbers and

turbulence was obtained at the upper end of the foil. Some qualitative features were observed and discussed. However, no temperature or velocity profiles were presented.

This dissertation seems to be the only theoretical solution of unsteady turbulent free convection available at the present time. A manuscript based on a part of this work has been submitted for publication to the International Journal of Heat and Mass Transfer.

3. MATHEMATICAL FORMULATION

In the first Section of this Chapter, the definition of our problem is given. This definition must be translated into a mathematical model, from which quantitative results can be obtained. Fluid flow and heat transfer, just as other physical processes, are governed by certain basic physical laws. The mathematical formulation of these laws provides us with a system of partial differential equations. These equations are very complicated, and before an attempt to obtain a solution for a particular problem is made, the equations usually are suitably simplified. We will also follow this traditional path here.

3.1 Definition of the Problem

Consider a vertical half-infinite smooth flat plate submerged into a stagnant infinite fluid having a constant temperature T_f, the same as the wall. Let the wall temperature instantaneously arise to $T_w > T_f$. The temperature and therefore also the density of the fluid immediately adjacent to the wall are evidently affected by this change and the resulting buoyancy force generates an upward fluid movement in the neighbourhood of the wall. The situation is illustrated in Fig. 1 .

The cooling rate of the wall is considerably enhanced in this way, compared with pure conduction mode of heat transfer. The flow has the character of boundary layer and is always laminar at the lower end of the wall. However, during its advance along the wall, it becomes sooner or later turbulent. The causes of this change are not well known yet and are the subject of intensive research.

Our task is to predict the development of the flow and temperature fields in the case of the turbulent flow regime. Knowledge of temperature profiles (more specifically temperature gradients at the wall) enables us to predict heat transfer coefficients for the wall.

3.2 Conservation Principles and the Fundamental Equations

The basic physical laws, which must be satisfied in any problem of fluid mechanics and/or heat transfer, are the principles of

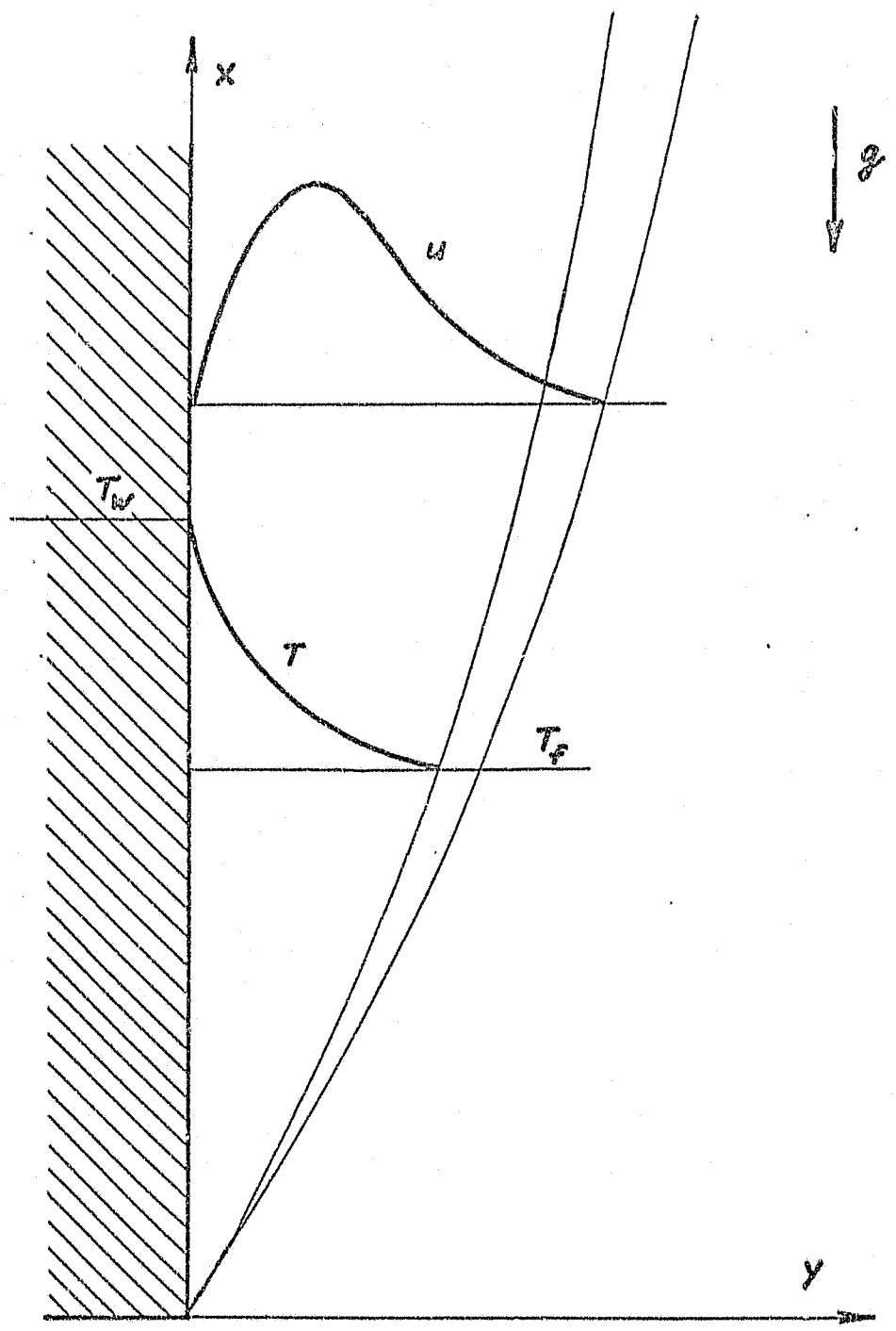

FIG. 1. FREE CONVECTION HEAT TRANSFER OVER A VERTICAL FLAT PLATE

mass, momentum, and energy conservation. Their mathematical counterpart is a system of partial differential equations, which are given here in tensor notation and in a quite general form, but for Newtonian fluids only. The derivation of these equations can be found in any advanced fluid mechanics book, e.g. Loitsianskii /143/ or Schlichting /157/.

The equations are

the continuity equation (conservation of mass)

$$\frac{\partial \rho}{\partial t} + \frac{\partial}{\partial x_k}(\rho V_k) = 0 \qquad (1)$$

the Navier-Stokes or momentum equation (corresponding to the Newton's second law of motion, i.e. conservation of momentum)

$$\rho\left(\frac{\partial V_i}{\partial t} + V_k \frac{\partial V_i}{\partial x_k}\right) = \rho F_i - \frac{\partial p}{\partial x_i} + \frac{\partial}{\partial x_k}\left[\mu\left(\frac{\partial V_i}{\partial x_k} + \frac{\partial V_k}{\partial x_i}\right)\right] - \frac{2}{3}\frac{\partial}{\partial x_i}\left(\mu \frac{\partial V_k}{\partial x_k}\right) \qquad (2)$$

and the energy equation (corresponding to the first law of thermodynamics, i.e. conservation of energy)

$$\rho c\left(\frac{\partial T}{\partial t} + V_k \frac{\partial T}{\partial x_k}\right) = Q + \frac{\partial}{\partial x_k}\left(k \frac{\partial T}{\partial x_k}\right) + \frac{\partial p}{\partial t} + V_i \frac{\partial p}{\partial x_k} + \mu\left[\frac{\partial V_i}{\partial x_k}\left(\frac{\partial V_i}{\partial x_k} + \frac{\partial V_k}{\partial x_i}\right) - \frac{2}{3}\left(\frac{\partial V_k}{\partial x_k}\right)^2\right] \qquad (3)$$

The system of equations (1-3) is the cornerstone of theoretical investigations in the field of convective heat transfer.

3.3 Simplification of the Fundamental Equations

The system of equations (1-3) is very complicated, and before an attempt to obtain a solution is made, the equations are usually simplified according to the conditions of a particular case. Also we shall introduce a number of assumptions, which will make the system more amenable to mathematical treatment.

The equations will be written in vector notation now. We assume first, that the fluid properties k and μ are constant. At this stage, the continuity equation remains unchanged, although it is

now written as

$$\frac{\partial \varrho}{\partial t} + div\ \varrho \vec{V} = 0 \qquad (4)$$

We assume further, that the body force in the momentum equation is due to the Earth's gravitational field only. After rearrangement of the last two terms, the momentum equation now becomes

$$\varrho \frac{D\vec{V}}{Dt} = \varrho \vec{g} - grad\ p + \mu \nabla^2 \vec{V} + \frac{\mu}{3} grad\ div\ \vec{V} \qquad (5)$$

We shall consider fluids without heat sources only, i.e. $Q = 0$. Furthermore, the viscous dissipation, represented by the last term in equation (3), is significant only in the flow of high viscosity liquids and the presence of steep velocity gradients, and shall be neglected here. We can write the energy equation now a:

$$\varrho c \frac{DT}{Dt} = k \nabla^2 T + \frac{Dp}{Dt} \qquad (6)$$

The system of equations (4-6) is still quite generally valid, the restrictions being of a relatively minor nature. In the treatment of natural convection some further assumptions are usually made. These assumptions were proposed by Boussinesq /102/ and the simplification is called the Boussinesq approximation. Its feasibility can be proven by an order-of-magnitude analysis, which can be found e.g. in Gebhart /120/. The basic assumption is that the density of the fluid is constant, with the exception of the buoyancy term. This means, that the flow is considered to be effectively incompressible.

The continuity equation now becomes

$$div\ \vec{V} = 0 \qquad (7)$$

We shall consider pressure as a sum of hydrostatic and dynamic pressure, writing

$$p = -\varrho g x + p_{dyn} \qquad (8)$$

If volumetric expansion coefficient is used, the body force,

according to Archimedes' law, is

$$\rho \vec{g} = \rho_f \vec{g} - \beta \rho_f \vec{g} \, (T - T_f) \qquad (9)$$

Using equations (8) and (9), we get

$$\rho \vec{g} - grad\ p = -\beta \rho_f \vec{g} \, (T - T_f) - grad\ p_{dyn} \qquad (10)$$

We can see also, by comparison with equation (7), that the last term in equation (5) becomes zero. After division by ρ (all properties, including the density, will be evaluated at the same reference temperature, so that $\rho = \rho_f$ here), the momentum equation can be now written as

$$\frac{D\vec{V}}{Dt} = -\beta \vec{g} \, (T - T_f) - \frac{1}{\rho} grad\ p_{dyn} + \nu \nabla^2 \vec{V} \qquad (11)$$

The vector $\vec{g}$ has a negative value in our coordinate system (see Fig. 1), so that the local driving force is directly proportional to the local temperature increase.

The magnitude of the substantial derivative of pressure is negligible in flows with moderate velocities. Therefore, after dividing by $c_p \rho$, the energy equation becomes

$$\frac{DT}{Dt} = \alpha \nabla^2 T \qquad (12)$$

The system of equations (7),(11) and (12) is valid for both laminar and turbulent flows.

3.4 Introduction of Turbulence

We are considering an unsteady problem here, and for this reason the customary definitions of mean and fluctuating quantities do not apply. The difference between a steady and unsteady turbulent flow was discussed in a simple way by Bradshaw /103/.

The mean value is obtained in the unsteady case by ensemble--averaging instead of the usual time-averaging in the steady case. If an experiment with unsteady turbulent flow is repeated many times, an instantaneous quantity $\phi(\vec{x}, t)$ at a certain point in space and time contains a random fluctuating part, probably always different. The mean value is defined as the arithmetic average

over a sufficiently high number of experiments, so that

$$\overline{\phi}(\vec{x},t) = \lim_{n\to\infty} \sum_{k=1}^{n} \frac{\phi_k(\vec{x},t)}{n} \qquad (13)$$

The instantaneous value and the fluctuating component are defined in the same way as in the case of steady state turbulent flow, viz.

$$\phi = \overline{\phi} + \phi' \qquad (14)$$

From the definition, the mean value of a fluctuating component is zero, i.e.

$$\overline{\phi'} = 0 \qquad (15)$$

The equations (7),(11) and (12) are valid for instant values in the case of turbulent flow. We shall insert now into these equations the instant values, written as a sum of the mean value and the fluctuating component, according to equation (14). The values of all coefficients (i.e. the physical properties) are considered to be nonfluctuating.

The continuity equation now becomes

$$\frac{\partial(\bar{u}+u')}{\partial x} + \frac{\partial(\bar{v}+v')}{\partial y} + \frac{\partial(\bar{w}+w')}{\partial z} = 0 \qquad (16)$$

Recalling the continuity equation, the momentum equation written for the x-direction is

$$\frac{\partial(\bar{u}+u')}{\partial t} + \frac{\partial(\bar{u}+u')(\bar{u}+u')}{\partial x} + \frac{\partial(\bar{v}+v')(\bar{u}+u')}{\partial y} + \frac{\partial(\bar{w}+w')(\bar{u}+u')}{\partial z} =$$
$$= \nu \nabla^2(\bar{u}+u') + \beta g (\bar{T}+T'-T_f) - \frac{1}{\rho}\frac{\partial(\bar{p}_{dyn}+p'_{dyn})}{\partial x} \qquad (17)$$

and for the y-direction

$$\frac{\partial(\bar{v}+v')}{\partial t} + \frac{\partial(\bar{u}+u')(\bar{v}+v')}{\partial x} + \frac{\partial(\bar{v}+v')(\bar{v}+v')}{\partial y} + \frac{\partial(\bar{w}+w')(\bar{v}+v')}{\partial z} =$$
$$= \nu \nabla^2(\bar{v}+v') - \frac{1}{\rho}\frac{\partial(\bar{p}_{dyn}+p'_{dyn})}{\partial y} \qquad (18)$$

The equation for the z-direction is analogous to equation (18).

Recalling again the continuity equation, the energy equation becomes

$$\frac{\partial(\bar{T}+T')}{\partial t} + \frac{\partial(\bar{u}+u')(\bar{T}+T')}{\partial x} + \frac{\partial(\bar{v}+v')(\bar{T}+T')}{\partial y} + \frac{\partial(\bar{w}+w')(\bar{T}+T')}{\partial z} =$$

$$= \alpha \nabla^2 (\bar{T}+T') \qquad (19)$$

We are now in possession of a system of partial differential equations, describing the problem of unsteady turbulent free convection, but the equations cannot be used in this form yet.

3.5 Smoothing of the Turbulent Equations

The next step usually undertaken in the case of steady state turbulent flow is called time-averaging. We shall call the corresponding procedure in the unsteady case smoothing.

The averages of the equations (16-19) are (after some rearrangements)

$$\frac{\partial \bar{u}}{\partial x} + \frac{\partial \bar{v}}{\partial y} + \frac{\partial \bar{w}}{\partial z} = 0 \qquad (20)$$

$$\frac{\partial \bar{u}}{\partial t} + \frac{\partial(\bar{u}\bar{u})}{\partial x} + \frac{\partial(\bar{v}\bar{u})}{\partial y} + \frac{\partial(\bar{w}\bar{u})}{\partial z} =$$

$$= \nu \nabla^2 \bar{u} + \beta g (\bar{T} - T_f) - \frac{1}{\rho} \frac{\partial \bar{p}_{dyn}}{\partial x} -$$

$$- \left[\frac{\partial(\overline{u'u'})}{\partial x} + \frac{\partial(\overline{v'u'})}{\partial y} + \frac{\partial(\overline{w'u'})}{\partial z} \right] \qquad (21)$$

$$\frac{\partial \bar{v}}{\partial t} + \frac{\partial(\bar{u}\bar{v})}{\partial x} + \frac{\partial(\bar{v}\bar{v})}{\partial y} + \frac{\partial(\bar{w}\bar{v})}{\partial z} = \nu \nabla^2 \bar{v} -$$

$$- \frac{1}{\rho} \frac{\partial \bar{p}_{dyn}}{\partial y} - \left[\frac{\partial(\overline{u'v'})}{\partial x} + \frac{\partial(\overline{v'v'})}{\partial y} + \frac{\partial(\overline{w'v'})}{\partial z} \right] \qquad (22)$$

$$\frac{\partial \bar{T}}{\partial t} + \frac{\partial(\bar{u}\bar{T})}{\partial x} + \frac{\partial(\bar{v}\bar{T})}{\partial y} + \frac{\partial(\bar{w}\bar{T})}{\partial z} =$$

$$= \alpha \nabla^2 \bar{T} - \left[\frac{\partial(\overline{u'T'})}{\partial x} + \frac{\partial(\overline{v'T'})}{\partial y} + \frac{\partial(\overline{w'T'})}{\partial z} \right] \qquad (23)$$

taking into account, that

$$\overline{\phi\phi} = \overline{(\bar{\phi}+\phi')(\bar{\phi}+\phi')} = \overline{\bar{\phi}^2 + 2\bar{\phi}\phi' + \phi'^2} = \bar{\phi}^2 + \overline{\phi'^2} \qquad (24)$$

and recalling equation (15). The momentum equation for the z-direction is again analogous to the equation for y-direction, i.e. equation (22).

It can be seen, that equations (21-23) differ from equations (11) and (12) by the presence of the last terms on the right-hand side. In the case of the momentum equations, the name Reynolds' stresses is used for these terms, which represent the turbulence and obviously are not negligible. Therefore, they must always be taken into account, although their evaluation is very far from being simple.

3.6 The Problem of Closure

An inspection of the system of equations (20-23) reveals, that there are now more dependent variables than equations. This unpleasant situation arises from the appearance of the averaged products of fluctuating quantities in the momentum and energy equations. We can proceed only by equaling the number of equations and dependent variables, i.e. by closing the system. This is the central problem of theoretical turbulence investigations and is known as the problem of closure.

One of the oldest methods of treatment of this problem is due to Boussinesq /101/. The method is based on the observation, that the action of the terms containing the averaged products is analogous to viscous friction and molecular heat diffusion, respectively. Therefore, the averaged products of turbulent fluctuations are replaced by the so-called eddy diffusivity of momentum ε_M and eddy diffusivity of energy ε_H. According to this idea, we shall evaluate the effect of the tensors of Reynolds' stresses and turbulent heat fluxes in terms of these diffusivities, which are scalar properties of the field and as such can be directly added to kinematic viscosity and thermal diffusivity, respectively.

We shall omit the z-dimension in our equations, because the wall is infinite in that direction. In this way, the flow is assumed to be two-dimensional, although turbulence is essentially a three-dimensional phenomenon. The equations (20-23) now become (subsequently, all equations contain mean values only, and the bars overhead will be omitted for simplicity)

$$\frac{\partial u}{\partial x} + \frac{\partial v}{\partial y} = 0 \qquad (25)$$

$$\frac{\partial u}{\partial t} + u\frac{\partial u}{\partial x} + v\frac{\partial u}{\partial y} = \frac{\partial}{\partial x}\left[(\nu+\varepsilon_M)\frac{\partial u}{\partial x}\right] + \frac{\partial}{\partial y}\left[(\nu+\varepsilon_M)\frac{\partial u}{\partial y}\right] + \beta g (T - T_f) - \frac{1}{\rho}\frac{\partial p_{dyn}}{\partial x} \qquad (26)$$

$$\frac{\partial v}{\partial t} + u\frac{\partial v}{\partial x} + v\frac{\partial v}{\partial y} = \frac{\partial}{\partial x}\left[(\nu+\varepsilon_M)\frac{\partial v}{\partial x}\right] + \frac{\partial}{\partial y}\left[(\nu+\varepsilon_M)\frac{\partial v}{\partial y}\right] - \frac{1}{\rho}\frac{\partial p_{dyn}}{\partial y} \qquad (27)$$

$$\frac{\partial T}{\partial t} + u\frac{\partial T}{\partial x} + v\frac{\partial T}{\partial y} = \frac{\partial}{\partial x}\left[(\alpha+\varepsilon_H)\frac{\partial T}{\partial x}\right] + \frac{\partial}{\partial y}\left[(\alpha+\varepsilon_H)\frac{\partial T}{\partial y}\right] \qquad (28)$$

It is obvious, that the eddy diffusivities are not material properties, such as kinematic viscosity or thermal conductivity. Their main purpose is to eliminate the averaged products of turbulent fluctuating quantities. It is inherently assumed in this concept, that turbulence can be evaluated from local mean values of dependent variables. This assumption is of course questionable, and also the smoothing procedure (Section 3.5) has not been rigorously justified. Unfortunately, our present understanding of turbulent processes is still quite limited and for this reason the foregoing heuristic approximations are commonly used in contemporary calculations of turbulent flow and/or heat transfer. Strictly speaking, such methods can be regarded as useful working hypotheses only.

3.7 Boundary Layer Approximation

Experimental investigations of natural convection have shown, that the flow region thickness is usually small in comparison with other flow dimensions. The concept of boundary layer, as introduced by Prandtl /151/, may be conveniently employed in such a situation.

From the relative thinness of the flow region it follows that

$$u \gg v \qquad (29)$$

and

$$\frac{\partial u}{\partial y} \gg \frac{\partial u}{\partial x}\ ,\ \frac{\partial v}{\partial x}\ ,\ \frac{\partial v}{\partial y} \qquad (30)$$

Moreover, the variation of the dynamic pressure in the flow region also becomes negligible. The region of appreciable temperature changes is also thin, and it follows that

$$\frac{\partial T}{\partial y} \gg \frac{\partial T}{\partial x} \qquad (31)$$

After an order-of-magnitude analysis, the boundary layer approximation, resulting from the system of equations (25-28), is

$$\frac{\partial u}{\partial x} + \frac{\partial v}{\partial y} = 0 \qquad (32)$$

$$\frac{\partial u}{\partial t} + u\frac{\partial u}{\partial x} + v\frac{\partial u}{\partial y} = \frac{\partial}{\partial y}\left[(\nu + \varepsilon_M)\frac{\partial u}{\partial y}\right] + \beta g (T - T_f) \qquad (33)$$

$$\frac{\partial T}{\partial t} + u\frac{\partial T}{\partial x} + v\frac{\partial T}{\partial y} = \frac{\partial}{\partial y}\left[(\alpha + \varepsilon_H)\frac{\partial T}{\partial y}\right] \qquad (34)$$

The boundary layer assumption means physically, that the situation at a given station depends on the upstream conditions only. This is a fundamental difference, compared with the 'jury-type' problem given by the system of equations (25-28).

From the mathematical point of view, the nature of the system was changed from an elliptic to a parabolic one. This change shall considerably simplify the numerical treatment of the system.

The basic difference between forced and free convection can be readily seen from equation (33), which is coupled through the last right-hand term with the energy equation (34). This means, that both these equations must be solved simultaneously. In the case of forced convection, there is no such coupling and the flow field can be solved independently before the temperature field is calculated. It is clear, that calculations of natural convection are for this reason intrinsically more complicated than similar calculations of forced convection.

3.8 Initial and Boundary Conditions

The complete formulation of a problem described by partial differential equations must include appropriate boundary and/or initial conditions. We are considering a parabolic problem here, and therefore both initial and boundary conditions are required.

Initial conditions must be given in the whole domain at $t = 0$. Moreover, boundary conditions for $x = 0$, $y = 0$, and $y \to \infty$ must be specified. The boundary conditions could be a function of time. No condition is required for $x = L$, because our equations are parabolic in that direction.

In agreement with the definition of our problem, as given in Section 3.1, we specify the following initial conditions

$$t = 0 \quad : \qquad u = 0, \quad v = 0, \quad T = T_f \qquad (35)$$

and boundary conditions

$$\left.\begin{array}{lll} x=0\ ,\ y>0 & : & u=0\ , \qquad T=T_f \\ y=0 & : & u=0\ ,\ v=0\ ,\ T=T_w \\ y\to\infty & : & u=0\ , \qquad T=T_f \end{array}\right\} \qquad (36)$$

A difficulty arises at the left lower corner of the field (see Fig. 1). At this point, the temperature specified for $y=0$ is T_w , but

$$\lim_{y\to 0+} T(0,y) = T_f \neq T_w \qquad (37)$$

However, such singularities are relatively common in the numerical treatment of partial differential equations. This singular point deformates the solution in its neighbourhood, and under certain circumstances can become the focal point of a numerical instability. Its influence upon the solution shall be seen from the discussion of our results.

4. TURBULENCE MODEL

We have formulated in the preceding Chapter a system of partial differential equations, employing the concept of eddy diffusivities. These diffusivities are not material properties, but are functions of the mean flow field. Therefore, a necessary condition for proceeding further with our analysis is that a method for their calculation from the mean flow field be prescribed. Such a method is usually called a turbulence model.

4.1 Phenomenological Models of Turbulence

The first suggestion how to determine the value of ε_M is due to Prandtl /152/. He proposed the well-known mixing-length hypothesis

$$\varepsilon_M = \ell^2 \left| \frac{\partial u}{\partial y} \right| \qquad (38)$$

This does not seem to be a big progress, as another unknown parameter was introduced by this equation. However, the mixing length ℓ can be evaluated from the geometry of the flow system and, moreover, it varies much less than the eddy diffusivity ε_M.

Subsequently, more sophisticated approaches were proposed by other authors. An important formulation was that of Kolmogorov /136/, who connected ε_M with the kinetic energy of the fluctuating velocities. In his model of turbulence, it is possible to derive a differential equation with the turbulent kinetic energy as its main dependent variable. Rotta /155/ proceeded further and proposed a differential equation for the length scale also.

Turbulence models employing differential equations are quite abundant today (see e.g. Bradshaw et al. /105/, Ng & Spalding /148/, Hanjalić & Launder /124/), but all of them have a serious drawback: they contain empirical coefficients, which must be suitably adjusted by comparison with experimental data. This whole approach is in a certain sense nothing else but a sophisticated curve fitting. The number of the empirical coefficients usually increases much more rapidly than the accuracy of the predictions, and there does not seem to be any justification for the use of some of the more complicated models.

These methods were applied exclusively to forced convection problems. The only exception is the recent work of Mason & Seban /69/, who employed the turbulent kinetic energy equation for their calculations of steady turbulent natural convection.

4.2 The Turbulence Model of Nee & Kovasznay

One of the recently proposed models is that of Nee & Kovasznay /147/. This model appeals mainly by its relative simplicity. On the other hand, its accuracy and predictive ability also seem to be satisfactory. In fact, Wassel & Catton /164/ in their calculations of forced convection boundary layers obtained better results with this model than with the more complicated turbulent kinetic energy equations. For its relative simplicity and good accuracy, this model was chosen also for our calculations.

We define effective viscosity as the sum of kinematic viscosity and eddy diffusivity of momentum, i.e.

$$\omega = \nu + \varepsilon_M \qquad (39)$$

The basic idea of the Nee-Kovasznay model is to write a rate equation with the effective viscosity as the dependent variable. For a boundary layer, this equation is

$$\frac{\partial \omega}{\partial t} + u\frac{\partial \omega}{\partial x} + v\frac{\partial \omega}{\partial y} = \frac{\partial}{\partial y}\left[\omega \frac{\partial \omega}{\partial y}\right] + G - D \qquad (40)$$

The left-hand side represents convection of the effective viscosity by the mean flow. The name advection instead of convection is sometimes used in turbulence models of this type. The first term on the right-hand side represents nonlinear diffusion. The turbulent motion diffuses by itself, and it seems reasonable to use the effective viscosity as its own diffusion coefficient.

The generation term G is formed from a rough analogy with production of turbulent kinetic energy. It is known, that this production is increasing with the magnitude of $\left|\frac{\partial u}{\partial y}\right|$ and also with the level of turbulence, i.e. with ε_M. The generation term is constructed as the simplest form compatible with the two requirements, which is

$$G = A\,(\omega - \nu)\left|\frac{\partial u}{\partial y}\right| \qquad (41)$$

In this equation, A is an empirical constant. The dissipation term D is again constructed from an analogy with turbulent kinetic energy, for which the rate of decay, in a rough approximation, is

$$\frac{d\overline{u'^2}}{dt} = -c\left(\overline{u'^2}\right)^2 \qquad (42)$$

The rate equation (40) in absence of the convection, diffusion, and generation terms is reduced to

$$\frac{\partial \omega}{\partial t} = -D \qquad (43)$$

Comparing this equation with equation (42), the form of the dissipation term is chosen as

$$D \sim c\,\omega^2 \qquad (44)$$

In order to obtain a more appropriate behaviour for $\varepsilon_M \to 0$, and for dimensional considerations, the final form of the dissipation (or decay) term is chosen as

$$D = \frac{B}{\ell^2}\,\omega\,(\omega - \nu) \qquad (45)$$

In this equation, B is another empirical constant and ℓ is a characteristic length. The authors suggest (see /147/) $\ell = y$ for boundary layer flows and we shall adopt this idea.

Inserting the generation term (41) and the decay term (45) into the rate equation (40), we have now

$$\frac{\partial \omega}{\partial t} + u\frac{\partial \omega}{\partial x} + v\frac{\partial \omega}{\partial y} = \frac{\partial}{\partial y}\left[\omega\frac{\partial \omega}{\partial y}\right] + A\,(\omega - \nu)\left|\frac{\partial u}{\partial y}\right| - \frac{B}{y^2}\,\omega\,(\omega - \nu) \qquad (46)$$

However, solutions obtained from this equation in a region where the kinematic viscosity is dominant cannot be accurate. For this reason the equation (46) is used in the outer part of the boundary layer only, and its solution is matched to a law of the wall somewhere near the surface, but still outside of the viscous sublayer.

4.3 Law of the Wall

It had been observed that experimental turbulent velocity profiles in the vicinity of a wall could be correlated by a universal curve in nondimensional coordinates. Various research workers subsequently formulated different algebraic correlations, from which the universal velocity profile can be calculated. Such a formula is usually called a law of the wall.

Compilations of these formulae were given by Kestin & Richardson /134/, Herring & Mellor /127/, and also in the Kays' textbook /133/.

One of the best-known models is due to von Kármán /132/, who divided the boundary layer into three distinct regions and wrote an algebraic equation for each of them. Later, Reichardt /153/, van Driest /116/ and Spalding /160/ suggested models covering the entire boundary layer by one equation only.

We shall use here the law of the wall as formulated by Deissler /115/. This model consists of two equations, but the first one is valid for $y^+ \leqq 26$ and covers the laminar sublayer and almost the whole buffer layer.

The velocity profile is expressed as

$$u^+ = \int_0^{y^+} \frac{dy^+}{1 + n^2 u^+ y^+ \left[1 - \exp(-n^2 u^+ y^+)\right]} \qquad (47)$$

This formidable formula is certainly not very practical, but we are interested in $\omega^+ = \phi(y^+)$ and not so much in $u^+ = \phi(y^+)$. The required formula can be readily obtained from equation (47), if we remember that

$$\omega^+ = \frac{dy^+}{du^+} \qquad (48)$$

The resulting formula for ω^+ is

$$\omega^+ = 1 + n^2 u^+ y^+ \left[1 - \exp(-n^2 u^+ y^+)\right] \qquad (49)$$

This formula is convenient from the computational point of view, as it is relatively simple, but at the same time covers the whole region of interest by one equation. Moreover, it has been successfully applied in many heat transfer calculations. Writing (49) in dimensional form, we have

$$\omega = \nu \left\{ 1 + n^2 \frac{uy}{\nu} \left[1 - \exp\left(-n^2 \frac{uy}{\nu}\right) \right] \right\} \qquad (50)$$

The effective viscosity shall be calculated in the inner region, covering the whole laminar sublayer and a part of the buffer zone, from the equation (50).

4.4 Turbulent Prandtl Number

By means of the equations (46) and (50), we are in a position to calculate the eddy diffusivity of momentum. However, it is necessary to evaluate also the eddy diffusivity of energy. This is usually accomplished by introducing the so-called turbulent Prandtl number. Its definition, in analogy with the 'normal' Prandtl number, is

$$Pr_t = \frac{\varepsilon_M}{\varepsilon_H} \qquad (51)$$

Unfortunately, its evaluation is somewhat more difficult than its definition. The usual approach to the evaluation is based on an analogy between turbulent diffusion of heat and momentum. These analogies were extensively discussed by Knudsen & Katz /135/, Kays /133/, and in the field of mass transfer (diffusion of mass instead of heat) by Skelland /159/. The first such analogy is due to Reynolds, who simply postulated $\varepsilon_H = \varepsilon_M$. This means, of course, that the turbulent Prandtl number becomes constant and equal to one. In spite of its crudity, this hypothesis yielded surprisingly good results.

The simple Reynolds' analogy was later refined by many research workers, and some of them, e.g. Jenkins /131/, derived quite complicated formulae for $\varepsilon_H = \phi(\varepsilon_M)$. Recently, such correlations were proposed by Tyldesley & Silver /163/, Cebeci /107/, and Wassel & Catton /164/.

The available experimental data were evaluated by Kestin & Richardson /134/, and it can be clearly seen from their comparisons, that the agreement among the results of various investigators is not very good. However, most of the data lie between $Pr_t = 0,6$ and $Pr_t = 1,0$. Moreover, the variation of the turbulent Prandtl number with distance from the wall is practically insignificant.

The uncertainty does not warrant the use of a sophisticated model, and a constant value of the turbulent Prandtl number, approximately equal to one, is used in most applications. We shall also apply this method here.

4.5 Empirical Constants

Each phenomenological model of turbulence contains a number of empirical constants, which must be adjusted in such a way, that agreement with empirical data is obtained. In our case, altogether five constants must be given appropriate values. These constants are: A and B in the Nee-Kovasznay partial differential equation (46); n in the Deissler's law of the wall (50); the boundary y^+_{lim} between the inner and outer region; and the turbulent Prandtl number Pr_t. Fortunately, with only one exception, their values can be taken from literature.

Nee & Kovasznay propose in their original publication /147/ the values A = 0,133 and B = 0,8. In a later article, Kovasznay /137/ suggests A = 0,1 and B = 1,0. Wassel & Catton /164/, who applied this model to forced convection boundary layers, also used the values A = 0,1 and B = 1,0 with good results. Therefore, the values A = 0,1 and B = 1,0 have been chosen also for our calculations.

The constant n in the law of the wall (50) was calculated by Deissler /115/, and its value is $n = 0{,}124$.

Kestin & Richardson /134/ recommend the value of the turbulent Prandtl number around $Pr_t = 0{,}78$, while Gröber et al. /123/ suggest $Pr_t = 0{,}8$. The later value shall be also used in our calculations.

The only remaining constant is the boundary between the inner and outer region, y^+_{lim}. The law of the wall must cover the whole laminar sublayer, and therefore $y^+_{lim} > 5$. Kovasznay /137/ suggests $30 < y^+_{lim} < 100$, but after some numerical experiments, $y^+_{lim} = 15$ was chosen as the optimum value for our calculations. This relatively small value obviously results from the small magnitude of wall friction in natural convection flows.

4.6 Complete Mathematical Formulation of the Problem

We shall give here for convenience the complete mathematical formulation of our problem. The system of equations consists from the continuity equation

$$\frac{\partial u}{\partial x} + \frac{\partial v}{\partial y} = 0 \qquad (52)$$

the momentum equation

$$\frac{\partial u}{\partial t} + u\frac{\partial u}{\partial x} + v\frac{\partial u}{\partial y} = \frac{\partial}{\partial y}\left[\omega \frac{\partial u}{\partial y}\right] + \beta g (T - T_f) \qquad (53)$$

the energy equation

$$\frac{\partial T}{\partial t} + u\frac{\partial T}{\partial x} + v\frac{\partial T}{\partial y} = \frac{\partial}{\partial y}\left[\left(\alpha + \frac{\omega - \nu}{Pr_t}\right)\frac{\partial T}{\partial y}\right] \qquad (54)$$

the effective viscosity rate equation

$$\frac{\partial \omega}{\partial t} + u\frac{\partial \omega}{\partial x} + v\frac{\partial \omega}{\partial y} = \frac{\partial}{\partial y}\left[\omega\frac{\partial \omega}{\partial y}\right] + A(\omega - \nu)\left|\frac{\partial u}{\partial y}\right| - \frac{B}{y^2}\,\omega(\omega - \nu) \quad \text{for} \quad y \geq \frac{y^+_{eim}\,\nu}{\sqrt{\frac{\tau_w}{\varrho}}} \qquad (55)$$

and the law of the wall

$$\omega = \nu\left\{1 + n^2\frac{uy}{\nu}\left[1 - \exp\left(-n^2\frac{uy}{\nu}\right)\right]\right\}$$

$$\text{for} \quad y \leq \frac{y^+_{eim}\,\nu}{\sqrt{\frac{\tau_w}{\varrho}}} \qquad (56)$$

It is obviously required, that the effective viscosity profile be continuous at y^+_{eim}, i.e.

$$\lim_{y^+ \to y^+_{eim}-} \omega(y^+) = \lim_{y^+ \to y^+_{eim}+} \omega(y^+) \qquad (57)$$

It shall be assumed, that equations (52-56) apply for the entire boundary layer, starting from the leading edge of the plate.

The initial and boundary conditions must now include also the appropriate values of effective viscosity.

The complete initial conditions

$$t = 0 : \quad u = 0,\ v = 0,\ T = T_f,\ \omega = \nu \qquad (58)$$

and the complete boundary conditions

$$\left.\begin{array}{lll} x = 0,\ y > 0 & : & u = 0, \quad T = T_f, \quad \omega = \nu \\ y = 0 & : & u = 0,\ v = 0,\ T = T_w, \quad \omega = \nu \\ y \to \infty & : & u = 0 \quad\quad T = T_f, \quad \omega = \nu \end{array}\right\} \qquad (59)$$

describe, together with the system of equations (52-56), the problem of unsteady turbulent free convection, as defined in Section 3.1. This system must be solved by a numerical method and that will be the subject of the following Chapter.

5. NUMERICAL METHOD

It is impossible to solve our system of equations (52-56) analytically, and resort to a numerical method must be taken. A sufficient number of various numerical methods has been developed to select from, e.g. the finite-element method, employing variational principles and used mainly in stress analysis, the method of lines, transforming a partial differential equation into a system of ordinary differential equations, or the Monte Carlo method, based on random walk and utilised for treatment of some diffusion problems.

However, the most widely used numerical approach is the method of finite differences, which shall be used also in our case. There is a number of fine books describing this method, and at least the treatises of Forsythe & Wasow /176/, Richtmyer & Morton /189/ and Ames /166/ should be mentioned here. Dusinberre /117/ described the applications of this method in the field of heat transfer, but his book is somewhat outdated now. Our system of equations is of the parabolic nature and with this special case the publications of Saul'yev /190/, Douglas /173/ or Keller /183/ are concerned.

5.1 Finite Differences

The basic principle of this method is transformation of a partial differential equation into a finite-difference equation, which is algebraic and can be solved numerically.

Consider a two-dimensional rectangular region, in which a partial differential equation is defined. Let us superimpose a parallel rectangular grid on this region, with grid steps Δx and Δy. The grid points are denoted by indices as shown in Fig. 2. At a grid point, the function ϕ, which is a solution of the partial differential equation, can be expanded into Taylor series

$$\phi(x+\Delta x, y) = \phi(x,y) + \Delta x \frac{\partial \phi(x,y)}{\partial x} + \\ + \frac{(\Delta x)^2}{2!} \frac{\partial^2 \phi(x,y)}{\partial x^2} + \frac{(\Delta x)^3}{3!} \frac{\partial^3 \phi(x,y)}{\partial x^3} + O[(\Delta x)^4] \qquad (60)$$

and after dividing by Δx, we obtain the relation

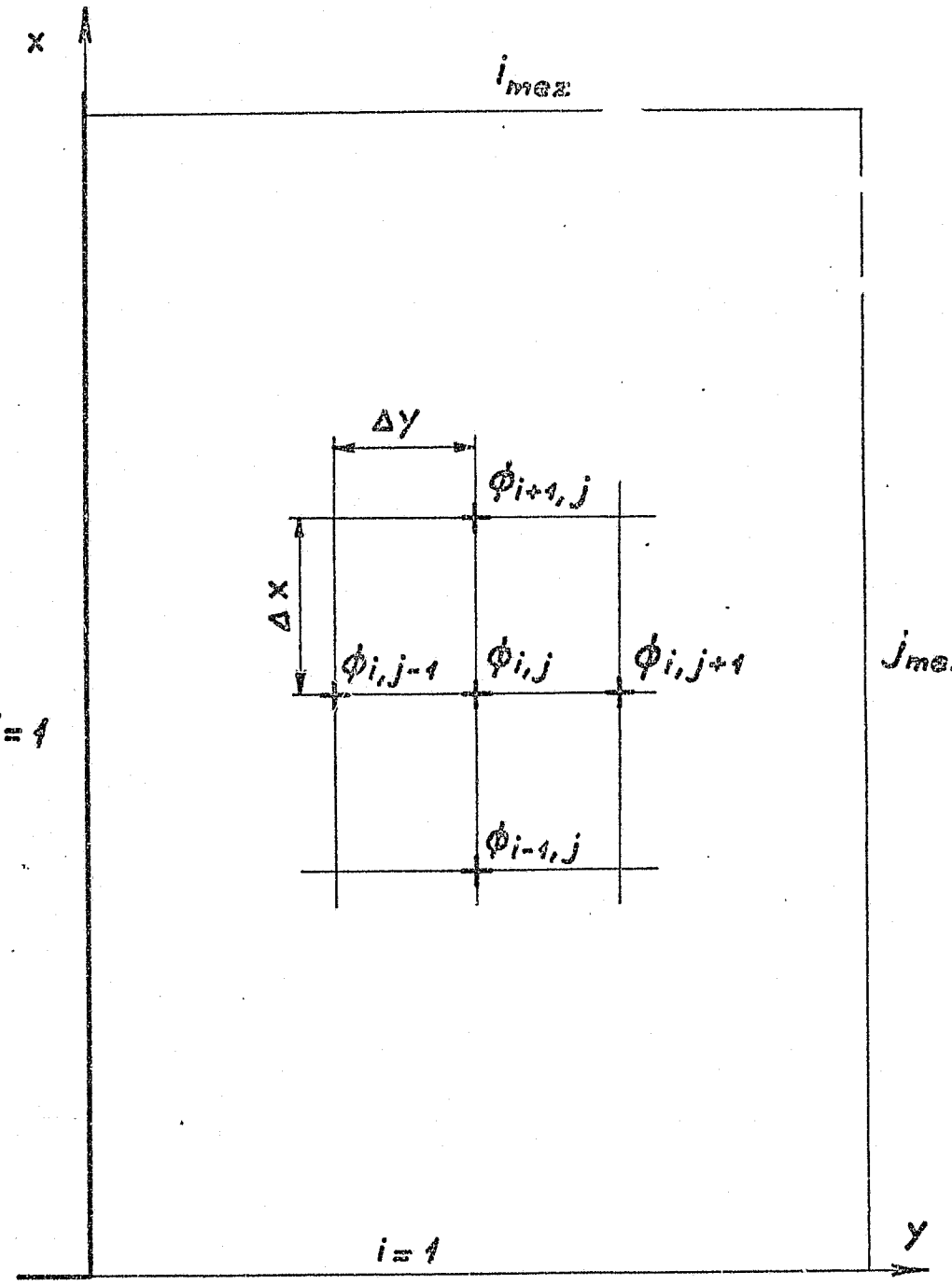

FIG. 2. FINITE DIFFERENCES

$$\frac{\partial \phi(x,y)}{\partial x} = \frac{\phi(x+\Delta x,y) - \phi(x,y)}{\Delta x} + O[\Delta x] \qquad (61)$$

This is called the forward-difference approximation. The analogous backward-difference approximation

$$\frac{\partial \phi(x,y)}{\partial x} = \frac{\phi(x,y) - \phi(x-\Delta x,y)}{\Delta x} + O[\Delta x] \qquad (62)$$

is obtained in a similar way. It can easily be shown, using again the Taylor series development, that the second partial derivative is approximated by

$$\frac{\partial^2 \phi(x,y)}{\partial x^2} = \frac{\phi(x-\Delta x,y) - 2\phi(x,y) + \phi(x+\Delta x,y)}{(\Delta x)^2} + O[(\Delta x)^2] \qquad (63)$$

The corresponding approximations for partial derivatives in the y-direction are obtained in a similar fashion.

The finite-difference equation results from a partial differential equation, if the partial derivatives are replaced by their finite--difference approximations. The solution of the finite-difference equation is represented by numerical values at a set of discrete points in the region. These values approximate the exact solution of the continuous problem defined by the partial differential equation.

5.2 System of Equations to be Solved

We shall now replace the partial derivatives in equations (52-55) by finite differences. The analogous laminar problem has been successfully treated by Hellums & Churchill /41,42/ and we shall use a similar approach here. The numerical stability of the algorithm is closely connected with proper choice of the finite--difference approximations to the first-order partial derivatives in the convective terms. As discussed by Hellums & Churchill /41/, some choices lead to unconditional instability, and we certainly do not desire anything like that.

The backward difference shall be used for the replacement of the first derivative associated with the vertical velocity component, which is always positive. On the other hand, the forward difference shall replace the first derivative associated with the horizontal velocity component, which is always negative. The reason

for this particular choice shall be explained in our discussion of numerical stability in Section 5.4 . These so-called 'upwind' differences were probably used for the first time by Courant et al. /169/ in a finite-difference solution of nonlinear hyperbolic partial differential equations. Charney & Phillips /111/ applied this method shortly afterwards to a meteorological problem, which seems to be the origin of the name.

The system of equations (52-56) is then approximated, with reference to Fig. 2 , by the following system of finite-difference equations:

$$T_{i,j}^{N} = T_{i,j} - \frac{\Delta t}{\Delta x} u_{i,j} (T_{i,j} - T_{i-1,j}) - \frac{\Delta t}{\Delta y} v_{i,j} (T_{i,j+1} - T_{i,j}) + \\ + \frac{\Delta t}{(\Delta y)^2} \left[(K_1 + K_2 \omega_{i,j+\frac{1}{2}})(T_{i,j+1} - T_{i,j}) - (K_1 + K_2 \omega_{i,j-\frac{1}{2}}) \cdot \right. \\ \left. \cdot (T_{i,j} - T_{i,j-1}) \right] \qquad (64)$$

$$u_{i,j}^{N} = u_{i,j} - \frac{\Delta t}{\Delta x} u_{i,j} (u_{i,j} - u_{i-1,j}) - \frac{\Delta t}{\Delta y} v_{i,j} (u_{i,j+1} - u_{i,j}) + \\ + \frac{\Delta t}{(\Delta y)^2} \left[\omega_{i,j+\frac{1}{2}} (u_{i,j+1} - u_{i,j}) - \omega_{i,j-\frac{1}{2}} (u_{i,j} - u_{i,j-1}) \right] + \\ + \Delta t \, \beta \, g \, (T_{i,j} - T_f) \qquad (65)$$

$$v_{i,j}^{N} = v_{i,j-1}^{N} - \frac{\Delta y}{\Delta x} (u_{i,j}^{N} - u_{i-1,j}^{N}) \quad \text{for} \quad i > 1 \qquad (66)$$

$$v_{1,j}^{N} = v_{1,j-1}^{N} - \frac{\Delta y}{\Delta x} (u_{2,j}^{N} - u_{1,j}^{N}) \qquad (67)$$

$$\omega_{i,j}^{N} = \nu + n^2 u_{i,j} y_j \left[1 - \exp\left(- n^2 \frac{u_{i,j} y_j}{\nu} \right) \right]$$

$$\text{for} \quad y_{i,j}^{+} \leqq y_{eim}^{+} \qquad (68)$$

$$\omega_{i,j}^{N} = \omega_{i,j} - \frac{\Delta t}{\Delta x} u_{i,j} (\omega_{i,j} - \omega_{i-1,j}) - \frac{\Delta t}{\Delta y} v_{i,j} (\omega_{i,j+1} - \omega_{i,j}) + \\ + \frac{\Delta t}{(\Delta y)^2} \left[\omega_{i,j+\frac{1}{2}} (\omega_{i,j+1} - \omega_{i,j}) - \omega_{i,j-\frac{1}{2}} (\omega_{i,j} - \omega_{i,j-1}) \right] + \\ + \frac{\Delta t}{\Delta y} A (\omega_{i,j} - \nu) \left| u_{i,j} - u_{i,j-1} \right| - \frac{\Delta t}{y_j^2} B \, \omega_{i,j} (\omega_{i,j} - \nu)$$

$$\text{for} \quad y_{i,j}^{+} > y_{eim}^{+} \qquad (69)$$

In this system, we take

$$\phi_{j\pm\frac{1}{2}} = \frac{\phi_j + \phi_{j\pm1}}{2} \qquad (70)$$

The Deissler's correlation (50) was derived purely for steady state. This is partly compensated by lagging the corresponding equation (68) one time step behind the solution.

It is not necessary to repeat the initial and boundary conditions here, as the formulation is straightforward. The asymptotic conditions for $y \to \infty$ are an exception, and they must be suitably approximated. In a transient, the thickness of the boundary layer is growing physically with time. The values of u, T, and ω on the last vertical grid line before the outer boundary will be checked at each time step, and if there is a change in any of these variables bigger than a specified criterion, the thickness of the region covered by the grid shall be increased. In this way, only a field of the necessary size shall be computed.

It can be seen, that an explicit scheme was chosen for the algorithm. Such a scheme is relatively simple and because of the parabolic nature of the system allows us 'to march forward' downstream along the wall and in time. The alternative is an implicit scheme, which permits a longer time step, but on the other hand, a large system of simultaneous nonlinear algebraic equations must be solved by iterations at each time level. In comparison with the explicit method, the longer permissible time step would hardly compensate for the substantial increase in computing time per one time step. Moreover, we are solving a transient problem here, in which the intermediate results of the explicit method can also be of interest to us. For these reasons, the explicit method seems to be more suitable for the treatment of our problem. If the steady state solution is required only, the algorithm (64-69) can be regarded as a special (although not especially economic) iterative procedure. In such a case, initial conditions approximating the expected steady state profiles would save some computing time.

5.3 Errors Associated with the Method

The finite-difference scheme is an approximation, and as all approximations, it is associated with some errors.

Round-off errors are common to almost all numerical calculations. These errors are introduced by our inability to perform

numerical calculations with infinite number of significant figures. For example, the single-precision arithmetic of the IBM/360 computers carries only 6 significant hexadecimal digits, corresponding approximately to 7 significant decimal figures.

However, there are also another errors, inherent to the finite--difference method. The error caused by the replacement of a continuous problem by a discrete model is called the discretization error. It is the difference between the exact solution of the partial differential equation and the exact solution of the corresponding finite-difference equation (which is supposed to be stable and convergent).

The error arising from cutting off the Taylor series development (60 etc.) is called the truncation error. This error is usually considered to be identical with the discretization error. However, this is not the case, strictly speaking. If the boundary conditions have to be also approximated by finite differences, an additional error is introduced, and the discretization error is larger than the truncation error.

Another error, which is peculiar to the use of the 'upwind' (or generally one-sided) differences, is called 'false' diffusion. However, it has been shown by Gosman et al. /122/, that this effect is negligible, if the velocity vector and one coordinate axis are parallel. This condition is practically satisfied in a boundary layer flow, so that it is not necessary to consider this effect further in our work.

5.4 Stability and Convergence

One very important property of a finite-difference scheme is its numerical stability. There is a number of different mathematical definitions of the stability, but the basic question is: If at a certain time level some small errors (e.g. round-off) are added to the solution, what happens in the subsequent time steps? The numerical scheme is stable, if these errors decay with time, or at least are bounded. On the other hand, if the errors are amplified, the numerical scheme is unstable. Such a scheme is practically useless, because the solution is very soon obliterated and in the end completely destroyed.

The problem of numerical stability of finite-difference schemes was extensively investigated by DuFort & Frankel /175/,

Lax & Richtmyer /185/, Douglas /171/ and others (see Richtmyer & Morton /189/). A frequently used method of stability analysis seems to be due to von Neumann. In this method, an initial row of errors is represented by a finite Fourier series. Its application to the one-dimensional equation of transient heat conduction is given e.g. by Schneider /158/. The result is the well-known stability criterion

$$\Delta t \leqq \frac{(\Delta x)^2}{2\,a} \tag{71}$$

However, this analysis is strictly valid for linear equations only. Moreover, it does not take boundary conditions into account.

Another method, due to John /181/ and also described by Forsythe & Wasow /176/ and others, seems to be more suitable in our case. It was also used by Torrance /89/ in his discussion of finite-difference methods for unsteady laminar free convection in cylindrical enclosures. John /181/ investigated the second-order parabolic partial differential equation

$$\frac{\partial \phi}{\partial t} = a(x,t)\frac{\partial^2 \phi}{\partial x^2} + b(x,t)\frac{\partial \phi}{\partial t} + c(x,t)\,\phi + d(x,t) \tag{72}$$

in which $a(x,t) \geqq 0$.

The mathematical discussion is complicated and transcends the scope of this dissertation. However, the resulting stability criteria are quite simple.

The explicit finite-difference scheme corresponding to the equation (72) can be written as a linear combination of known function values, viz.

$$\phi_i^N = \xi_{-1}\,\phi_{i-1} + \xi_0\,\phi_i + \xi_1\,\phi_{i+1} + \Delta t\; a_i \tag{73}$$

The essential requirement is that the norm of the matrix of the coefficients ξ_k be at all times bounded by unity. If the coefficients in equation (73) fulfil the inequalities

$$\xi_k \geqq 0 \tag{74}$$

and

$$\xi_{-1} + \xi_0 + \xi_1 \leqq 1 \tag{75}$$

the finite-difference scheme (73) is called approximation of positive type and is stable.

For nonlinear partial differential equations, the heuristic approach suggested by Richtmyer & Morton /189/ has to be used also in our case. This means, that the criteria (74) and (75) are used as local criteria only, because the coefficients depend on the solution being calculated.

For our finite-difference equations (64),(65), and (69), the linear combination analogous to (73) is

$$\phi^{N}_{i,j} = \xi_1 \phi_{i,j-1} + \xi_2 \phi_{i,j} + \xi_3 \phi_{i,j+1} + \xi_4 \phi_{i-1,j} + \Delta t\, d_{i,j} \qquad (76)$$

in which instead of the dummy variable ϕ either T or u or ω may be inserted. The stability condition, besides the requirement (74) of nonnegative coefficients, is now

$$\sum_{k=1}^{4} \xi_k \leqq 1 \qquad (77)$$

If equation (65) is written in the same form as (76), we obtain

$$\xi_1 = \frac{\Delta t\ \omega_{i,j-\frac{1}{2}}}{(\Delta y)^2} \qquad (78)$$

$$\xi_2 = 1 - \frac{\Delta t}{\Delta x} u_{i,j} + \frac{\Delta t}{\Delta y} v_{i,j} - \frac{\Delta t}{(\Delta y)^2} \omega_{i,j+\frac{1}{2}} - \frac{\Delta t}{(\Delta y)^2} \omega_{i,j-\frac{1}{2}} \qquad (79)$$

$$\xi_3 = -\frac{\Delta t}{\Delta y} v_{i,j} + \frac{\Delta t}{(\Delta y)^2} \omega_{i,j+\frac{1}{2}} \qquad (80)$$

$$\xi_4 = \frac{\Delta t\ u_{i,j}}{\Delta x} \qquad (81)$$

The coefficient ξ_1 is always positive, because $\omega > 0$. The use of the 'upwind' differences ensures, that ξ_3 and ξ_4 will always be nonnegative, because $u \geqq 0$ and $v \leqq 0$. (It can easily be shown, that if the backward and forward differences connected with the convective terms were interchanged, the corresponding coefficient ξ_4 becomes negative in the major part of the flow field, and the corresponding finite-difference equation is unconditionally unstable.) We can see also, that

$$\xi_2 = 1 - (\xi_1 + \xi_3 + \xi_4) \qquad (82)$$

so that the condition (77) is always fulfilled. The only remaining condition is that ξ_2 be nonnegative. This can be achieved by suitably adjusting Δt, so that

$$\Delta t \left\{ \frac{1}{(\Delta y)^2} \left[\omega_{i,j+\frac{1}{2}} + \omega_{i,j-\frac{1}{2}} \right] + \frac{u_{i,j}}{\Delta x} + \frac{|v_{i,j}|}{\Delta y} \right\} \leq 1 \qquad (83)$$

This condition must be satisfied at all grid points. In a similar way, we obtain for equation (64) the stability criterion

$$\Delta t \left\{ \frac{1}{(\Delta y)^2} \left[2K_1 + K_2 \left(\omega_{i,j+\frac{1}{2}} + \omega_{i,j-\frac{1}{2}} \right) \right] + \frac{u_{i,j}}{\Delta x} + \frac{|v_{i,j}|}{\Delta y} \right\} \leq 1 \qquad (84)$$

The stability analysis for equation (69) is somewhat more complicated because of the last two terms. Richtmyer & Morton /189/ investigated a similar problem and came to the conclusion, that the stability is practically unaffected by such low-order terms. Therefore, it seems to be justifiable to neglect these two terms, and in such a case the stability criterion for equation (69) is identical with the condition (84).

The permissible time step shall be determined by only one of the criteria (83) and (84), depending upon the magnitude of K_1 and K_2. Naturally, the shorter time step must be taken. From the time step limitations and especially from the dependence upon the square of Δy follows, that we are usually faced with a Scylla and Charybda situation, namely accuracy versus economy. It is evident from the stability criteria (83) and (84), that a finer mesh size (higher accuracy) is associated with a shorter permissible time step (longer computing time), and vice versa. It may sometimes be difficult to achieve sufficient accuracy together with acceptable computing times (and costs, of course).

Another important property of a finite-difference scheme is its convergence. A finite-difference equation is convergent, if with successive refinements of the mesh size the exact solution of the finite-difference equation approaches more and more closely the exact solution of the approximated partial differential equation, i.e. the discretization error is monotonously decreasing. The analysis of convergence is again very complicated. Rigorous analysis of this problem is available for linear equations only, and in the lack of anything better, it is applied heuristically also to nonlinear problems. Lax & Richtmyer /185/ investigated relations between consistency, stability, and convergence of

linear finite-difference problems, using Banach spaces. The result of these investigations is known as the Lax's Equivalence Theorem (see Richtmyer & Morton /189/) : 'Given a properly posed initial--value problem and a finite-difference approximation to it that satisfies the consistency condition, stability is the necessary and sufficient condition for convergence.' Physical problems are normally properly posed and consistent in the sense of this theorem. Therefore, convergence and stability are equivalent in our case, and satisfaction of the stability criteria (83) and (84) also ensures convergence.

5.5 Calculation of Wall Gradients and Nusselt Numbers

The most important results of our calculations will be heat transfer coefficients, which are evaluated by means of the non-dimensional Nusselt number

$$Nu_x = \frac{h\,x}{k} \tag{85}$$

Heat flux at the wall can be expressed either by the heat transfer coefficient

$$q_w = h\,(T_w - T_f) \tag{86}$$

or by temperature gradient at the wall

$$q_w = -k\left(\frac{\partial T}{\partial y}\right)_w \tag{87}$$

From equations (85-87), we have

$$Nu_x = -\frac{\left(\frac{\partial T}{\partial y}\right)_w \; x}{T_w - T_f} \tag{88}$$

It is obvious, that the evaluation of the temperature gradient at the wall is a necessary step before calculating the Nusselt number from equation (88). Temperature values are known at the grid points only, and for this reason a numerical differentiation formula must be employed. There is a sufficient number of such formulae to select from (see e.g. /160/ or /184/), and the four-point Lagrangian formula

$$\left(\frac{\partial T}{\partial y}\right)_w \doteq \frac{1}{6\,\Delta y}\left(-11\,T_1 + 18\,T_2 - 9\,T_3 + 2\,T_4\right) \tag{89}$$

was applied here. The knowledge of the wall friction

$$\tau_w = \mu \left(\frac{\partial u}{\partial y}\right)_w \qquad (90)$$

is not especially important in natural convection problems, but it shall also be evaluated in our calculations. For this purpose, the three-point Lagrangian formula

$$\left(\frac{\partial u}{\partial y}\right)_w \doteq \frac{1}{2\Delta y}\left(-3u_1 + 4u_2 - u_3\right) \qquad (91)$$

shall be used to evaluate the velocity gradient at the wall.

From the equation (88) together with equation (89) the local values of Nusselt number can be calculated at all stations along the wall. The overall Nusselt number for the entire wall is

$$Nu_L = \int_0^L \frac{Nu_x}{x}\, dx \qquad (92)$$

and as Nu_x is known at discrete points only, a numerical formula must be employed again. In this case, the five-point closed Newton-Cotes formula (sometimes called Boole's rule, see /180/)

$$\int_{x_0}^{x_4} \phi(x)\, dx \doteq \frac{2\Delta x}{45}\left(7\phi_0 + 32\phi_1 + 12\phi_2 + 32\phi_3 + 7\phi_4\right) \qquad (93)$$

was chosen. This formula is applied consecutively along the entire wall. The necessary condition is, of course, that the number of intervals be divisible by four.

The local Nusselt number is a function of position, and it can be assumed, that this function is of the form

$$Nu_x = a \cdot Gr_x^b \qquad (94)$$

for a constant Prandtl number. It cannot be expected, that all calculated points exactly satisfy the correlation (94). Therefore, the constants a and b must be evaluated according to an approximation method, and we shall use the least-squares criterion

$$\sum_{i=1}^{i_{max}} \left(Nu_i - a\, Gr_i^b\right)^2 \stackrel{!}{=} min. \qquad (95)$$

This formulation leads to a system of two simultaneous non-linear algebraic equations, which must be solved by iterations.

The overall Nusselt number can be then also calculated analytically from the equation (92), into which equation (94) has been inserted. After some elementary manipulations, we obtain

$$Nu_L = \frac{a}{3b} \, Gr_L^{\,b} \qquad (96)$$

5.6 Computer Programme

It is obviously impractical to solve our problem by hand calculations. A computer programme, based on the algorithm given by the equations (64-69) and incorporating the numerical techniques described in this Chapter, was written in FORTRAN IV, successfully compiled and employed for the calculations presented in the following Chapter. A short description of the programme and its listing are given in Appendix A. The programme can also be used for calculations of laminar free convection transients or as a special iterative method for calculations of steady state free convection. However, the later application of the programme cannot be recommended on the basis of economy, as convergence is very slow.

6. RESULTS OF CALCULATIONS

The calculations of complete transients are quite expensive (long computer times) and for this reason, only three transients were calculated. In this Chapter the scope of the results is described, but they will be discussed mainly in the following Chapter.

6.1 Common Features of the Calculations

The applicability of the programme was demonstrated by performing calculations for three different fluids. These fluids were dry air, water, and mercury, and they were chosen as representative for gases, liquids, and liquid metals. In all three cases, the calculations were done in a similar way and to the same extent.

The choice of a suitable combination of mesh size and time step always was the main problem. Although the stability criteria (83) and (84) were known, they could not be used beforehand, due to the lack of any a priori knowledge of the magnitude of the effective viscosity. For this reason, it was always necessary to run a number of test cases, from which the maximum permissible time step could be estimated. If a numerical instability did occur, it was always followed almost immediately by many under- and/or overflows in the calculated values, and the execution of the programme was automatically terminated by the diagnostics of the computer operating system. Therefore, no built-in safeguards in the programme itself were required.

The duration of a transient was estimated from the formula of Siegel /83/, which shall be later given here as equation (97).

For each fluid, two calculations are presented. The main calculation covers the whole duration of the transient. In this calculation, a short time step was required to satisfy the stability criteria, due to high velocity and effective viscosity values at the end of the transient. On the other hand, at the beginning of a transient the velocities and especially the effective viscosities are still quite small, and a considerably longer time step is permitted. Therefore, a control calculation for the same conditions, but with a longer time step was also carried out.

This calculation covered only a part of the transient. Its purpose was to estimate the discretization errors in the main calculation. In all three cases, the difference between the results of the two calculations was practically negligible. It was shown in this way, that the satisfaction of the stability criteria also ensured a sufficient accuracy.

The coefficients used in the turbulence model were the same in all three cases. For their values and discussion, see Section 4.5 . The value of the gravitational acceleration used in the calculations was $g = 980,665$ cm/s .

The results of a calculation were obtained in the form of computer printout and plotter drawings. The curves produced by the plotter show in the case of the main calculations the development of temperature, vertical velocity component, and effective viscosity profiles in the middle, three quarters and at the upper end of the plate. Moreover, drawings of the overall Nusselt number as a function of time and of a steady state heat transfer group as a function of the position along the plate also were produced. In the case of the control calculations, only the development of temperature and vertical velocity component profiles at the upper end of the plate is shown here. All these curves are presented in this Chapter.

The computer printout consists of a title page, on which all data defining a problem are printed, and five pages for each time step selected for printing. The first four pages give the vertical velocity component, horizontal velocity component, temperature and effective viscosity fields, respectively. The last page contains certain local values, such as wall stresses, local Grashof numbers, local Nusselt numbers etc. The overall Nusselt number, calculated by numerical integration, is also given here. Moreover, the coefficients of the formula (94) are printed on this page. Otherwise, the printout is largely selfexplanatory. It is quite voluminous and it shall be presented therefore in the Appendix B.

In all calculations, the medium was under normal atmospheric pressure. As mentioned in Chapter 3, all properties are evaluated at the same temperature. We shall use the mean film temperature equal to the arithmetic average of T_w and T_f . The effect of the choice of another reference temperature was not investigated.

All calculations were carried out on the IBM 370/145 computer of the University of the Witwatersrand.

6.2 Dry Air

The calculations were done for a plate of the length L = 80 cm. The initial temperature was $T_w = T_f$ = 20 degC, and the wall temperature was suddenly raised to T_w = 90 degC. The corresponding Rayleigh number is Ra_L = 2,223 . 10^9 and brings us into a region for which the use of turbulent correlations usually is prescribed (see e.g. /123/ or /140/). The physical properties of dry air were taken from a table given on p. 565 of Chapman /110/. A part of the table was approximated by polynomials in the sense of least squares (see Appendix C), and these polynomials were incorporated into the computer programme. The values of physical properties, together with all other data defining the example, are given on the title page of the computer printout, presented in the Appendix B.

The grid spacing of Δx = 5 mm and Δy = 1 mm is relatively coarse, but gives sufficient accuracy. With this spacing, time step Δt = 0,0025 s must be used to ensure numerical stability during the whole transient. The duration of the transient was estimated as approximately equal to 4,2 s, according to Siegel /83/. After 4 s real time, the temperature and velocity profiles reached practically steady state, and although the development of the effective viscosity field has not been fully completed, the execution of the programme was terminated. The results at t = 4 s are regarded as the steady state in the following text.

The main calculation took 157 min. CPU (central processing unit) time on the IBM 370/145, corresponding to 4 s in real time! The control calculation covered only the first 1 s of the transient. As the velocity and effective viscosity values are much smaller at this stage than in steady state, the time step Δt = 0,005 s can be used without any danger to the numerical stability. Moreover, the boundary layer thickness also is smaller than in the later part of the transient. Therefore, the required CPU time of 14 min. was naturally much shorter than for the complete transient.

Figs. 3-11 show the development of the temperature, vertical velocity, and effective viscosity profiles at stations x = 40 , 60 , and 80 cm, respectively. The symbols on the curves represent grid points of the finite-difference scheme. The points are relatively sparse and for this reason the curves in between them were interpolated by Lagrange polynomials (see e.g. /179/). A part of the corresponding computer printout is given in the Appendix B.

DRY AIR PR = 0.70179 GR(X) = 0.39597×10^9 STATION X = 40.00 CM

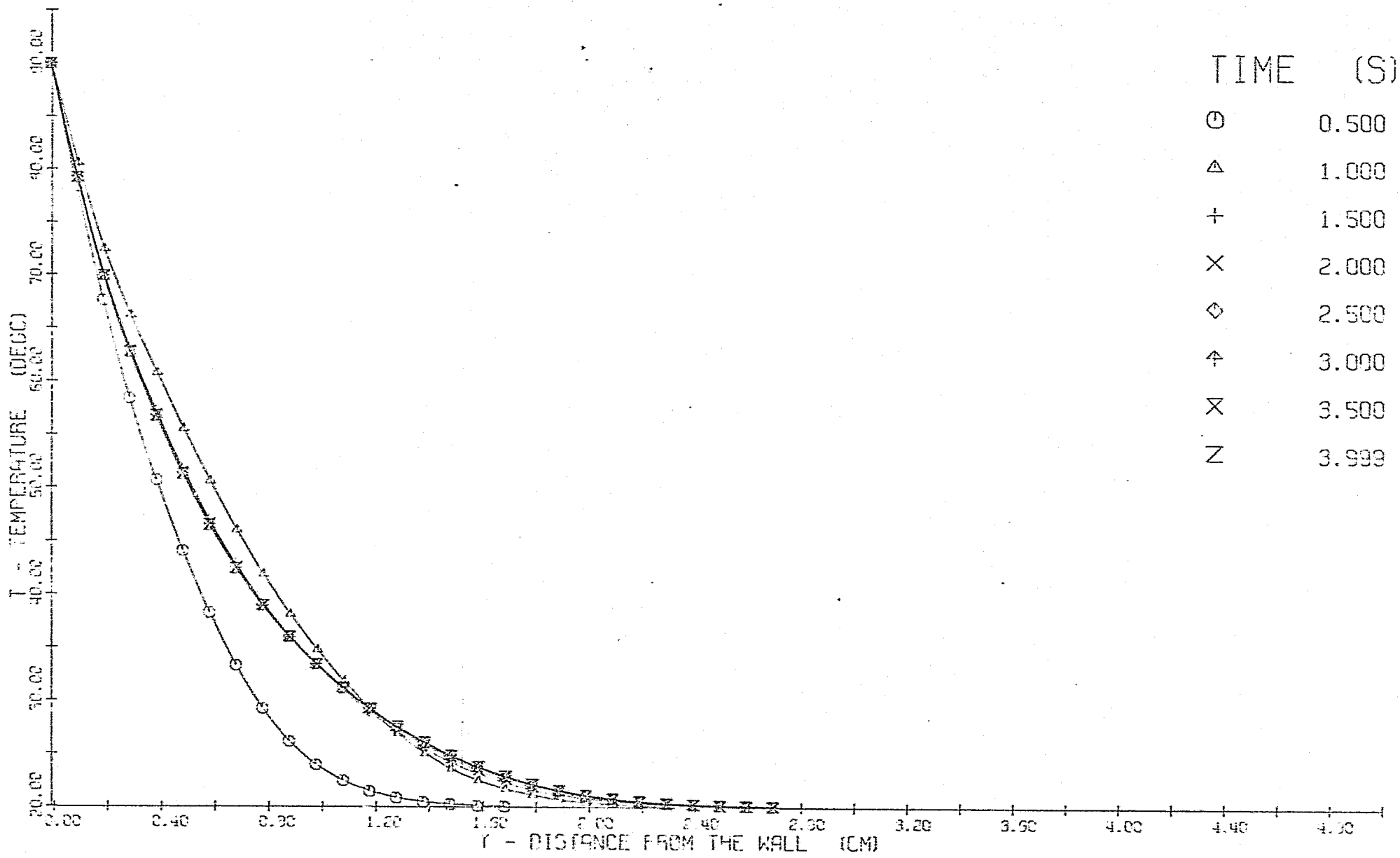

TIME	(S)
⊙	0.500
△	1.000
+	1.500
×	2.000
◇	2.500
⊕	3.000
⊠	3.500
Z	3.999

FIG. 3. TEMPERATURE PROFILES IN AIR AT x/L = 0,50

DRY AIR PR = 0.70179 GR(X) = 0.39597×10^9 STATION X = 40.00 CM

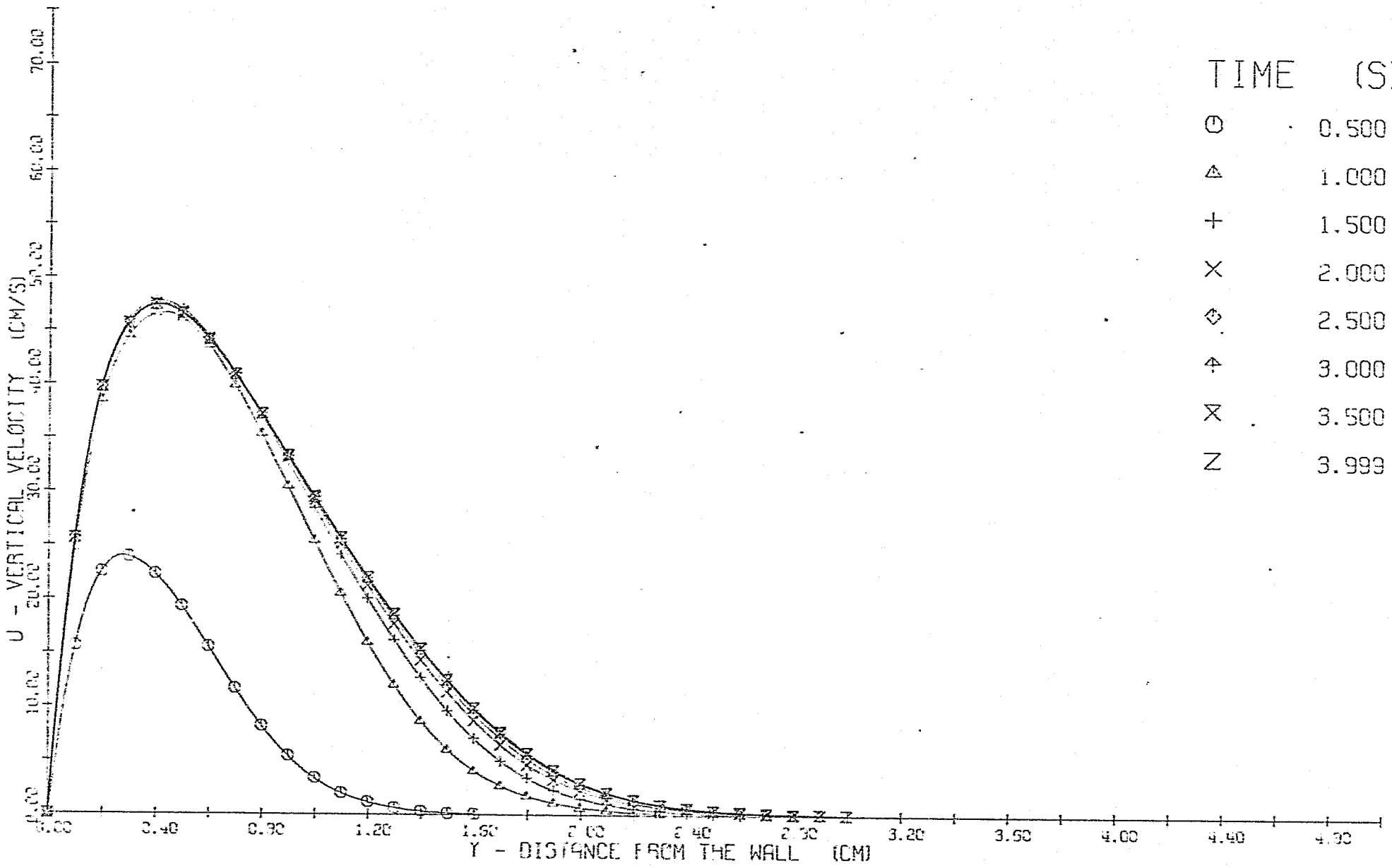

FIG. 4. VELOCITY PROFILES IN AIR AT x/L = 0,50

DRY AIR PR = 0.70179 GR(X) = 0.39597×10^{9} STATION X = 40.00 CM

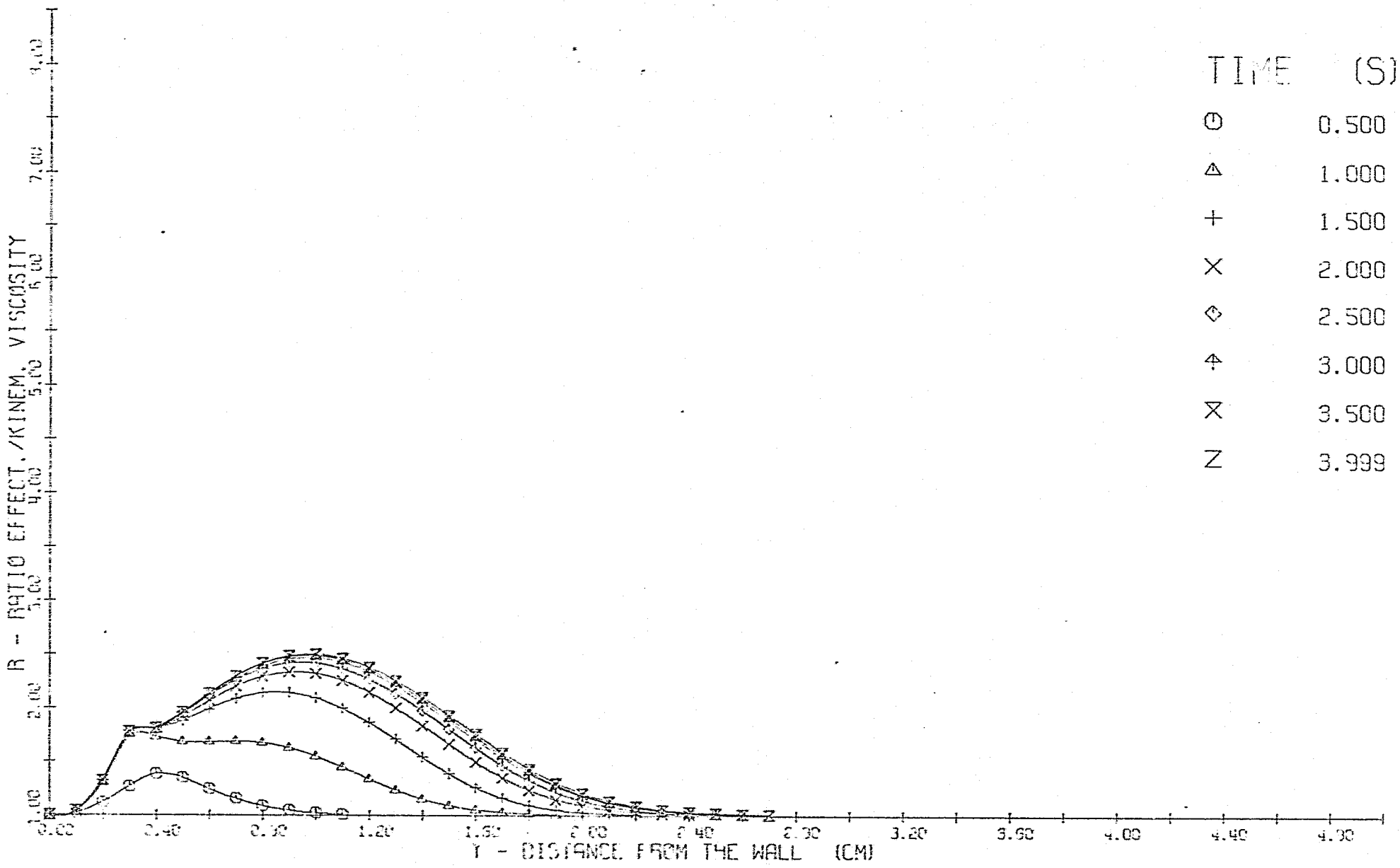

FIG. 5. EFFECTIVE VISCOSITY PROFILES IN AIR AT $x/L = 0,50$

DRY AIR PR = 0.70179 GR(X) = 1.33639×10^9 STATION X = 60.00 CM

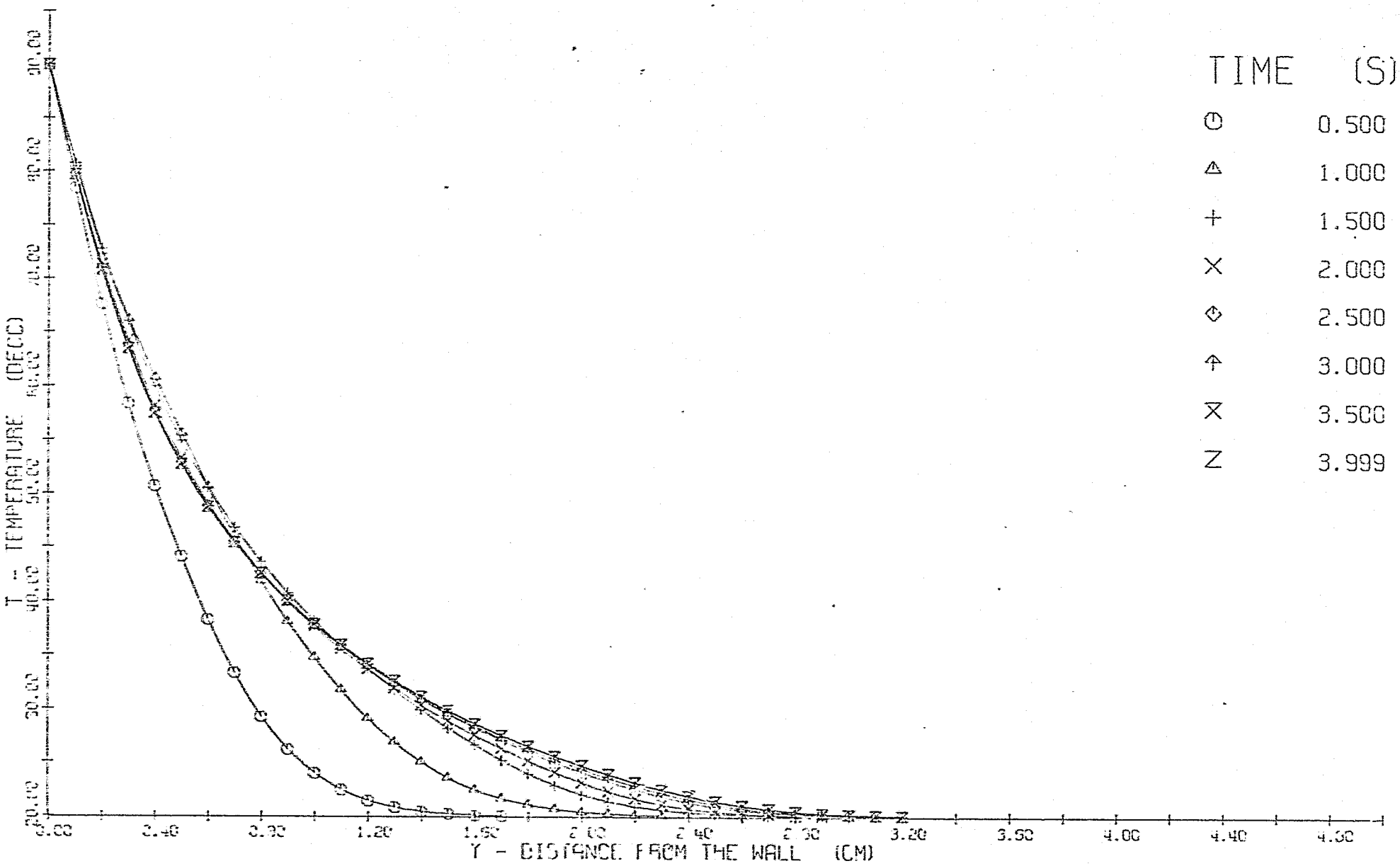

TIME (S)

⊙	0.500
△	1.000
+	1.500
×	2.000
◇	2.500
⊕	3.000
⊠	3.500
Z	3.999

FIG. 6. TEMPERATURE PROFILES IN AIR AT $x/L = 0,75$

DRY AIR PR = 0.70179 GR(X) = 1.33639×10^9 STATION X = 60.00 CM

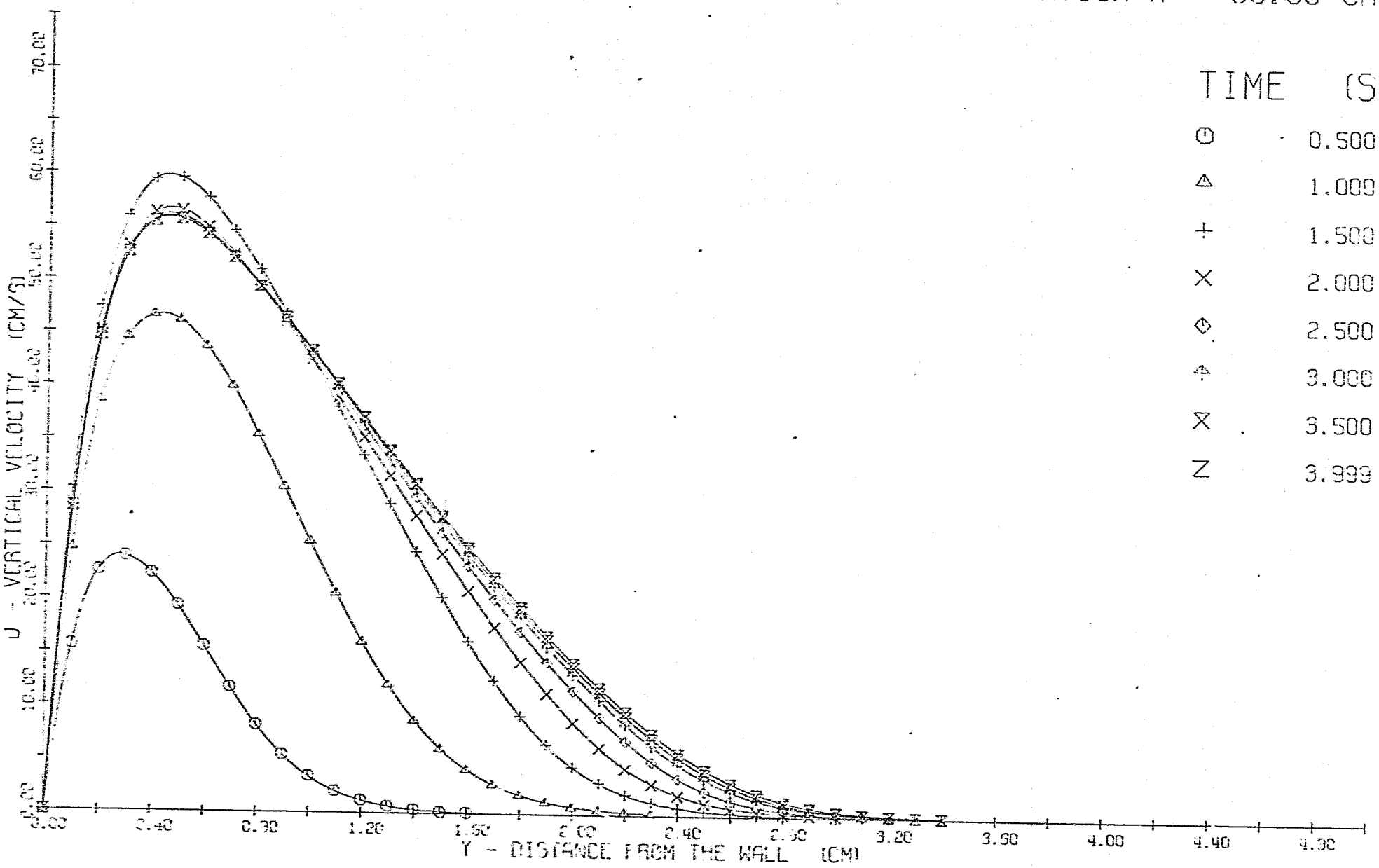

FIG. 7. VELOCITY PROFILES IN AIR AT $x/L = 0,75$

DRY AIR PR = 0.70179 GR(X) = 1.33639×10^9 STATION X = 60.00 CM

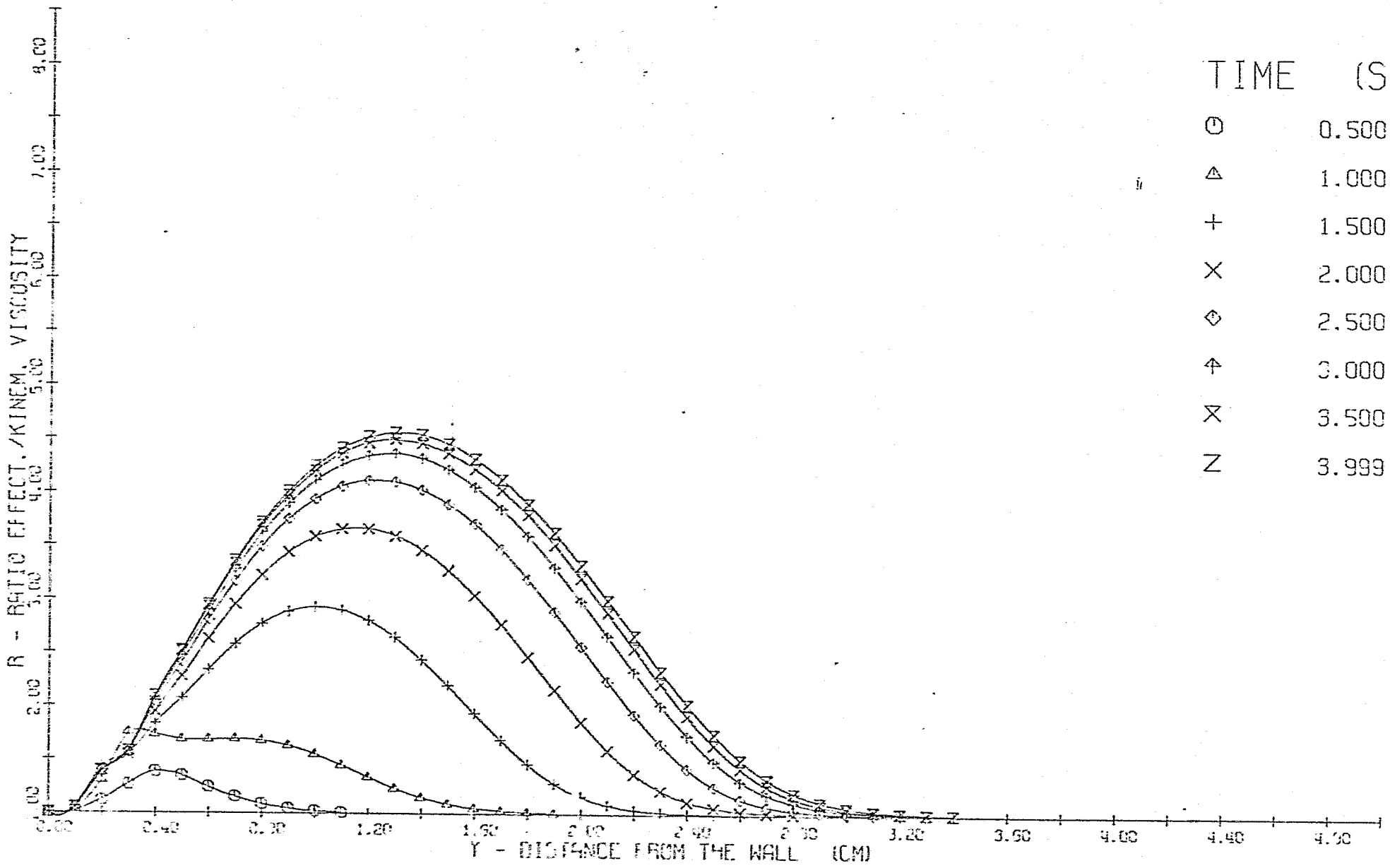

TIME	(S)
⊙	0.500
△	1.000
+	1.500
×	2.000
◇	2.500
⊕	3.000
X	3.500
Z	3.999

FIG. 8. EFFECTIVE VISCOSITY PROFILES IN AIR AT x/L = 0,75

DRY AIR PR = 0.70179 GR(X) = 3.16773×10^9 STATION X = 80.00 CM

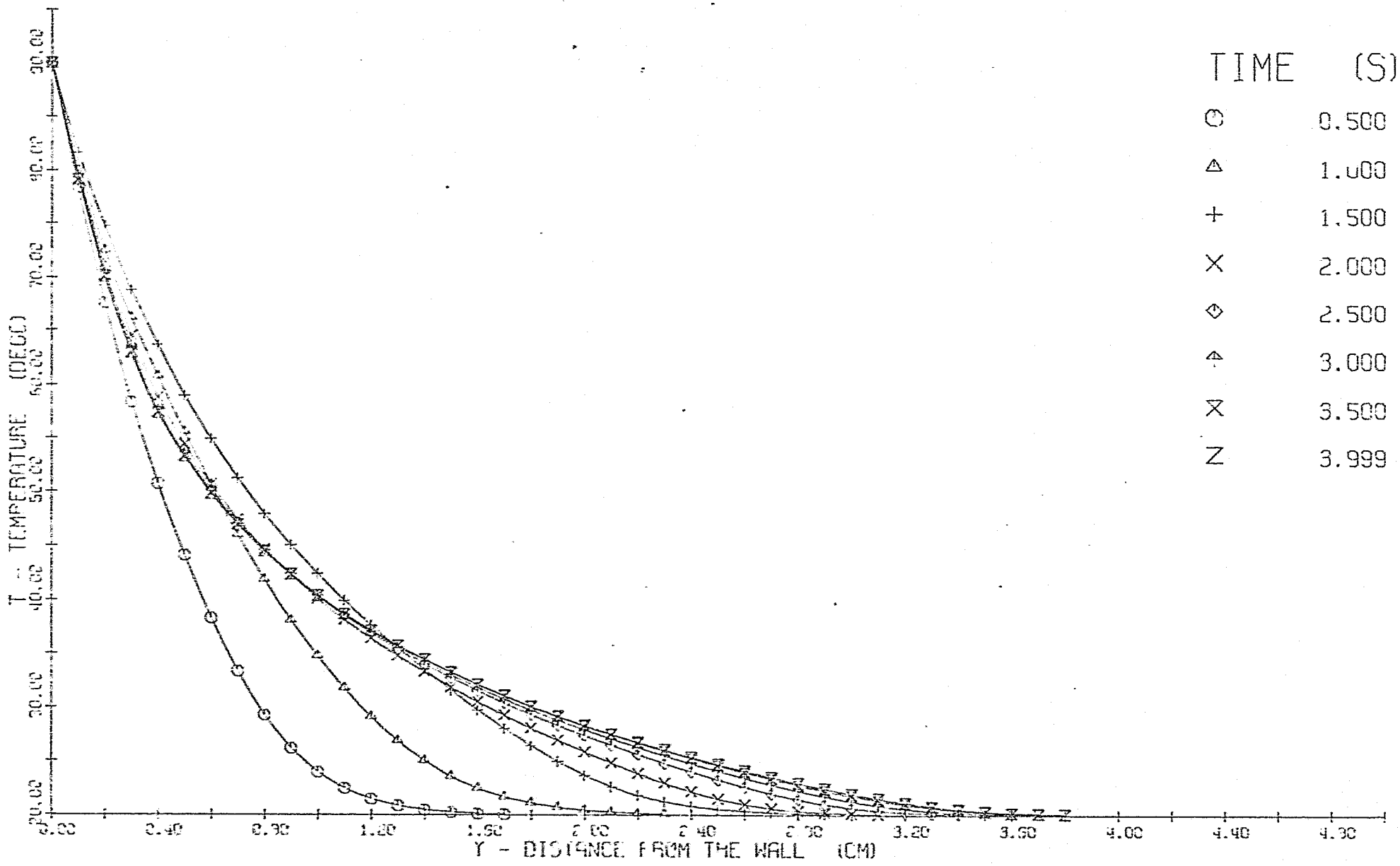

FIG.9. TEMPERATURE PROFILES IN AIR AT x/L = 1,00

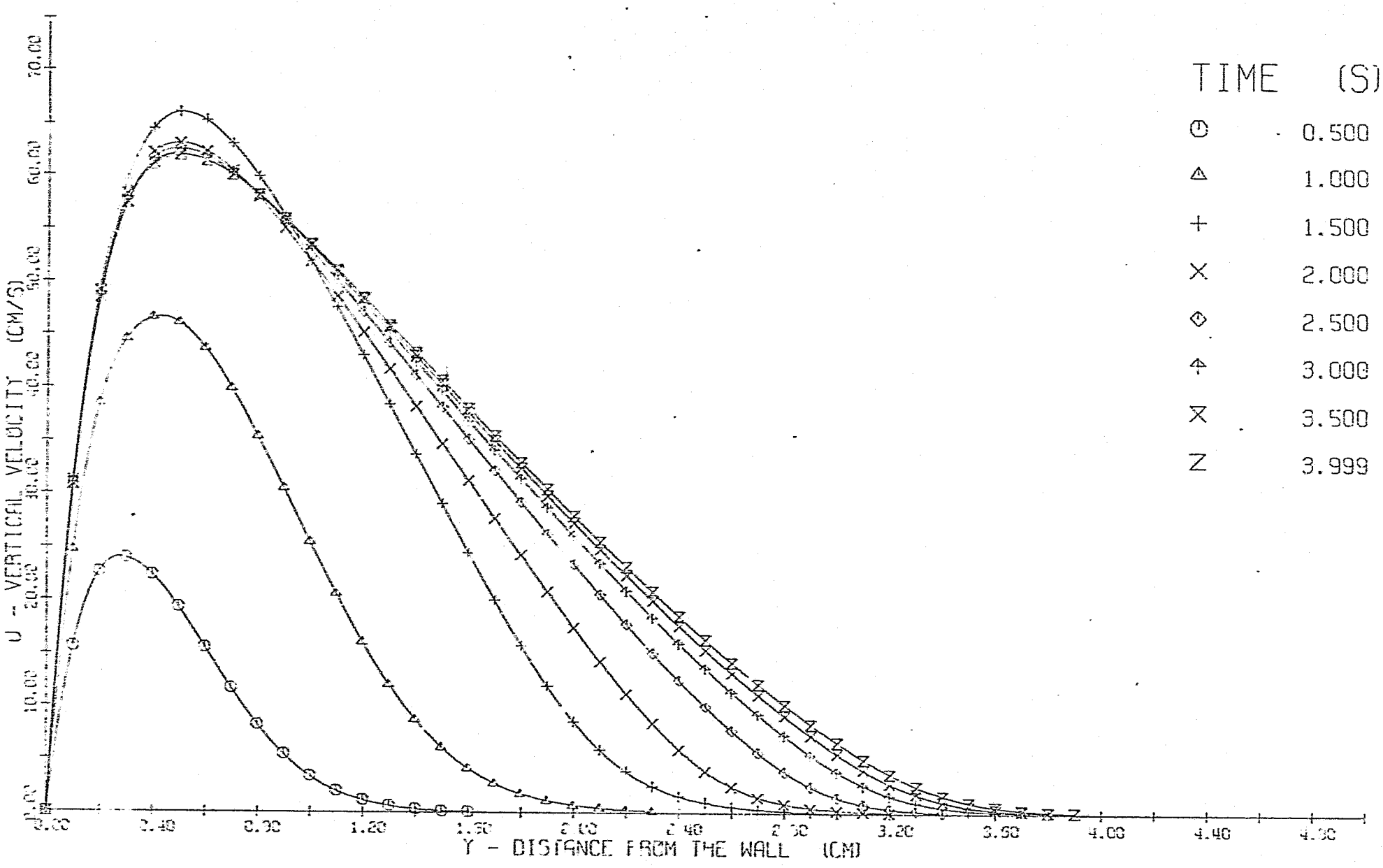

FIG. 10. VELOCITY PROFILES IN AIR AT x/L = 1,00

DRY AIR PR = 0.70179 GR(X) = 3.16773×10^9 STATION X = 80.00 CM

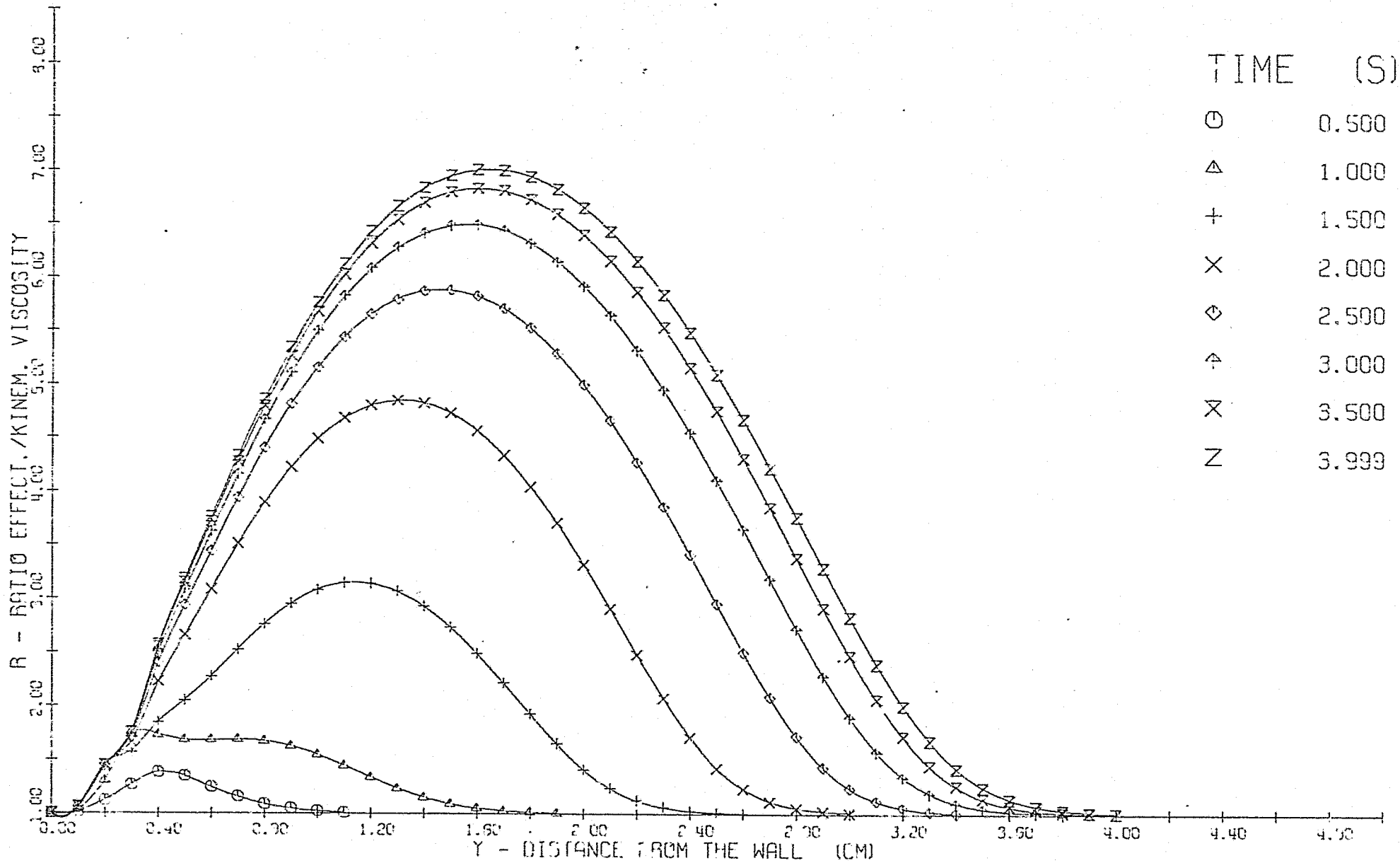

FIG. 11. EFFECTIVE VISCOSITY PROFILES IN AIR AT x/L = 1,00

The development of temperature and velocity profiles, obtained from the control calculation, is presented in Figs. 12 and 13 for the upper end of the plate only.

As expected, the thicknesses of the heat and momentum boundary layers are almost equal ($Pr \sim 1$). A quite interesting feature of the curves is the flattening of the outer part of both temperature and velocity profiles and the associated decrease of the peak velocity after reaching a maximum. This behaviour is obviously connected with the onset of turbulence and the consequent increase of the effective viscosity. A similar flattening effect of turbulence had been observed in forced-convection fluid flow and heat transfer studies.

The most important engineering aspect of the present study is the question, whether neat transfer coefficient goes through a minimum before reaching its steady state value. The existence of such a minimum was indeed confirmed by our results and this so-called 'overshoot' can be clearly seen in Fig. 14, giving the overall Nusselt number as a function of time. The 'overshoot' is about 8,5 % below the steady state value in this particular case.

In Fig. 15, the local steady state Nusselt numbers along the plate are given. At the leading edge, there is a singular point, with which an infinite heat transfer coefficient is theoretically associated. This leading edge effect disturbs local heat transfer coefficients in the lower quarter of the plate. However, in the remaining part of the plate, the local Nusselt numbers are very closely approximated by a correlation of the form (94).

If the overall Nusselt number is calculated analytically from the equation (96), the value of $Nu_L = 130,95$ is obtained. This is about 7,6 % below the value resulting from the numerical integration of local values along the wall. Naturally, a complete agreement cannot be expected due to the least-squares approximation, but the main contribution to this discrepancy seems to be coming from the leading-edge effect.

As mentioned above, a further discussion of the results is postponed to the next Chapter.

6.3 Water

The length of the plate considered in this example was $L = 10$ cm. The fluid and wall temperatures were the same as in the example with air, i.e. $T_f = 20$ degC and $T_w = 90$ degC. The resulting Rayleigh number $Ra_L = 4,195 \cdot 10^9$ is sufficiently high to bring us into the

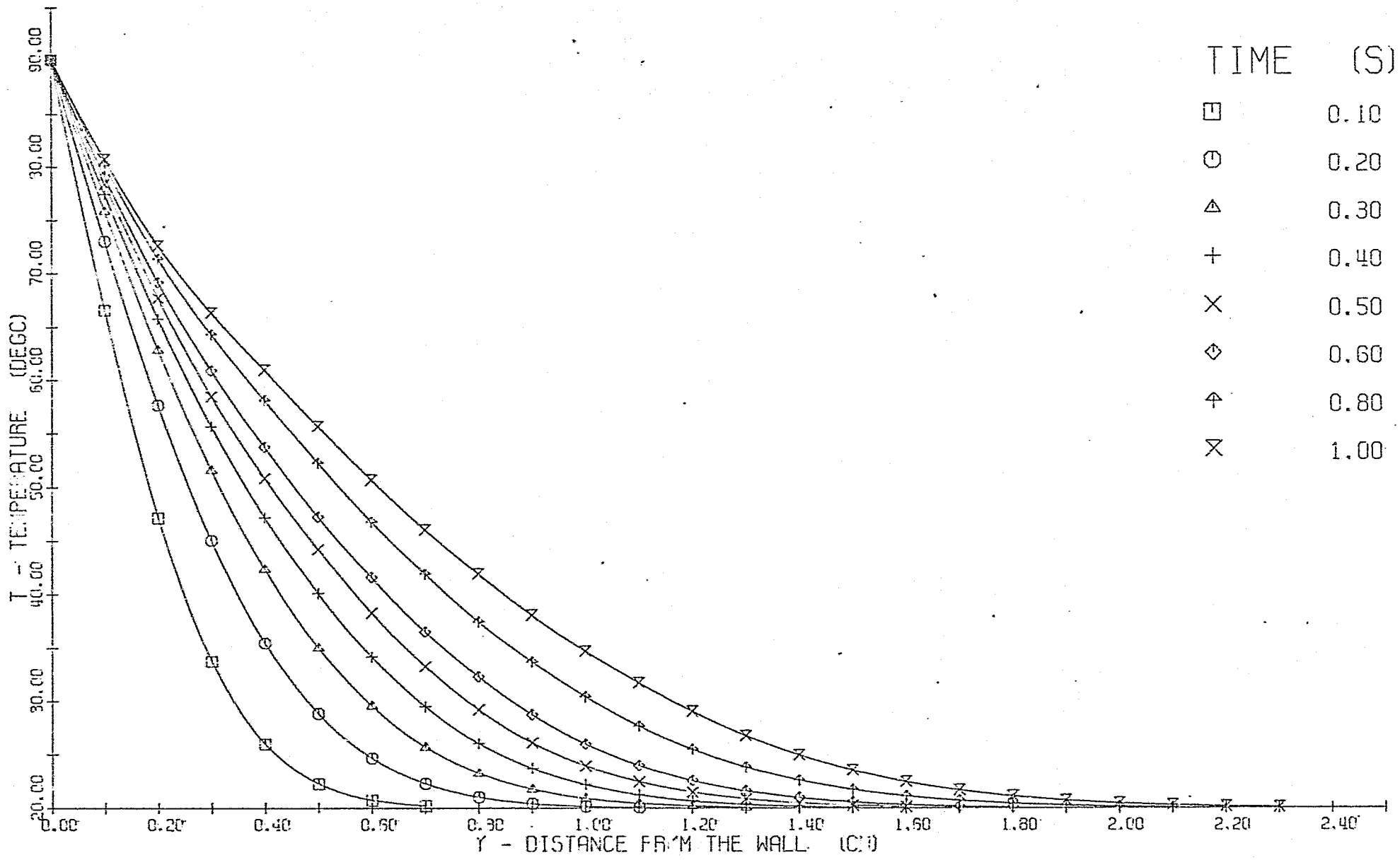

FIG. 12. TEMPERATURE PROFILES IN AIR AT x/L = 1,00 (CONTROL CALCULATION)

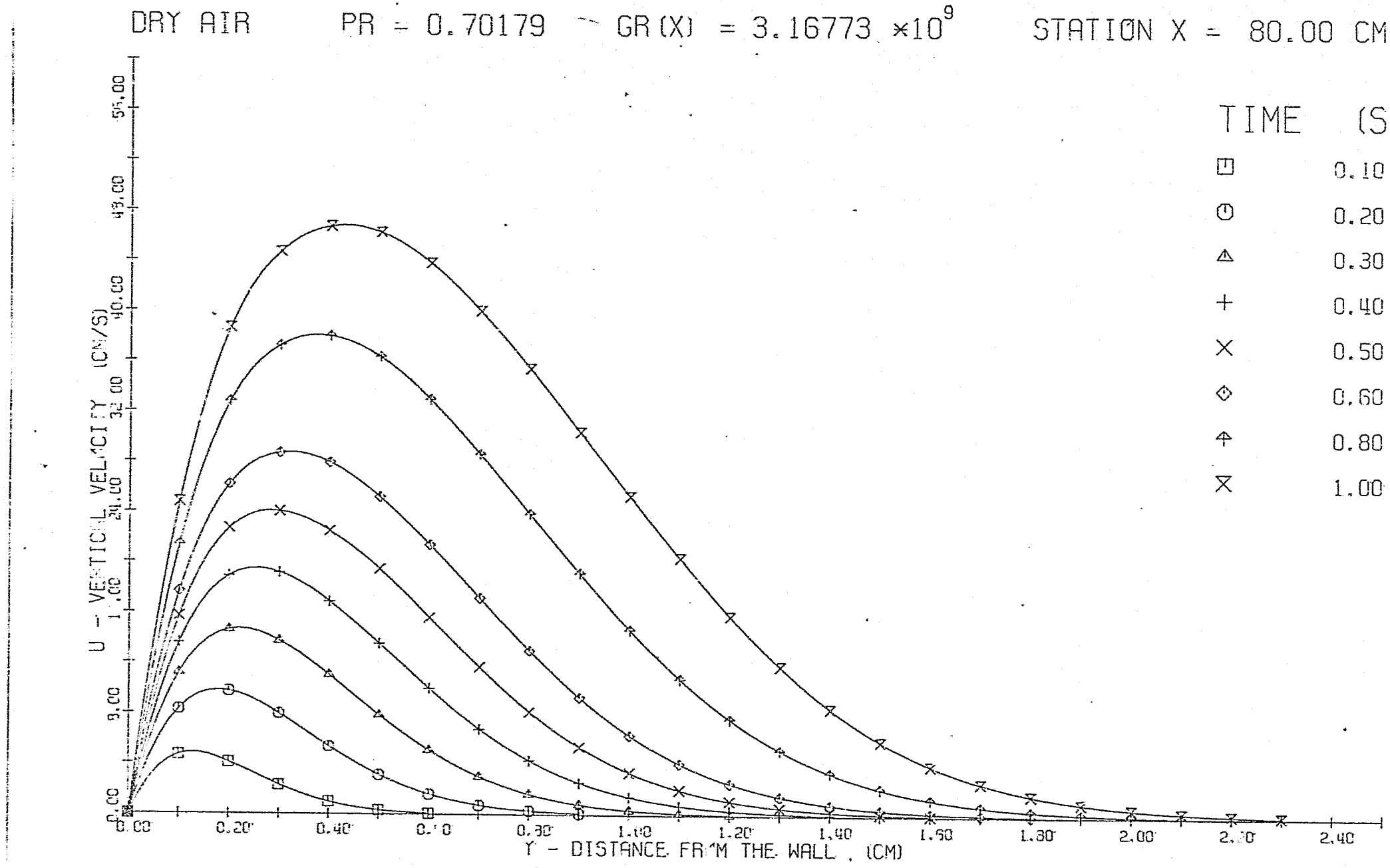

FIG. 13. VELOCITY PROFILES IN AIR AT x/L = 1,00 (CONTROL CALCULATION)

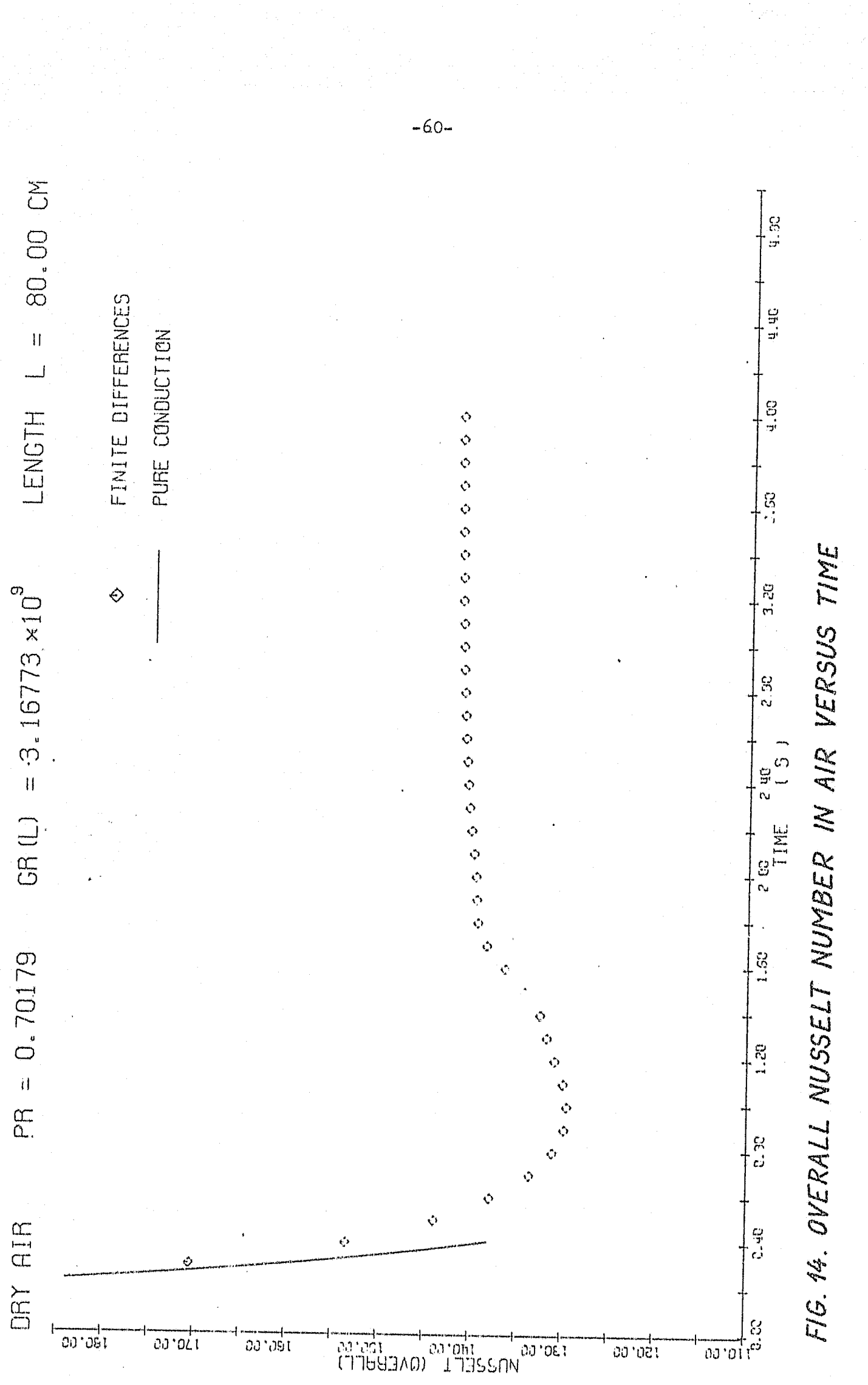

FIG. 14. OVERALL NUSSELT NUMBER IN AIR VERSUS TIME

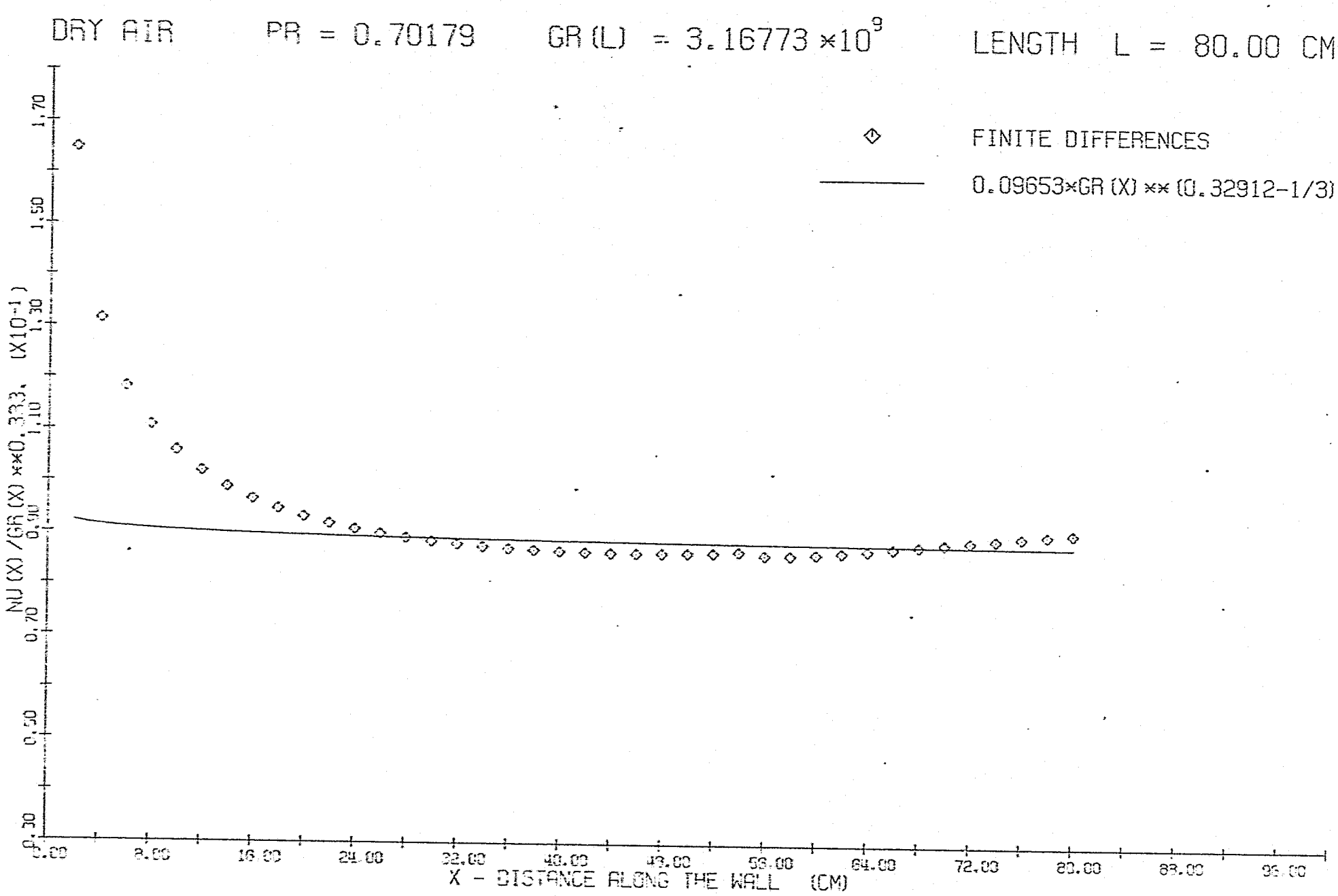

FIG. 15. STEADY STATE LOCAL HEAT TRANSFER IN AIR

region, which is usually considered to be turbulent. The physical properties were calculated in a similar way as in the case of air, but the source was this time a table given on p. 414 of Gröber et al. /123/. The evaluated properties and all other necessary data can be found on the first page of the computer printout, given in the Appendix B.

The grid spacing of Δx = 0,25 cm and Δy = 0,015 cm was chosen as suitable for this problem. The gradients of all profiles are much steeper now and therefore a much finer mesh size is required than in the case of air. The time step Δt = 0,005 s still ensures numerical stability. This doubling of the permissible time step in comparison with the case of air is rather surprising, especially in connection with the considerably refined mesh size. However, after an inspection of the stability criteria (83) and (84) it can readily be seen, that a simple explanation is the much smaller value of the kinematic viscosity of water.

The duration of this transient was again estimated according to Siegel /83/, and it was found to be approximately equal to 5,9 s. However, in order to obtain a perfect steady state, the main calculation was terminated after 8 s of real time. The required CPU time was 41 min. , which was much less than in the example with air, but still quite respectable.

The control calculation again covered the first quarter of the main calculation, i.e. in this case 2 s of real time. For reasons given in the preceding Section, a longer time step may be used. The value of Δt = 0,01 s was chosen, which means that the time step was also here doubled in comparison with the main calculation. This resulted into a much shorter CPU time of about 4 min. only.

The development of the temperature, vertical velocity, and effective viscosity profiles is shown in Figs. 16-24 at stations x = 5 , 7,5 , and 10 cm, respectively. The corresponding computer printout is given in the Appendix B. The temperature and velocity histories, Figs. 25 and 26, are the only results of the control calculation presented here.

In this case, the momentum boundary layer was somewhat thicker than the heat boundary layer. Such a result can be predicted from the Prandtl number, which is higher than one here.

A similar pattern as in the case of air can also now be observed, i.e. the 'turbulent flattening' of the profiles and a temporary maximum of the peak velocities.

WATER PR = 3.26368 GR(X) = 0.16069 $\times 10^9$ STATION X = 5.00 CM

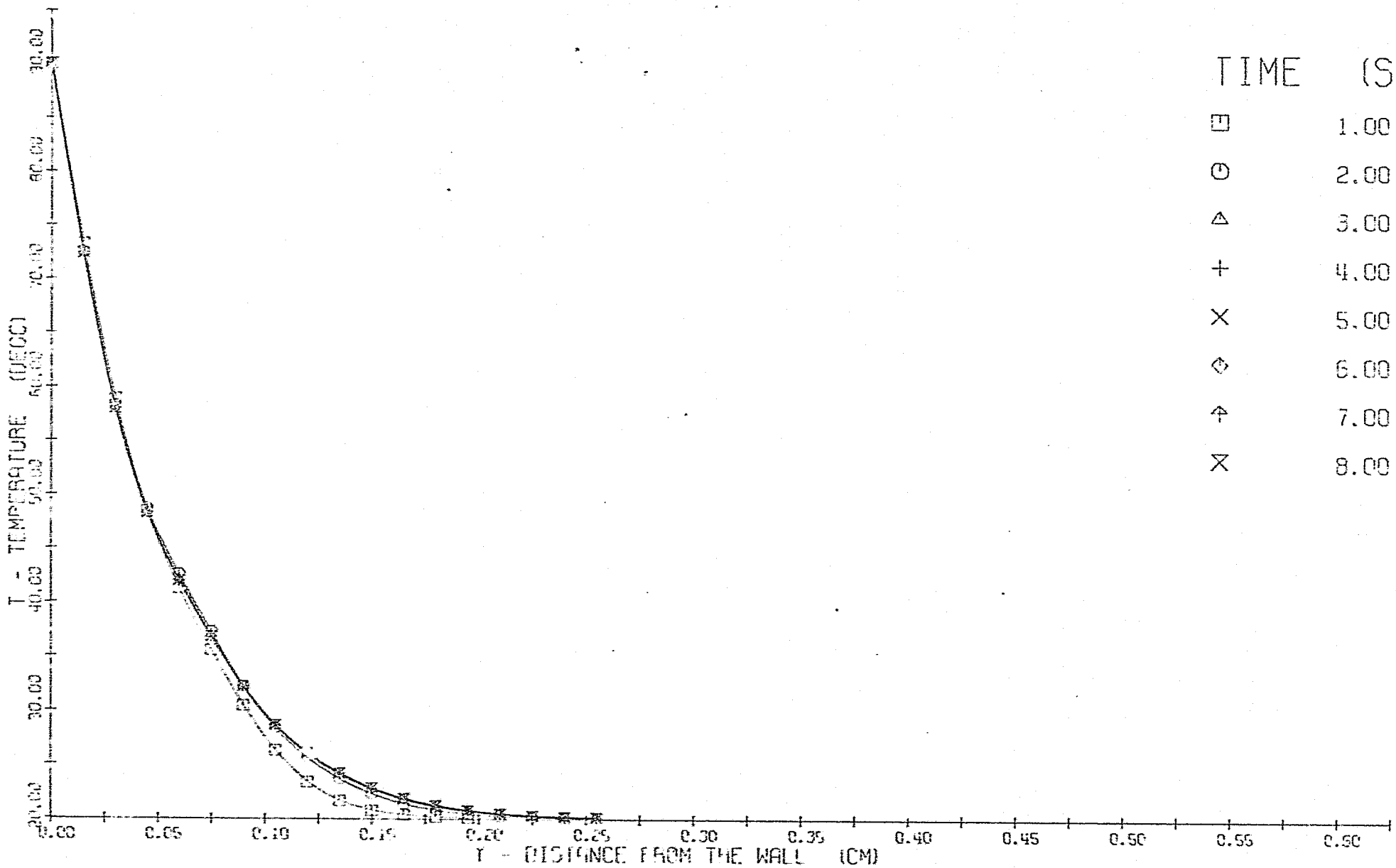

FIG. 16. TEMPERATURE PROFILES IN WATER AT x/L = 0,50

WATER PR = 3.26368 GR(X) = 0.16069 $\times 10^9$ STATION X = 5.00 CM

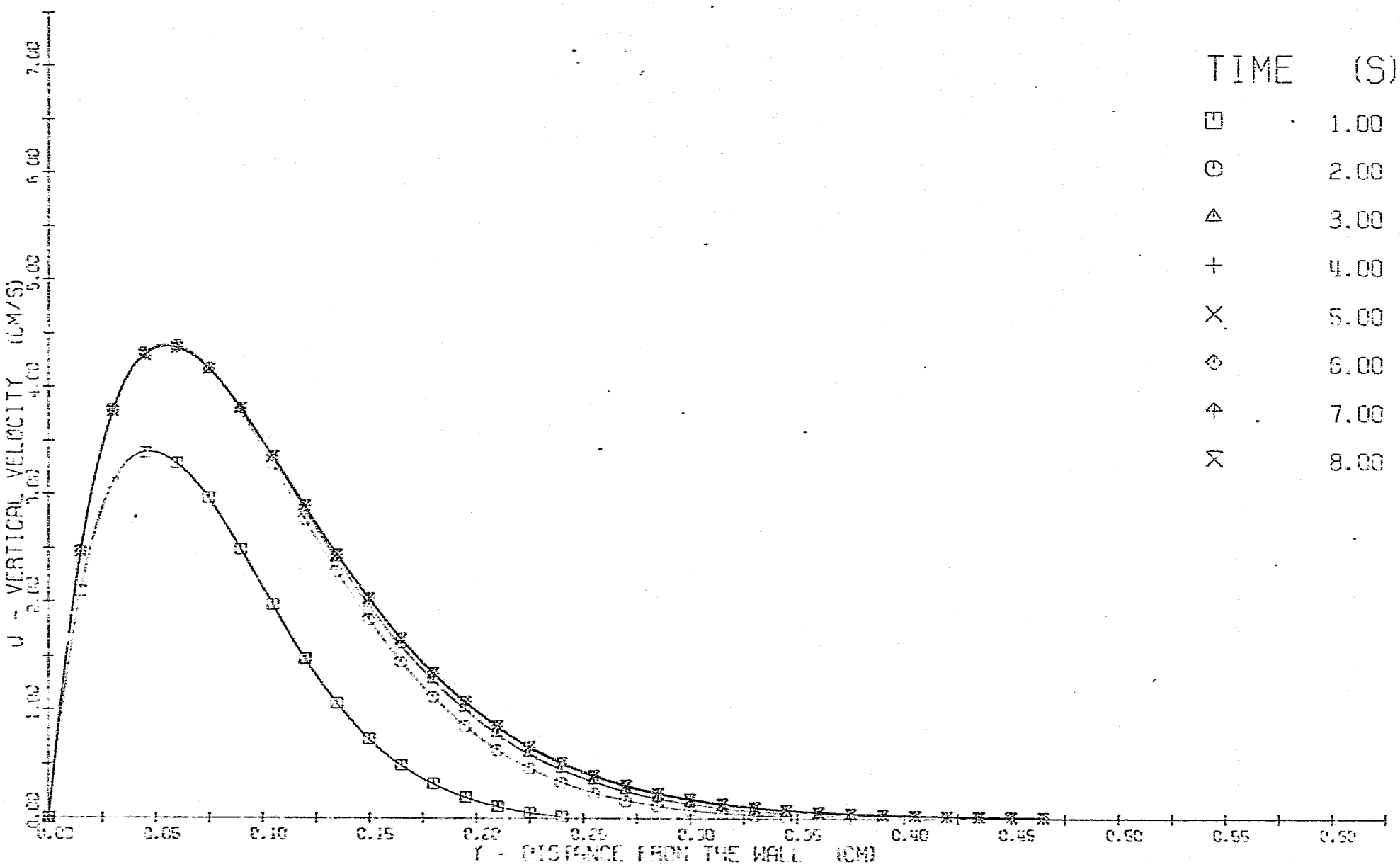

FIG. 17. VELOCITY PROFILES IN WATER AT $x/L = 0,50$

WATER PR = 3.26368 GR(X) = 0.16069 $\times 10^9$ STATION X = 5.00 CM

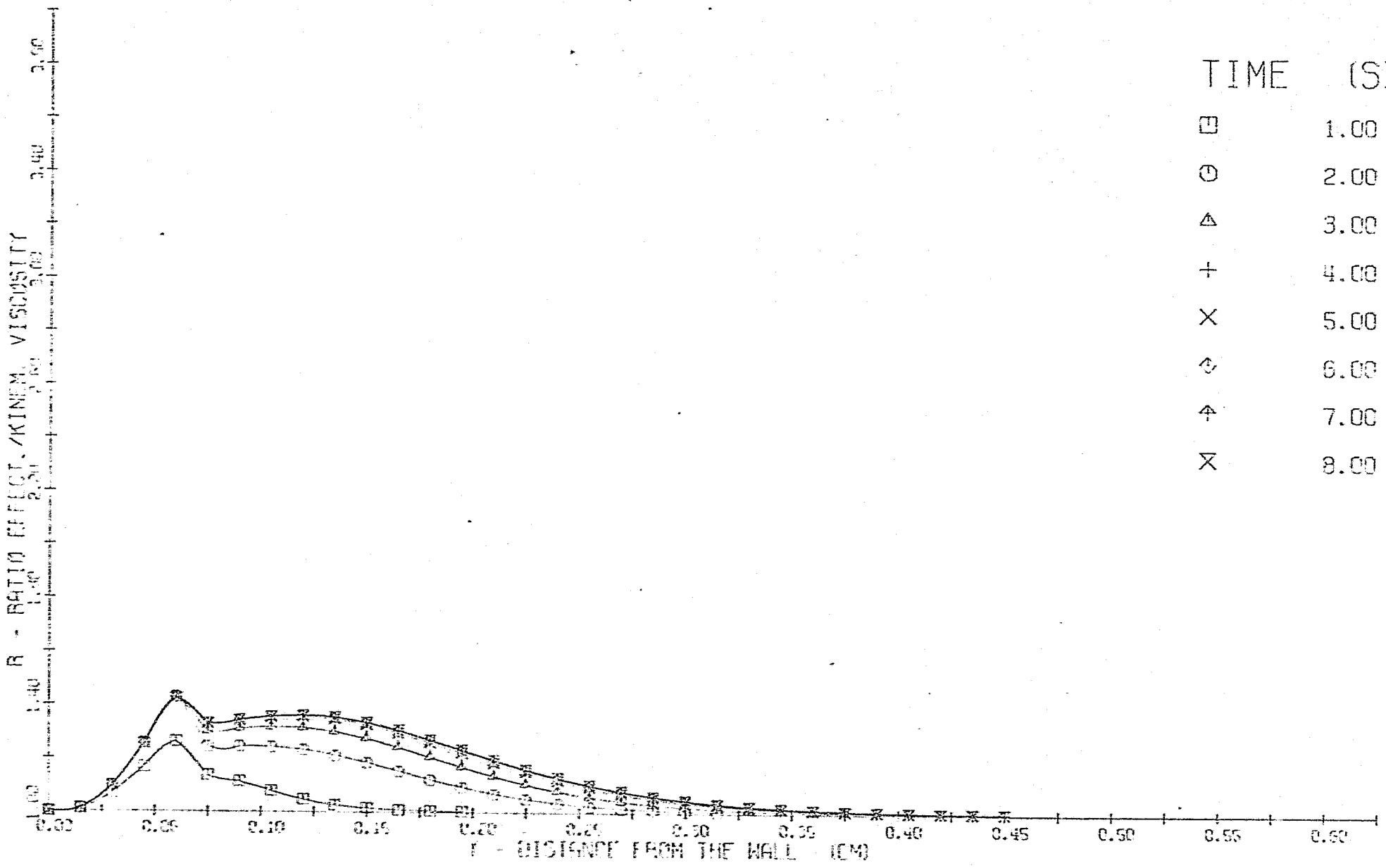

FIG. 18. EFFECTIVE VISCOSITY PROFILES IN WATER AT $x/L = 0{,}50$

WATER PR = 3.26368 GR(X) = 0.54232 $\times 10^9$ STATION X = 7.50 CM

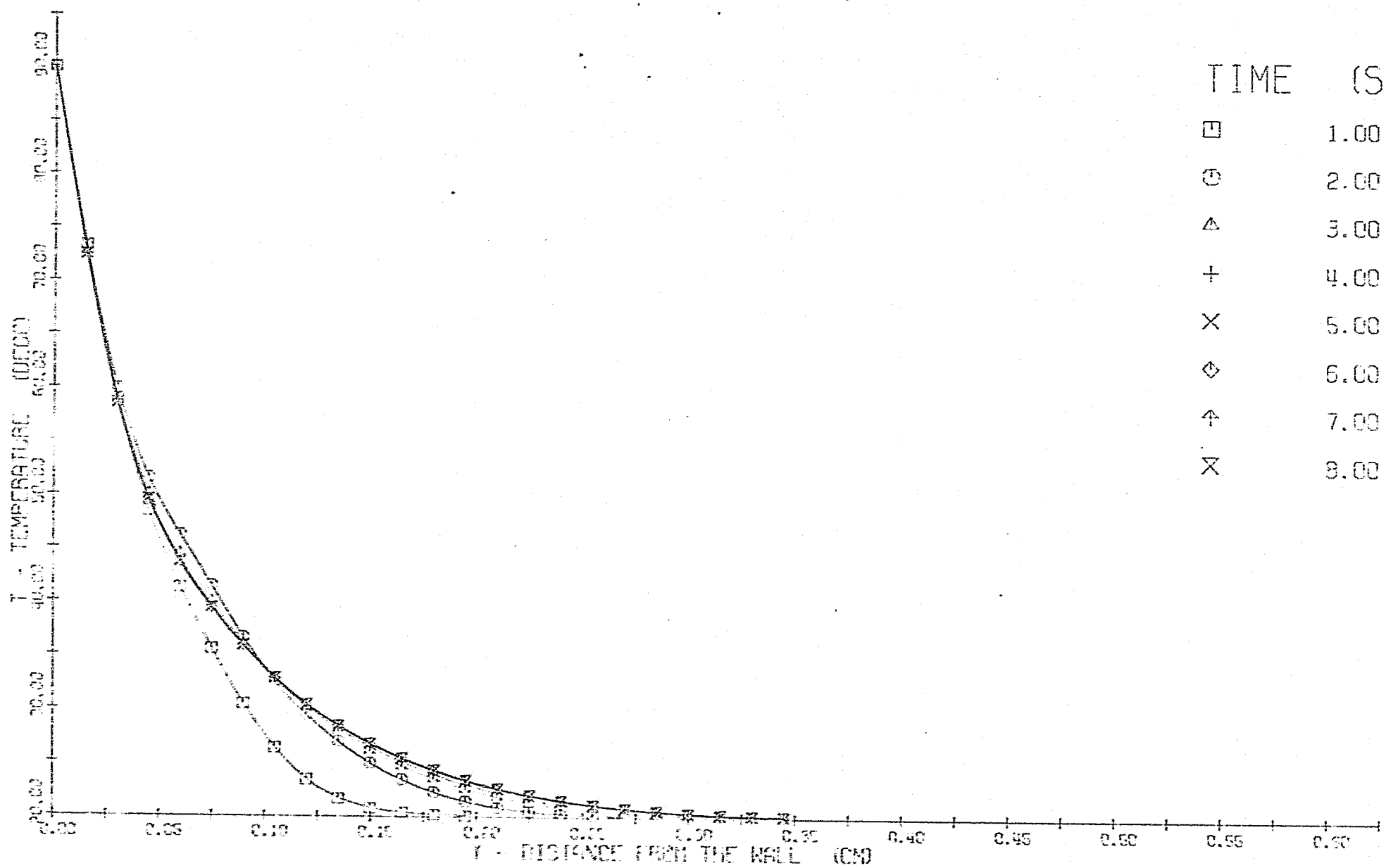

FIG. 19. TEMPERATURE PROFILES IN WATER AT $x/L = 0,75$

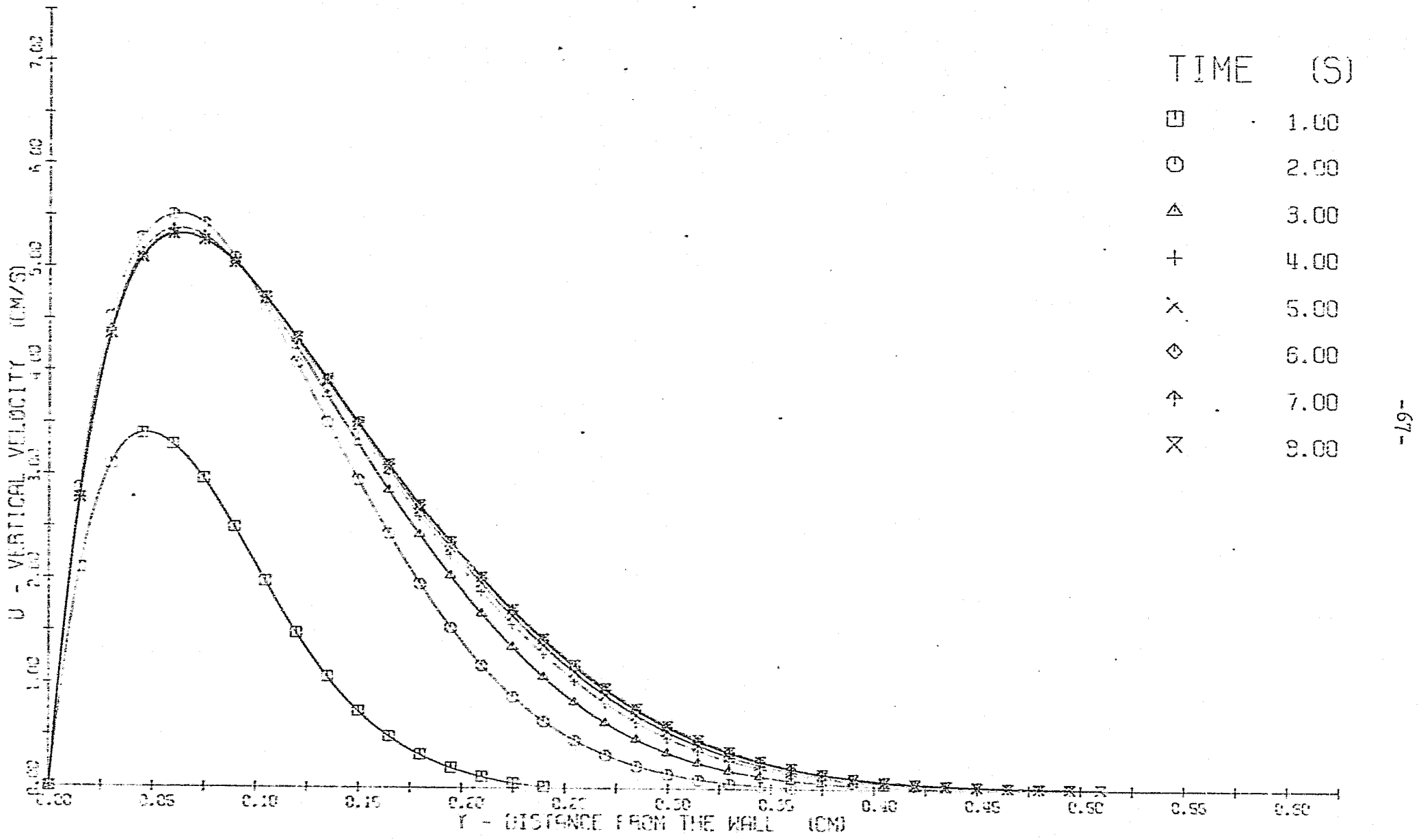

FIG. 20. VELOCITY PROFILES IN WATER AT x/L = 0,75

WATER PR = 3.26368 GR(X) = 0.54232 $\times 10^9$ STATION X = 7.50 CM

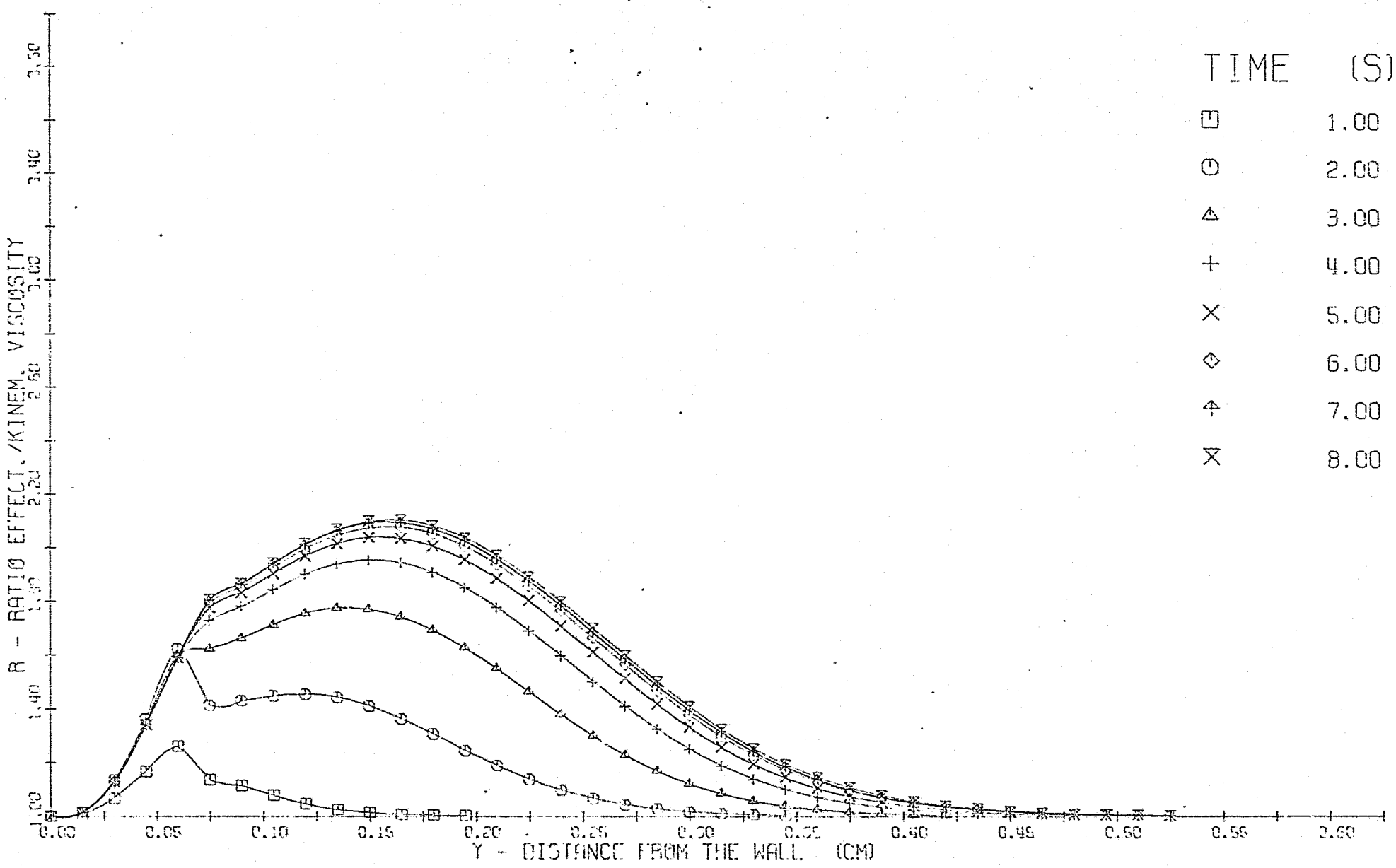

FIG. 21. EFFECTIVE VISCOSITY PROFILES IN WATER AT x/L = 0,75

WATER PR = 3.26368 GR(X) = 1.28550×10^9 STATION X = 10.00 CM

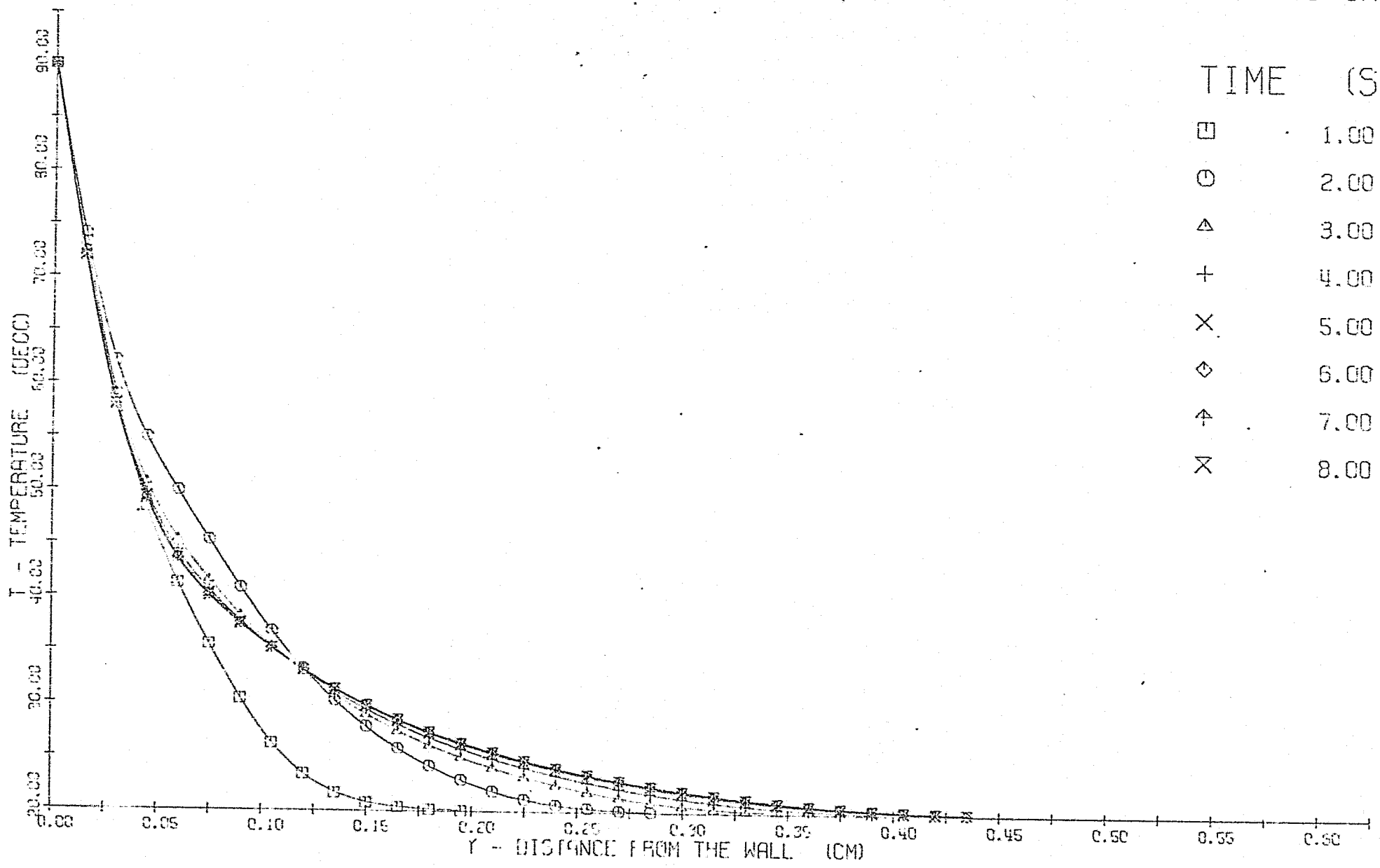

FIG. 22. TEMPERATURE PROFILES IN WATER AT $x/L = 1,00$

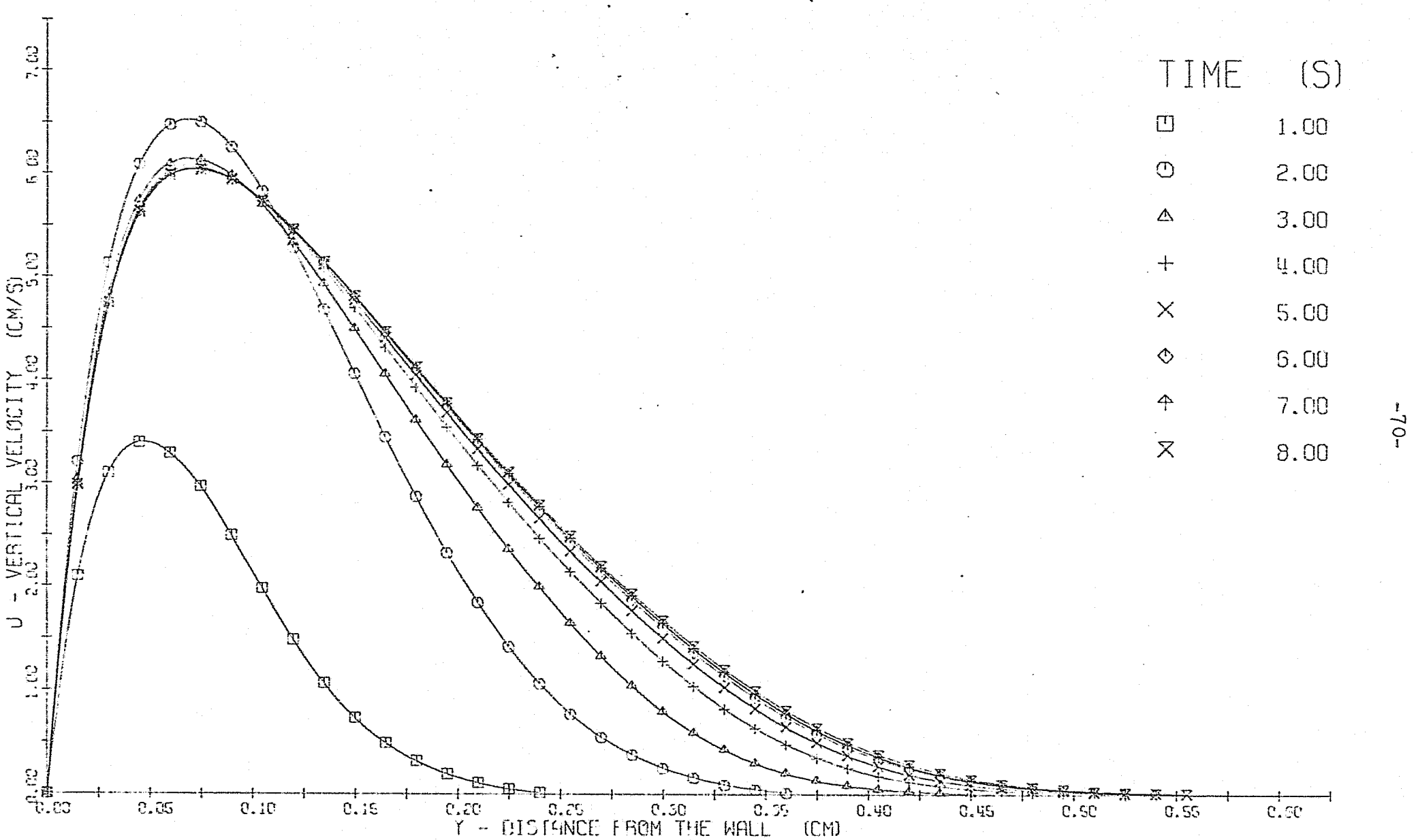

FIG. 23. VELOCITY PROFILES IN WATER AT x/L = 1,00

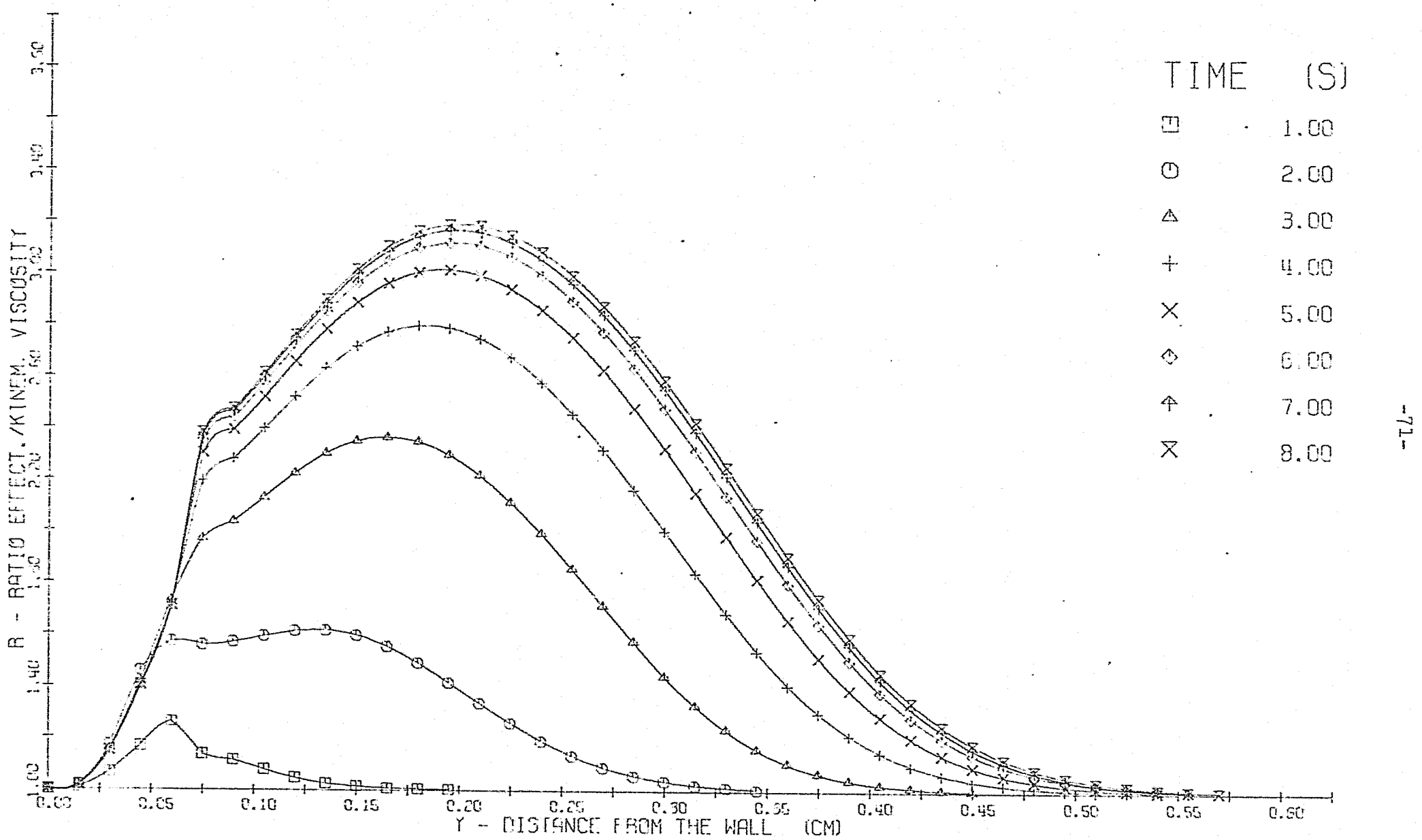

FIG. 24. EFFECTIVE VISCOSITY PROFILES IN WATER AT x/L = 1,00

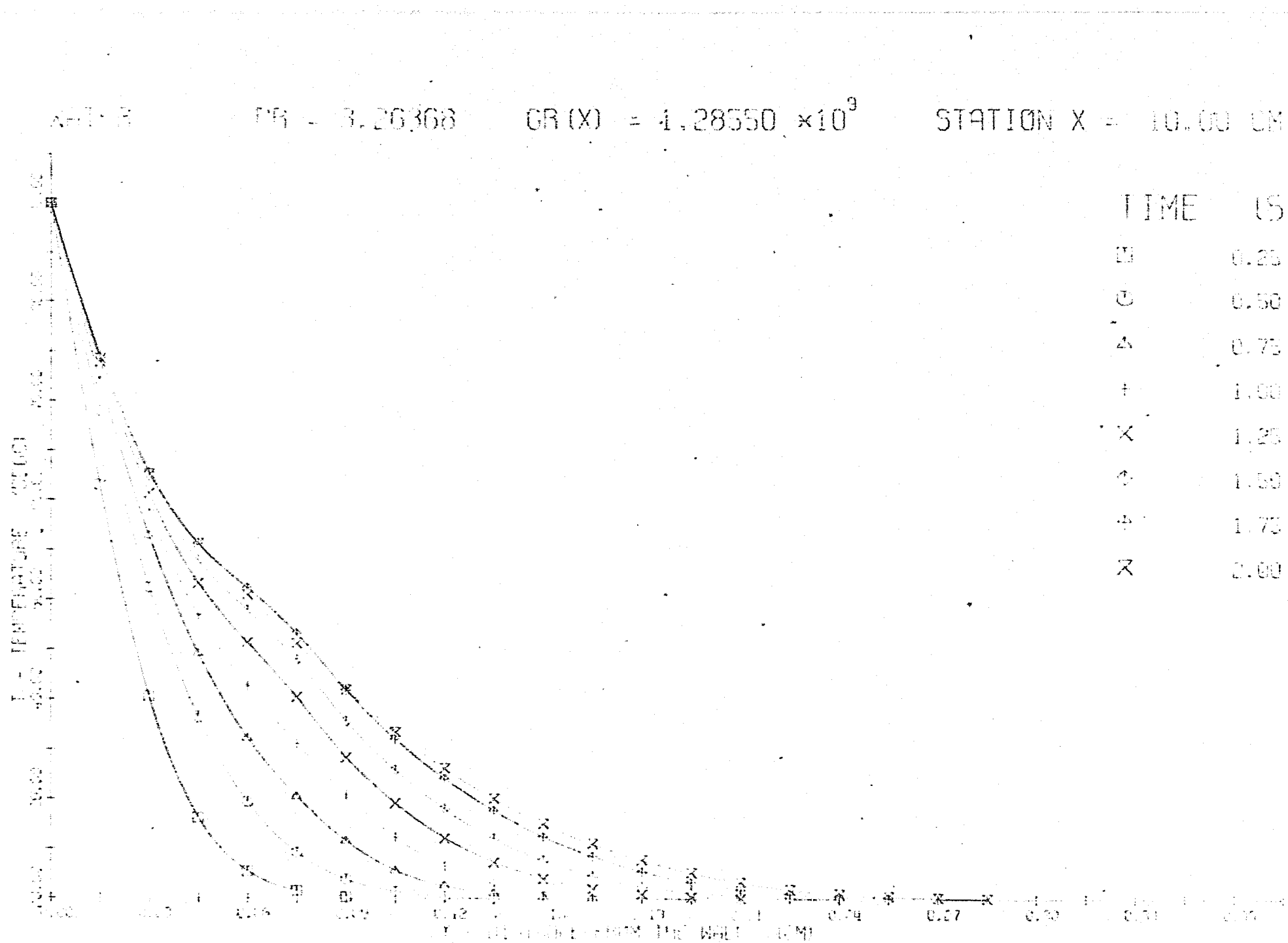

FIG. 25. TEMPERATURE PROFILES IN WATER AT x/L = 1,00 (CONTROL CALCULATION)

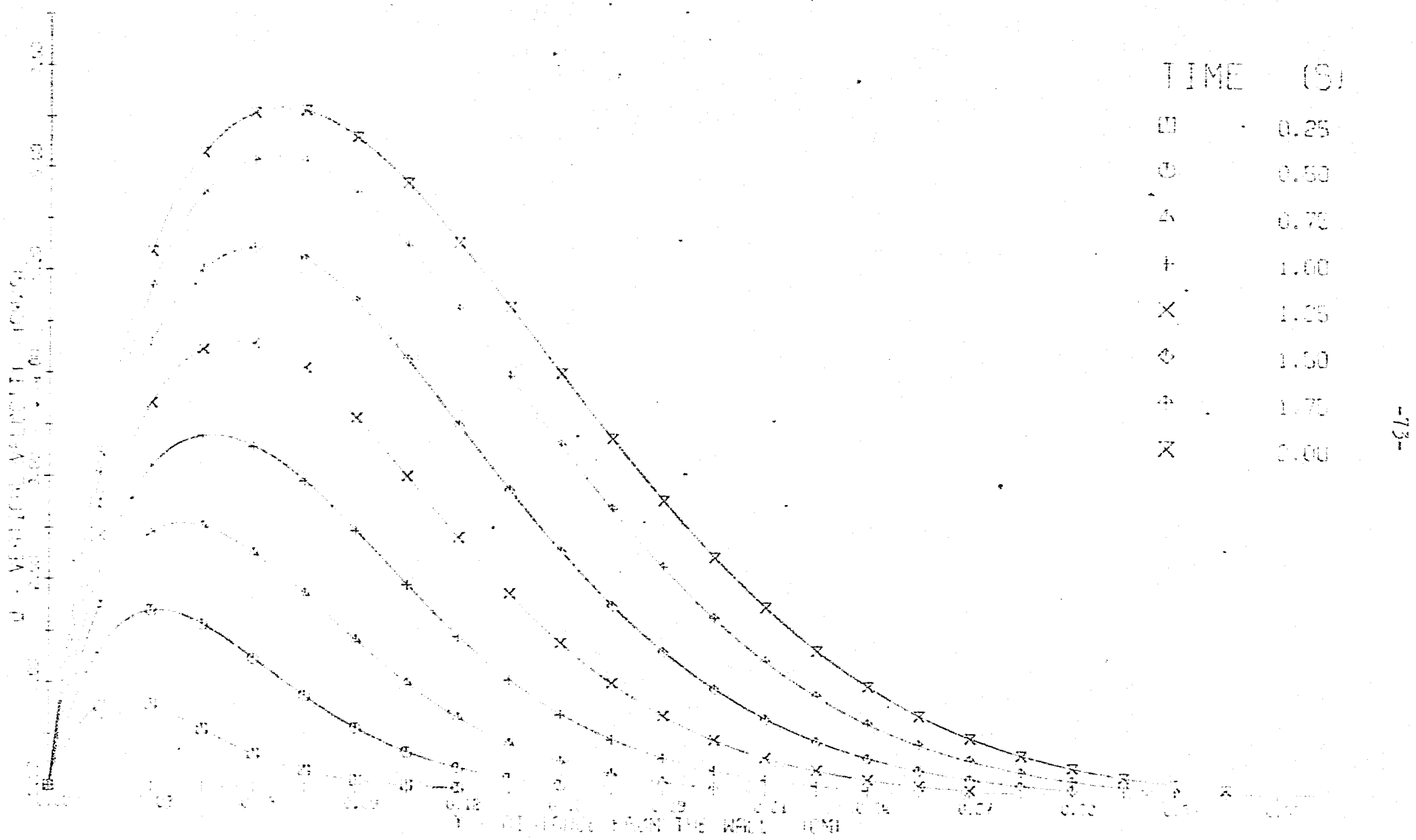

FIG. 26. VELOCITY PROFILES IN WATER AT x/L=1,00 (CONTROL CALCULATION)

Fig. 25 displays an interesting feature from the numerical--analysis point of view. The waves on the temperature profiles are the first symptoms that we are on the limits of numerical stability. And indeed, according to the stability criteria (83) and (84), the permissible time step in this situation is Δt = 0,0105 s . This is almost equal to the time step Δt = 0,01 s , which was actually used in the calculation. It can be seen, that the safety margin of the stability criteria is very small.

An 'overshoot' of the overall Nusselt number was again obtained, as shown in Fig. 27. The minimum is 6,3 % below the steady state value. The percentual difference is somewhat smaller than in the case of air.

Fig. 28 shows the local Nusselt numbers along the wall in steady state. The leading edge effect is exhibited also here and it again extends over the first quarter of the plate. Otherwise, the local Nusselt numbers are well approximated by a correlation of the form (94).

If the equation (96) is employed, the overall Nusselt number Nu_L = 163,13 is obtained. This value is about 8,3 % below the result of the numerical integration. The magnitude of this discrepancy is about the same as in the case of air and also the same comments apply here.

6.4 Mercury

After satisfactory results had been obtained for air and water, it was attempted to produce some results also for liquid metals. This attempt was quite questionable, as certain assumptions in the derivation of our basic equations could possibly exclude liquid metals from the range of applicability of our method. Mercury was chosen from this group of fluids for the study.

The length of the plate was selected as L = 12 cm . In this case, the initial equilibrium temperature was $T_w = T_f$ = 0 degC, and the wall temperature was suddenly raised to T_w = 40 degC. The corresponding Rayleigh number is Ra_L = 2,527 . 10^9, i.e. sufficiently high to require the application of turbulent formulae. The physical properties are a part of the input data in this case, and they were taken from a table given on p. 422 of Gröber et al. /123/. Their values and all other relevant data defining the problem are given on the first page of the computer printout, presented in the Appendix B.

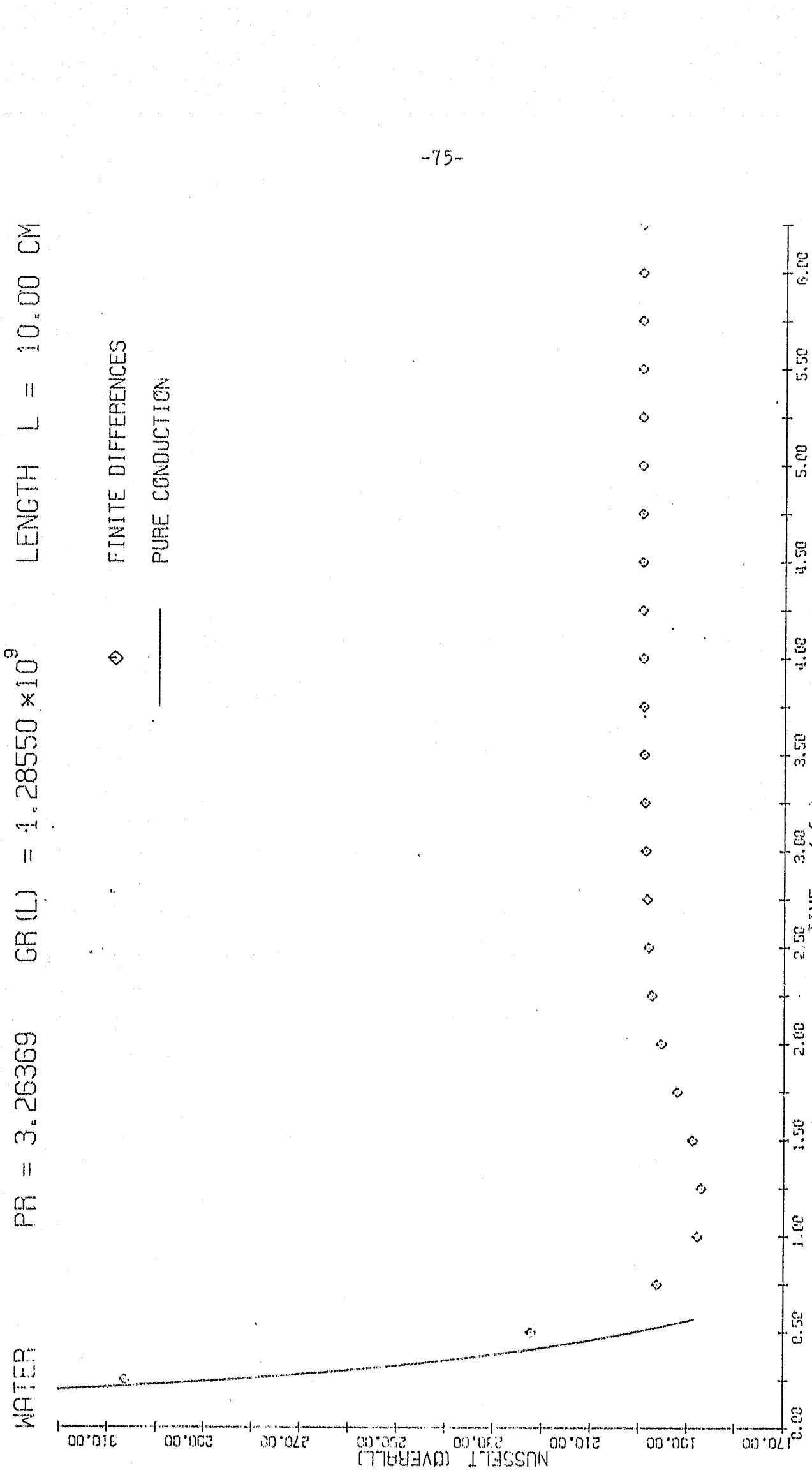

FIG. 27. OVERALL NUSSELT NUMBER IN WATER VERSUS TIME

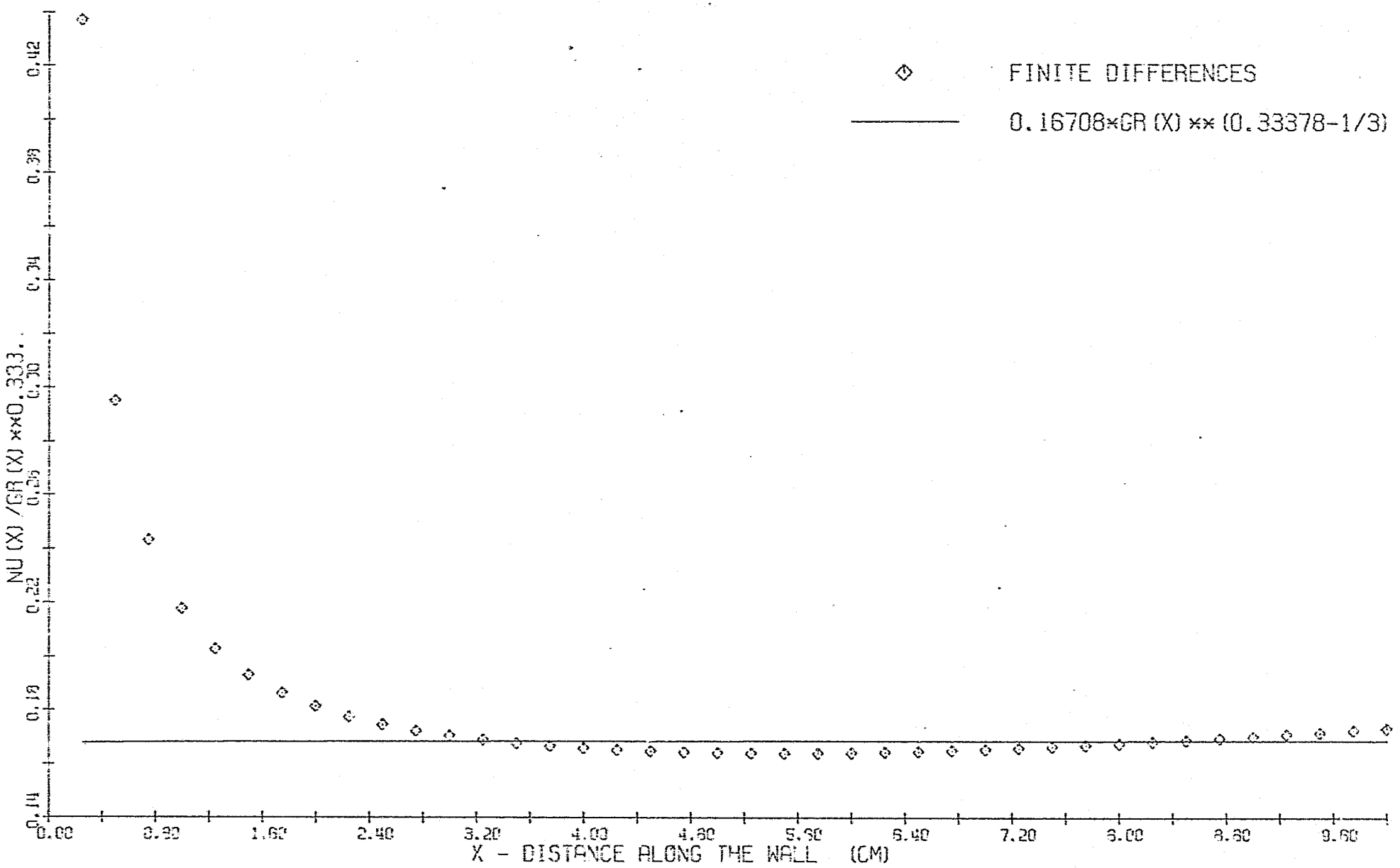

FIG. 28. STEADY STATE LOCAL HEAT TRANSFER IN WATER

The profile gradients are also in this case quite steep, and the grid spacing used for water was only slightly modified to Δx = 0,20 cm and Δy = 0,018 cm . However, because of much higher values of effective viscosity, a considerably shorter time step of Δt = 0,0015 s must be used now to ensure numerical stability during the whole transient.

The duration of the transient, as estimated according to Siegel /83/, should be 2,13 s . It was found out, however, that steady state is reached already sooner, and the main calculation was carried out for 1,8 s of real time only. The corresponding CPU time was 52 min. , somewhat more than in the case of water.

The control calculation covered 0,6 s of real time, i.e. one third of the main calculation. The time step was increased to Δt = 0,0025 s . The CPU time required for the control calculation was about 10 min.

The same set of curves as in the previous two cases is presented also here. Figs. 29-37 show development of the temperature, vertical velocity, and effective viscosity profiles at stations x = 6 , 9 , and 12 cm , respectively. The computer printout is given in the Appendix B. The control calculation is again presented only by temperature and velocity histories at the upper end of the plate, Figs. 38 and 39. All liquid metals have a very small Prandtl number, with the consequence that the heat boundary layer is thicker than the momentum boundary layer. This behaviour can be observed also in our results.

The profiles are now in some aspects quite different from the results obtained for air and water. An interesting feature is the peculiar shape of the velocity profiles. This is obviously caused by the eddy diffusivity of momentum, which reaches very high values compared with the kinematic viscosity, but the increase is limited to a narrow zone adjacent to the wall. Another interesting feature is the 'hump' on the outer part of the effective viscosity profiles in the later stages of development. It coincides with the region of peak velocity and seems to be caused by the small velocity gradients in this region.

Fig. 40 displays again an 'overshoot', but in this case the minimum is only 3,9 % below the steady state value.

The local Nusselt numbers along the wall in steady state are shown in Fig. 41. We can again see the leading-edge effect, but a part smaller than one quarter seems to be affected. The local

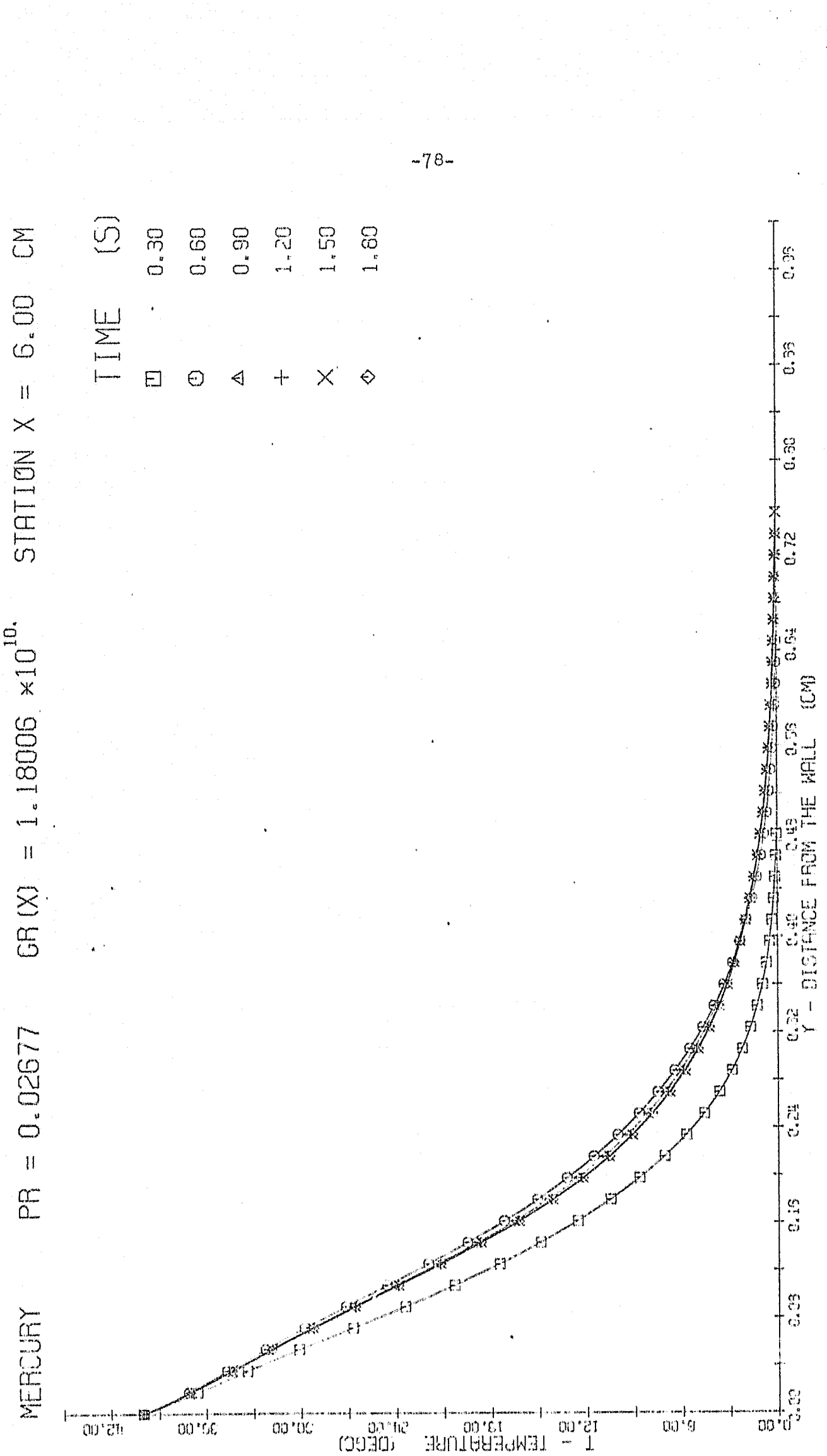

FIG. 29. TEMPERATURE PROFILES IN MERCURY AT x/L=0,50

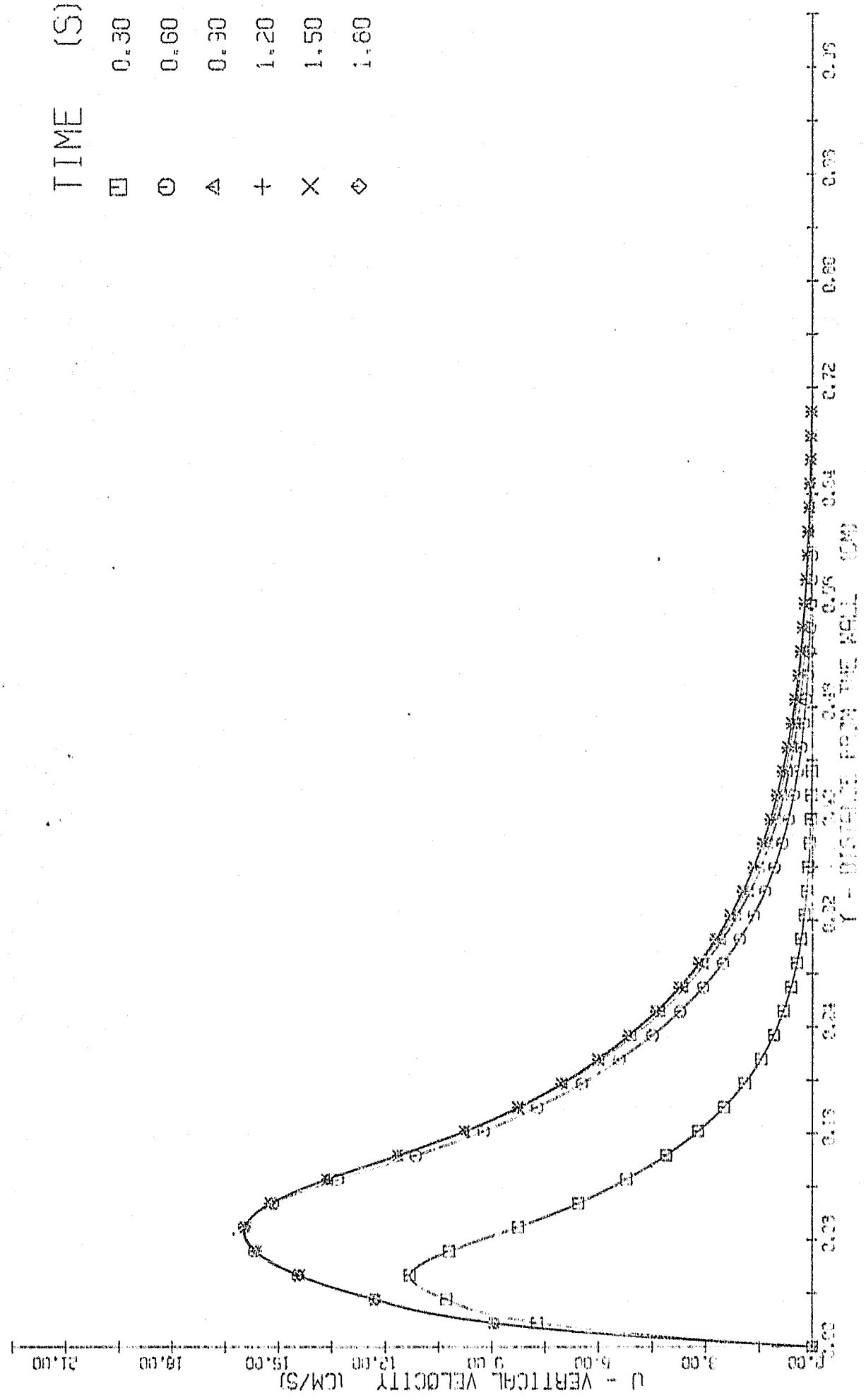

FIG. 30. VELOCITY PROFILES IN MERCURY AT x/L = 0,50

MERCURY PR = 0.02677 GR(X) = 1.18006 $\times 10^{10.}$ STATION X = 6.00 CM

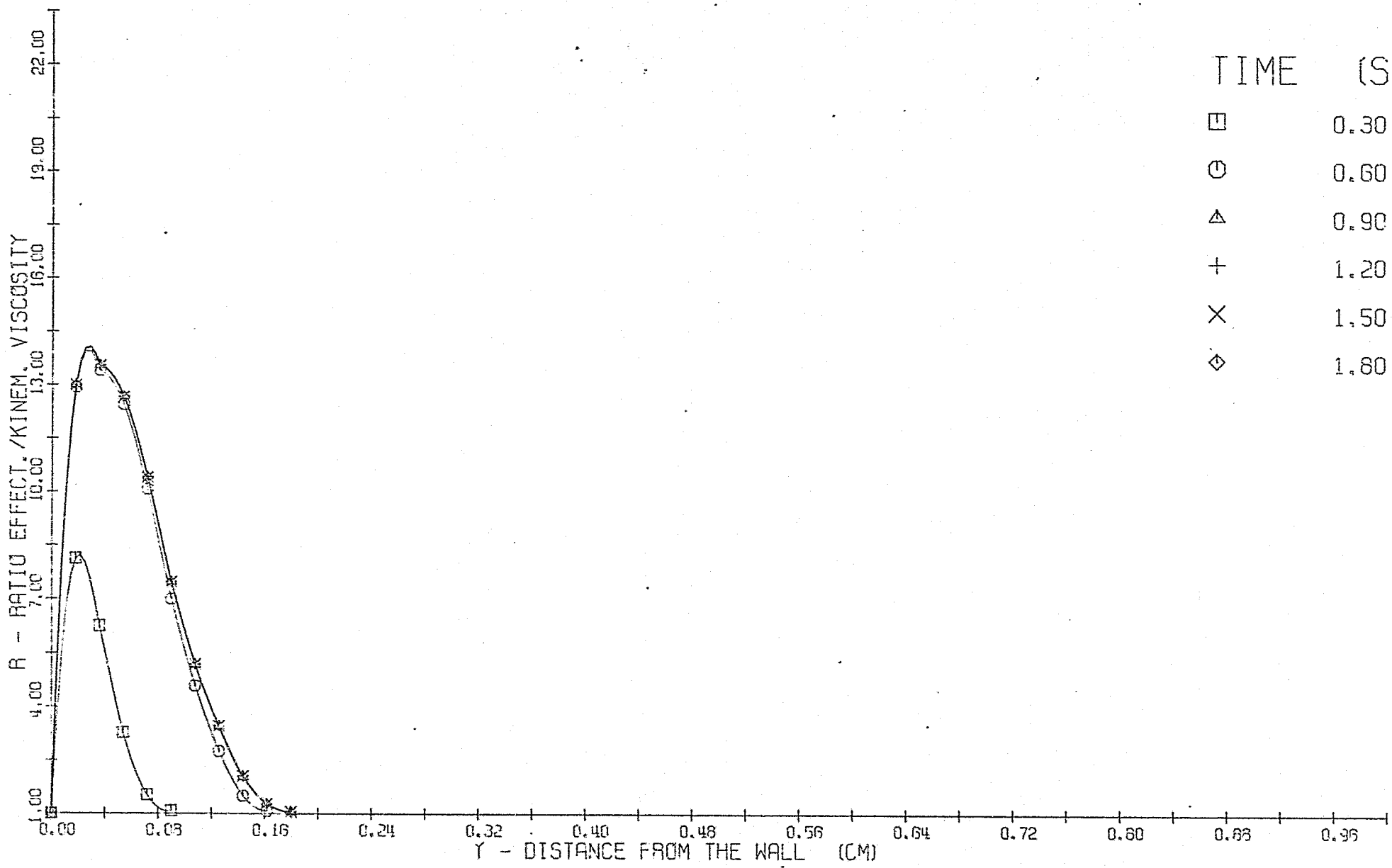

FIG. 31. EFFECTIVE VISCOSITY PROFILES IN MERCURY AT x/L = 0,50

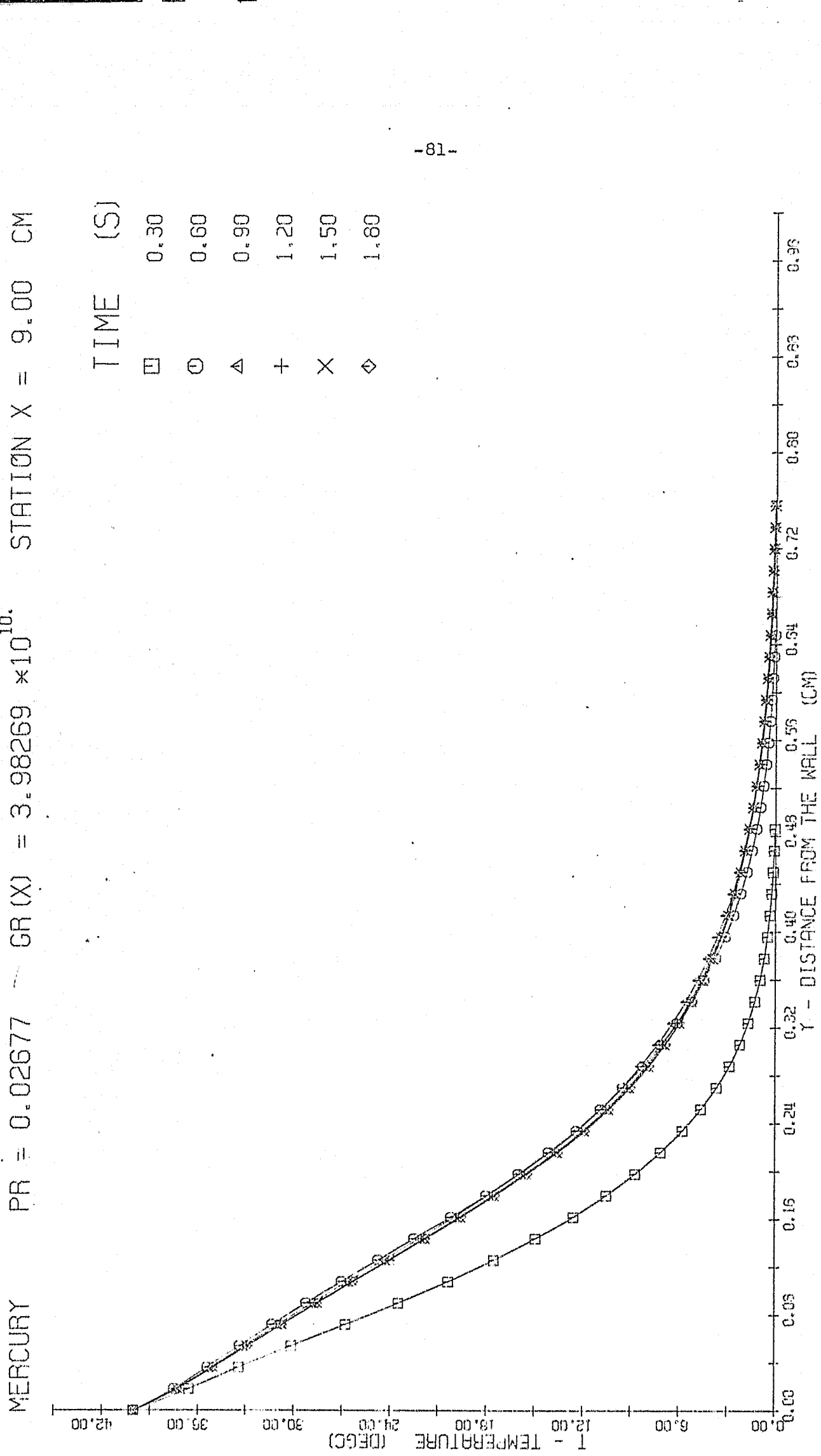

FIG. 32. TEMPERATURE PROFILES IN MERCURY AT $x/L = 0,75$

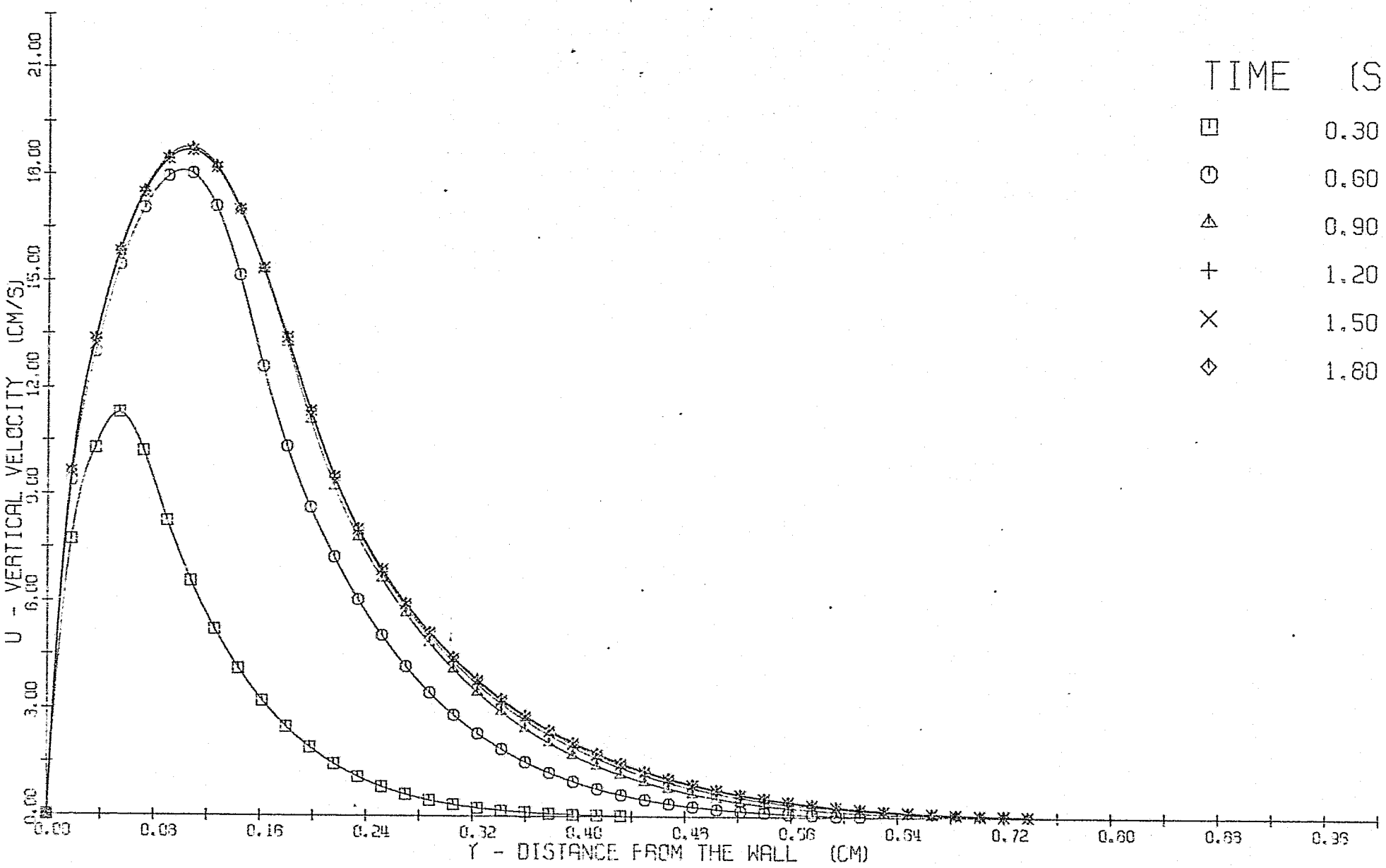

FIG. 33. VELOCITY PROFILES IN MERCURY AT $x/L = 0,75$

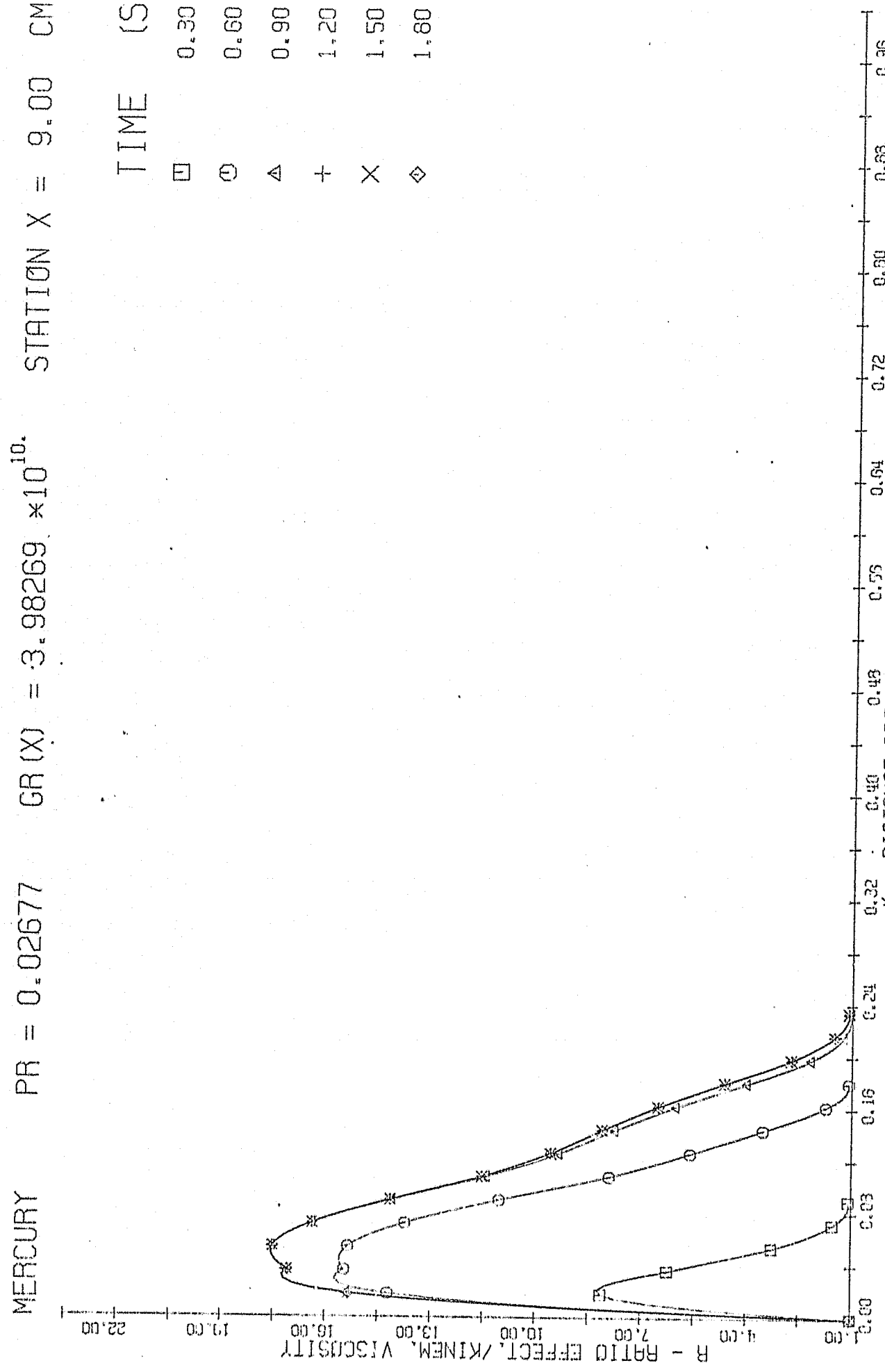

FIG. 34. EFFECTIVE VISCOSITY PROFILES IN MERCURY AT x/L = 0,75

MERCURY PR = 0.02677 GR(X) = $9.44045 \times 10^{10.}$ STATION X = 12.00 CM

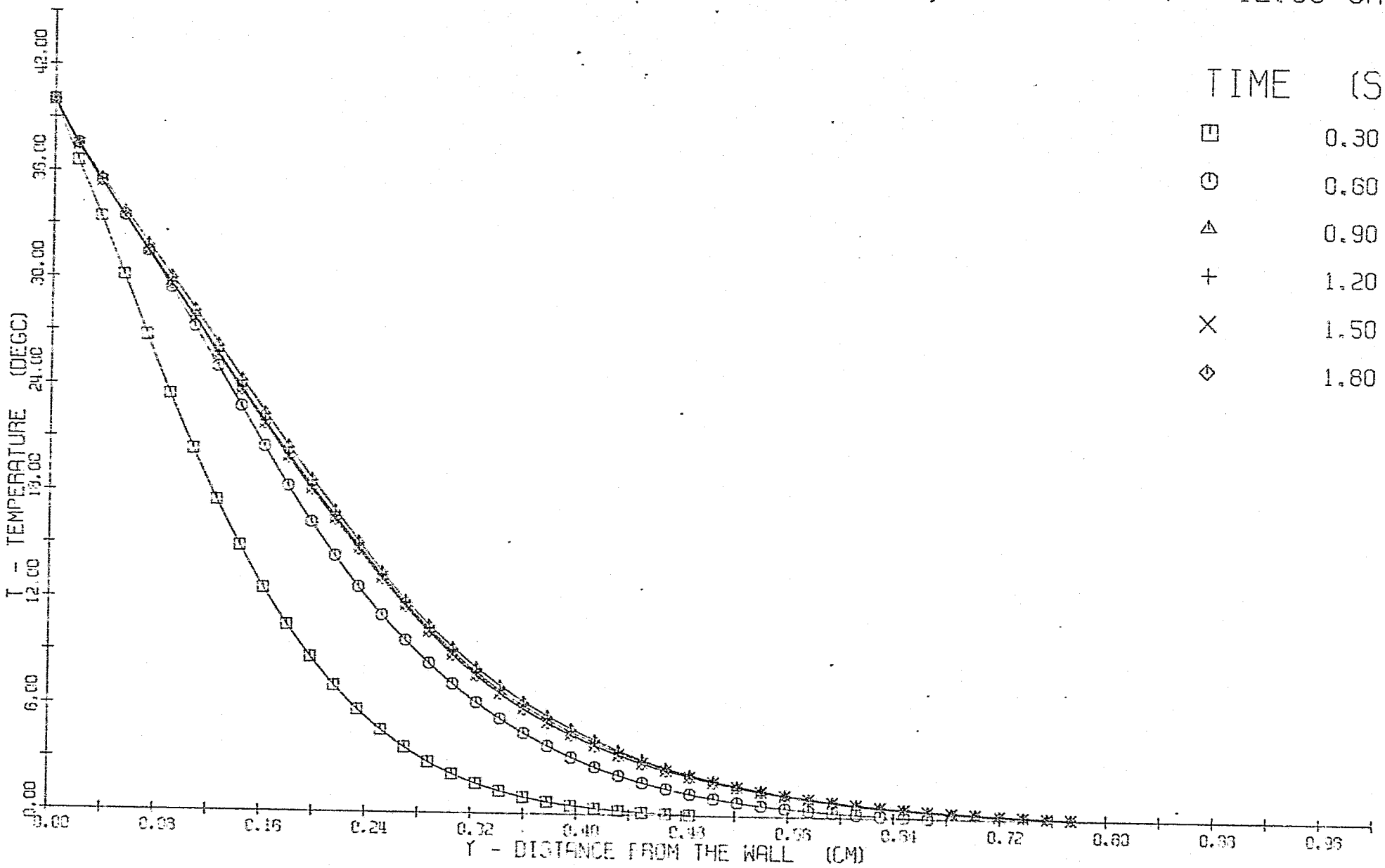

FIG. 35. TEMPERATURE PROFILES IN MERCURY AT x/L = 1,00

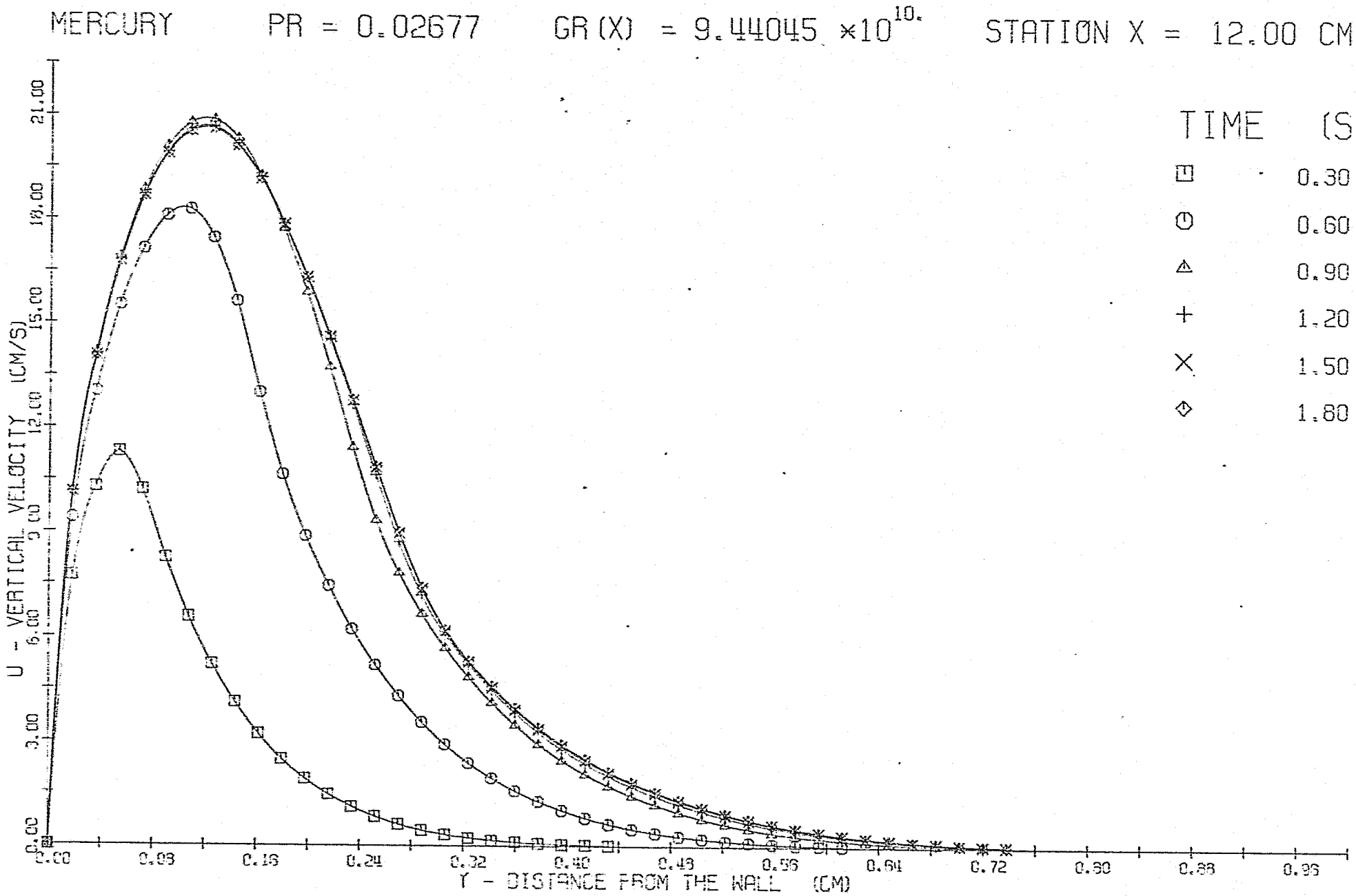

FIG. 36. VELOCITY PROFILES IN MERCURY AT x/L = 1,00

MERCURY PR = 0.02677 GR(X) = $9.44045 \times 10^{10.}$ STATIØN X = 12.00 CM

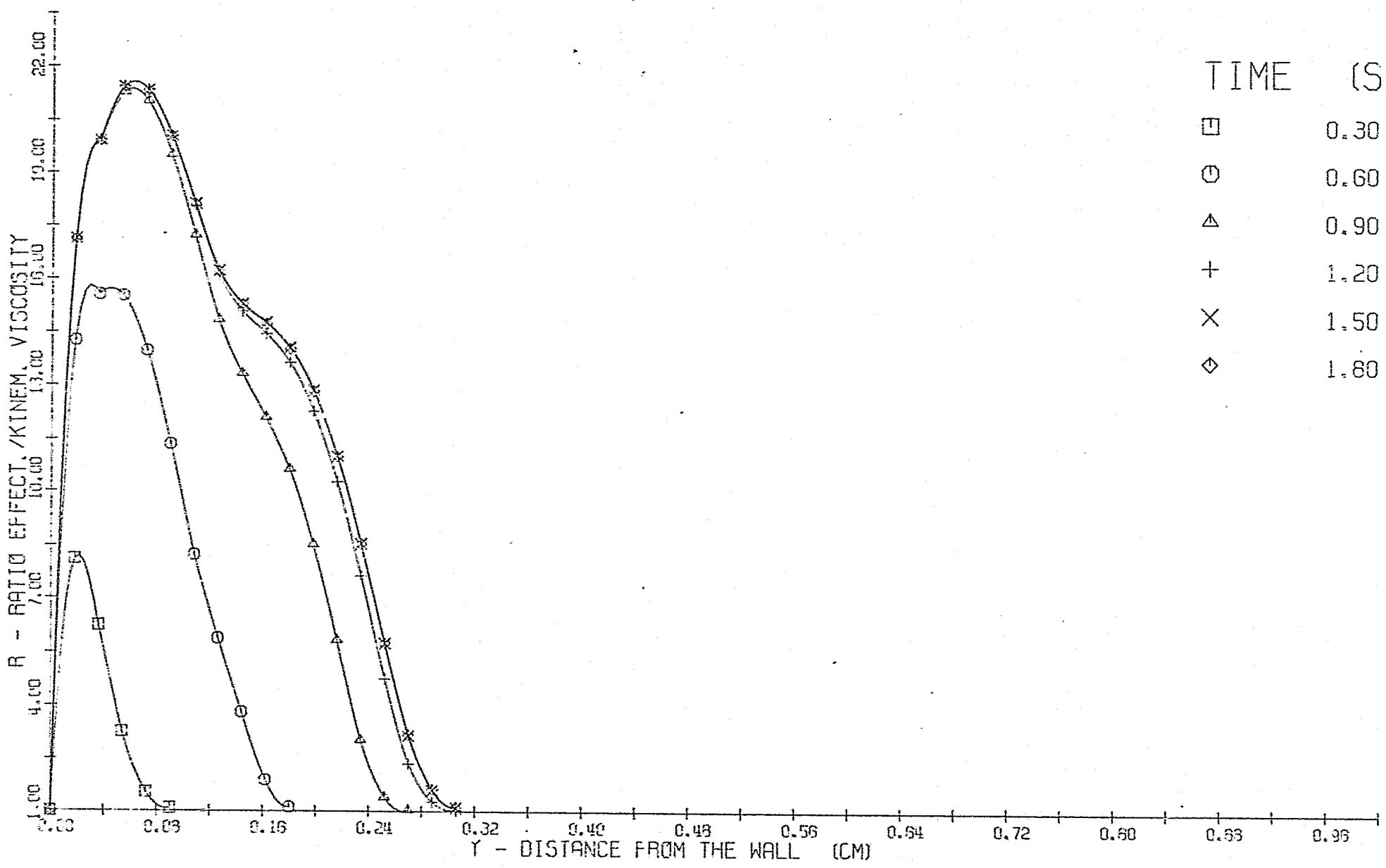

TIME	(S)
□	0.30
○	0.60
△	0.90
+	1.20
×	1.50
◇	1.80

FIG. 37. EFFECTIVE VISCOSITY PROFILES IN MERCURY AT $x/L = 1,00$

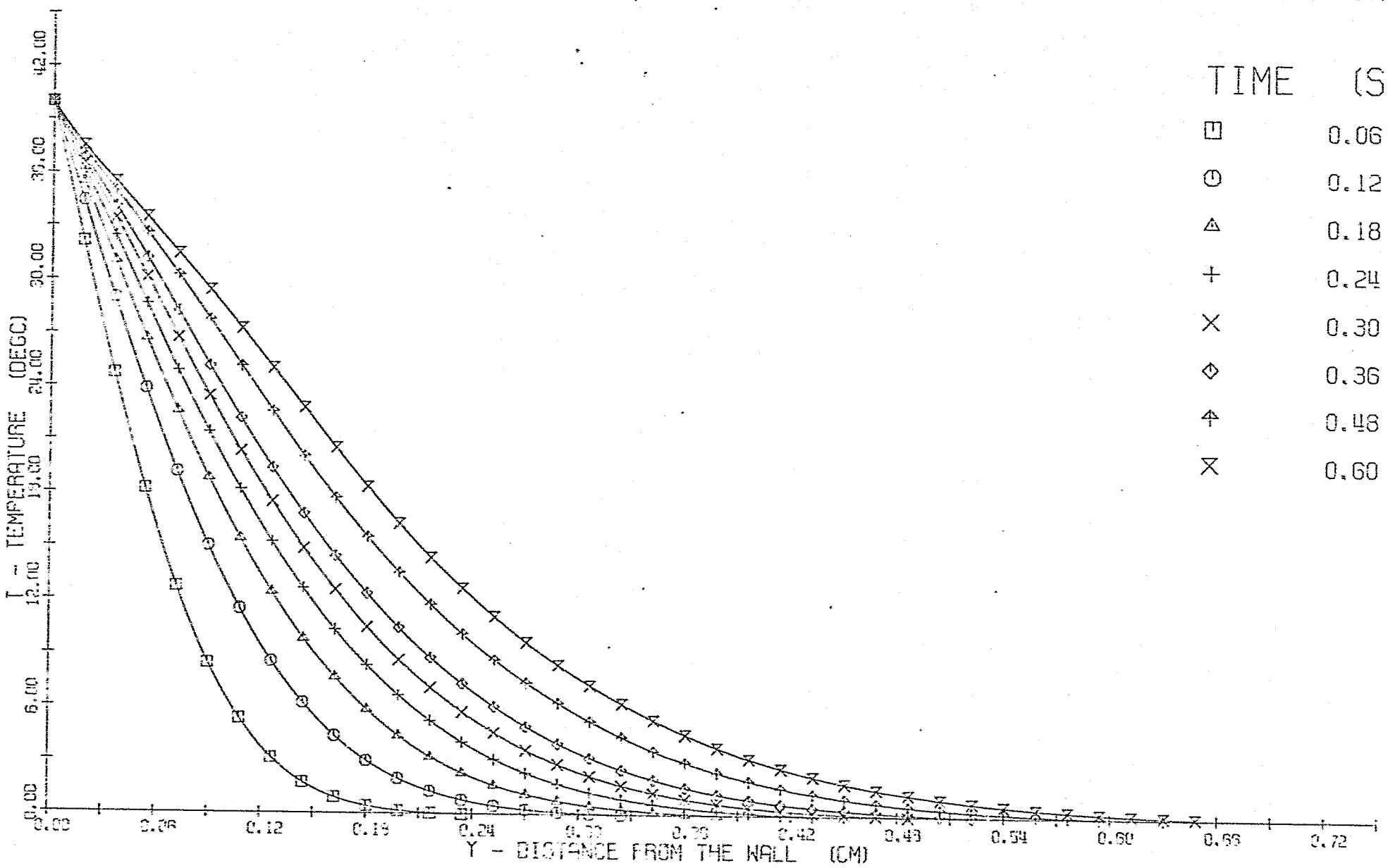

FIG. 38. TEMPERATURE PROFILES IN MERCURY AT x/L=1,00 (CONTROL CALCULATION)

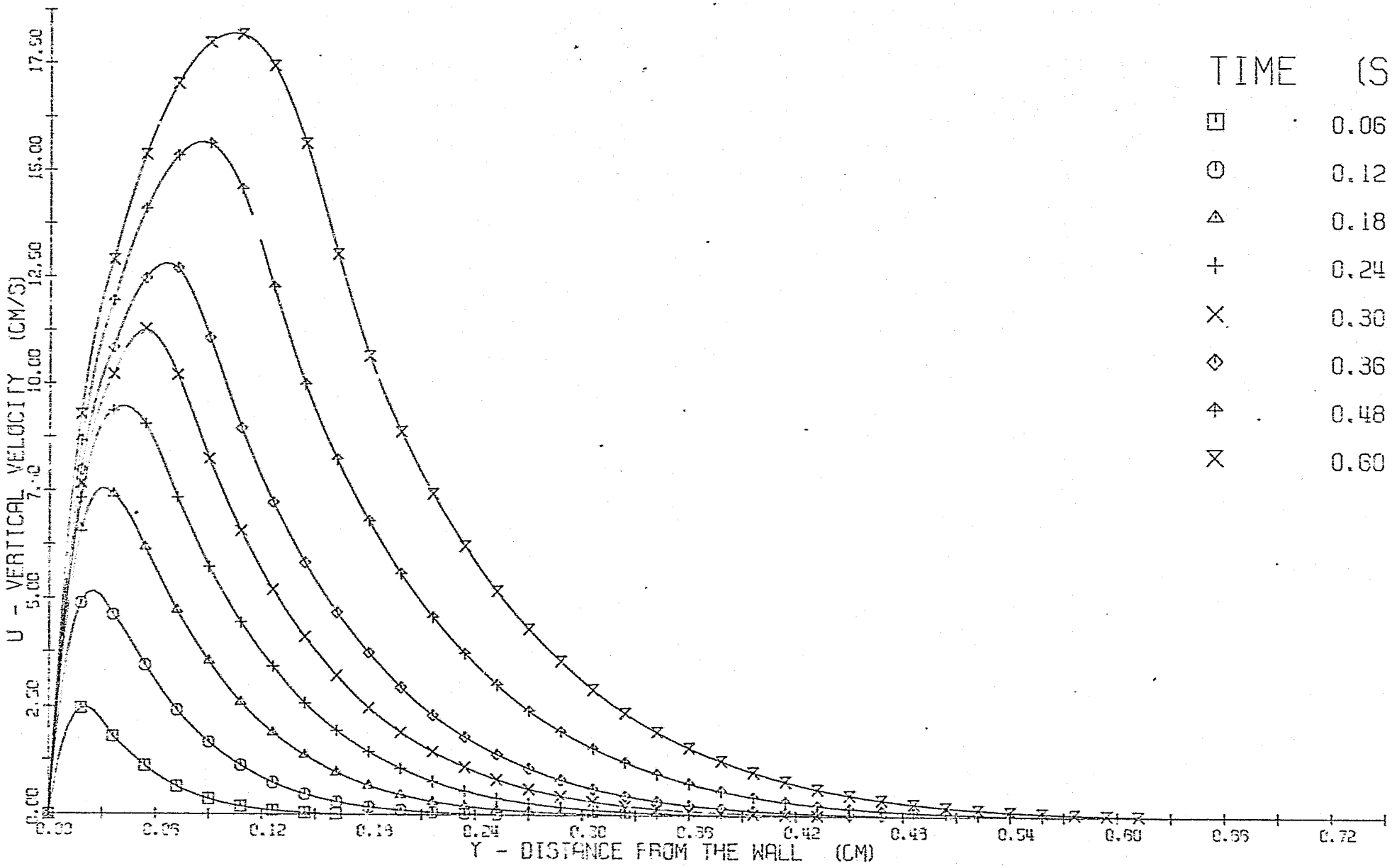

FIG. 39. VELOCITY PROFILES IN MERCURY AT x/L = 1,00 (CONTROL CALCULATION)

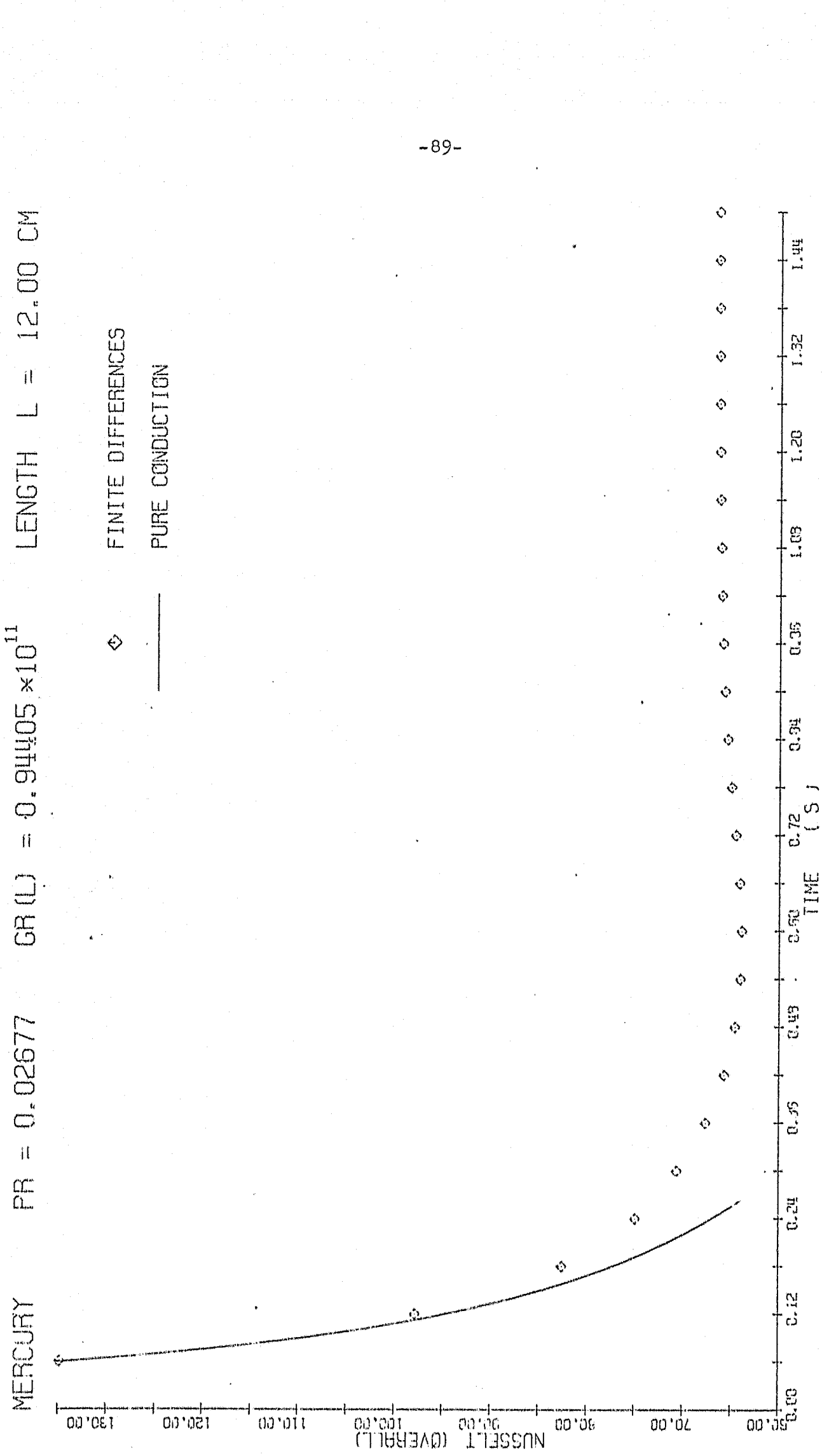

FIG. 40. OVERALL NUSSELT NUMBER IN MERCURY VERSUS TIME

MERCURY PR = 0.02677 GR(L) = 0.94405×10^{11} LENGTH L = 12.00 CM

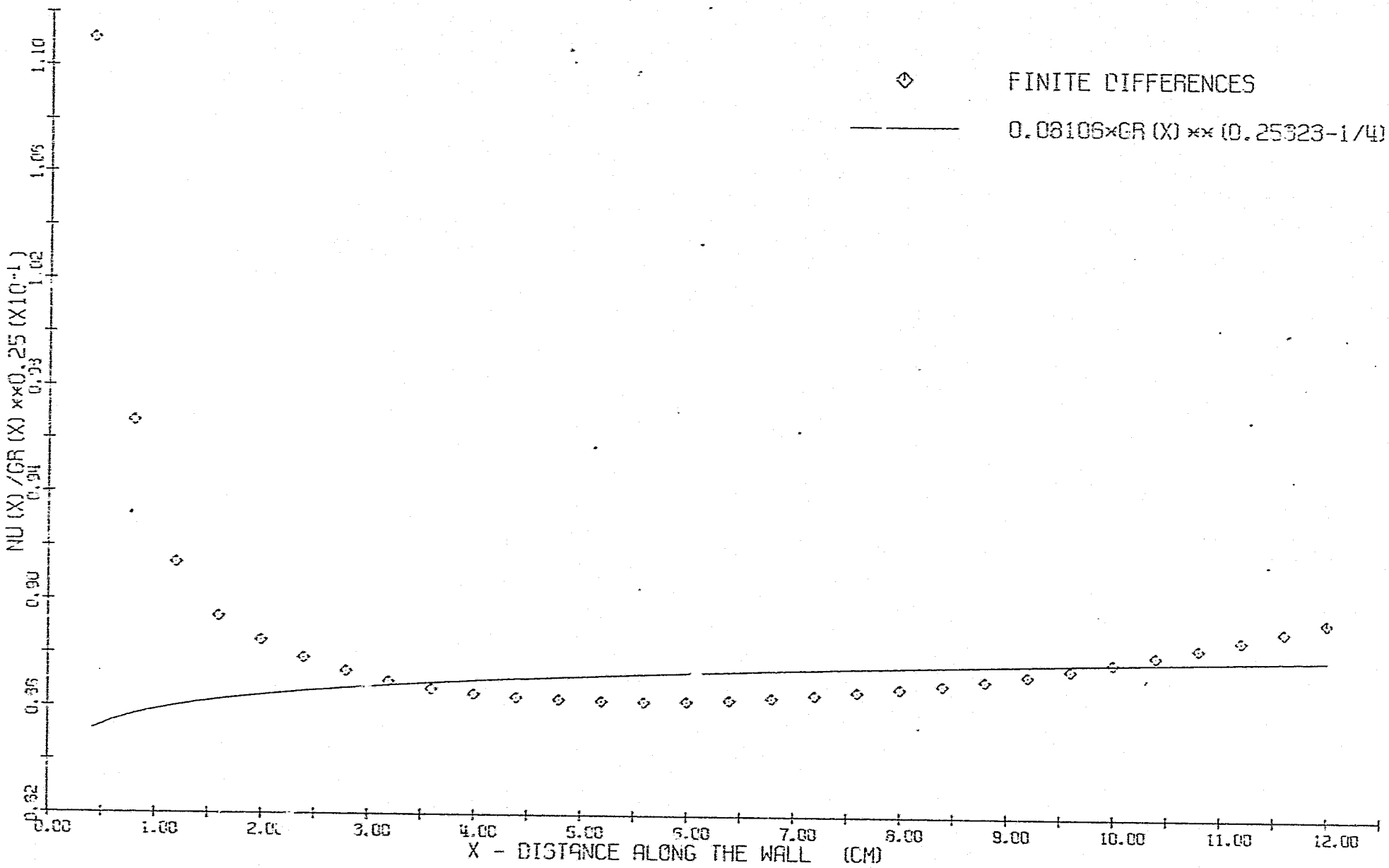

FIG. 41. STEADY STATE LOCAL HEAT TRANSFER IN MERCURY

Nusselt numbers are well approximated by a correlation of the form (94).

The overall Nusselt number, calculated from the equation (96), is $Nu_L = 64{,}18$. This is only 3,5 % less than the result of numerical integration of the local values along the wall, and the agreement is in this case surprisingly good.

We shall proceed now to the next Chapter, in which our results will be compared with data produced by other research workers.

7. COMPARISON WITH PUBLISHED DATA

It is always essential to know, how well our own results compare with the data produced by other research workers. Agreement with established data can serve as a verification of new results, while a severe disagreement indicates that something is wrong somewhere.

Unfortunately, there are no published data, theoretical or experimental, with which our results could be compared in their entirety. However, it is possible to employ as a substitution such data, which cover our results at least partially.

There are only a few formulae giving the duration of the transient and the velocity of the signal propagating from the leading edge, and all of them are for the laminar case only. Nevertheless, we shall make a comparison with them, to establish at least the possible deviations caused by turbulence.

In the initial stage of the transient, the heat transfer regime can be classified as an almost pure conduction. This enables us to obtain an analytical solution for a short initial period.

There are no data for the following intermediate stage, but it is clear, that at the other end of the transient a steady state must be established sooner or later. Relatively many data concerning the steady state are already available (see Section 2.4). They can be in some cases compared with our results, and this shall be done in the last four Sections of the present Chapter.

7.1 Duration of the Transient

It has been observed by all previous research workers, that natural convection transients are extremely fast. This is a fortunate circumstance from the economic point of view, as the required computer times are proportional to the duration of a transient.

To the author's knowledge, there is only one formula which gives the time required to reach steady state over an isothermal plate. The formula is

$$t = 5,24\,(0,952 + Pr)^{\frac{1}{2}}\,(g\beta\Delta T)^{-\frac{1}{2}}\,x^{\frac{1}{2}} \qquad (97)$$

and it was derived by Siegel /83/, who used an integral method for

the solution of transient laminar free convection boundary layer. He also investigated the sensitivity of the results with respect to the assumed profile shapes employed in the integral method and obtained an alternative formula with different numerical coefficients, but the results were almost identical.

If the time required to reach steady state is calculated from the equation (97), we obtain for our examples: 4,2 s for air, 5,9 s for water, and 2,1 s for mercury. In numerical calculations, this value depends of course on the definition of steady state, namely on the arbitrary choice of the fraction of the asymptotic steady state value which is attained. For this reason we shall limit here ourselves to a qualitative discussion, as anyone can easily draw his own conclusions from the Figures presented in the preceding Chapter.

Generally speaking, the steady state is first attained by the temperature field, which is closely followed by the velocity field. However, the development of the effective viscosity field usually takes somewhat more time and there are still some small changes of the effective viscosity profiles at a time, when heat transfer coefficients have attained completely steady values. Heat transfer is our main concern and if we consider Figs. 14, 27, and 40, respectively, we can see, that our results are more or less in agreement with the times predicted by means of the equation (97). However, as mentioned above, the degree of the agreement is to a great deal a question of the definition of the steady state.

7.2 Propagation of the Leading-Edge Effect

In the initial stage of a transient, the solution is dependent on time only. This phase is usually called the pure conduction regime. The singular point at the leading edge is source of a disturbance, which travells with a finite velocity downstream along the plate. When this signal reaches a station, the solution at this particular coordinate becomes dependent on both time and position. This is the intermediate stage. Finally, steady state is attained and the solution ceases to be dependent on time and is a function of position only.

It is evident, that the end of the pure conduction regime is identical with the propagation of the leading-edge effect. Formulae giving this signal velocity have been derived by two research

workers. It must be remembered, however, that both formulae were derived for the case of laminar flow.

Siegel /83/ derived, besides the formula (97) giving the end of the whole transient, also another formula giving the end of the pure conduction regime. This formula is

$$t = 1,80\ (1,5 + Pr)^{\frac{1}{2}} (g \beta \Delta T)^{-\frac{1}{2}} x^{\frac{1}{2}} \qquad (98)$$

The sensitivity with respect to the assumed profile shapes is again small.

Nanbu /64/ presented an analytical solution and his result can be written as

$$t = \phi (Pr)\ (g \beta \Delta T)^{-\frac{1}{2}} x^{\frac{1}{2}} \qquad (99)$$

This formula is very similar to equation (98), but the part which is a function of the Prandtl number is much more complicated here, involving multiply-integrated complementary error functions (see a table in Carslaw & Jaeger /106/). The interested reader is refered to Nanbu's paper /64/ for more details.

Our results are compared graphically in Figs. 42-44 with the predictions resulting from the equations (98) and (99). A similar problem is encountered here as in the previous Section, namely the question of a numerical definition of the end of the initial one-dimensional regime. It was defined here as the first occurrence of a change in the first three significant digits of the wall shear stress value, compared with the downstream values.

Figs. 42-44 show, that the disturbance defined in this way propagates with a velocity somewhat higher than those predicted by the equations (98) and (99). One possible explanation is that the increasing turbulence accelerates the propagation of the disturbance. However, the turbulence is still quite small at this stage and the discrepancy may simply be caused by our strict definition of a disturbance. Anyway, the agreement is quite reasonable.

7.3 Pure Conduction Regime

According to the initial conditions (56), all fluid is at rest when the transient starts. It can also be expected, that during a certain time after the start fluid velocities would be very small,

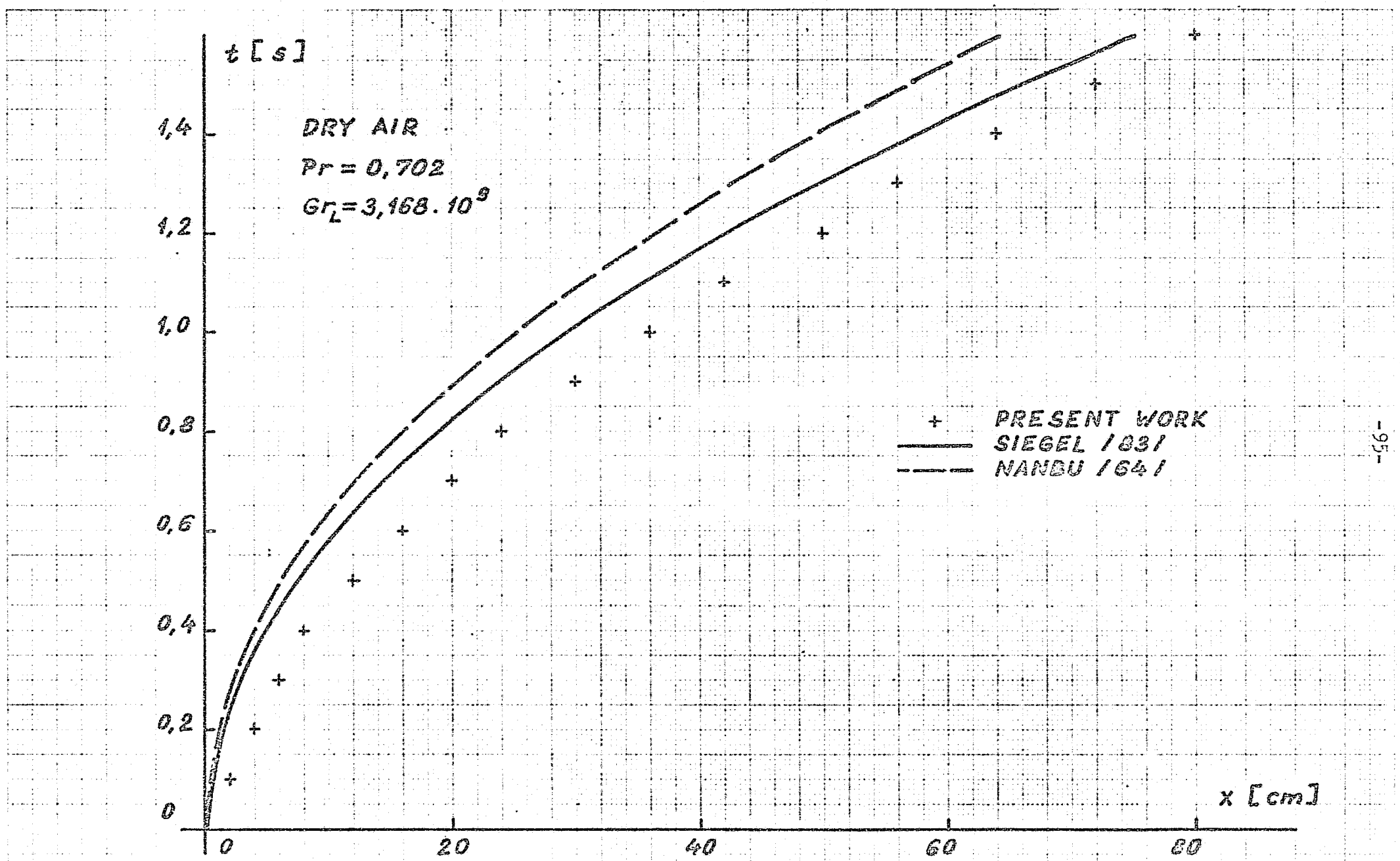

FIG. 42 . PROPAGATION OF THE LEADING-EDGE DISTURBANCE IN AIR

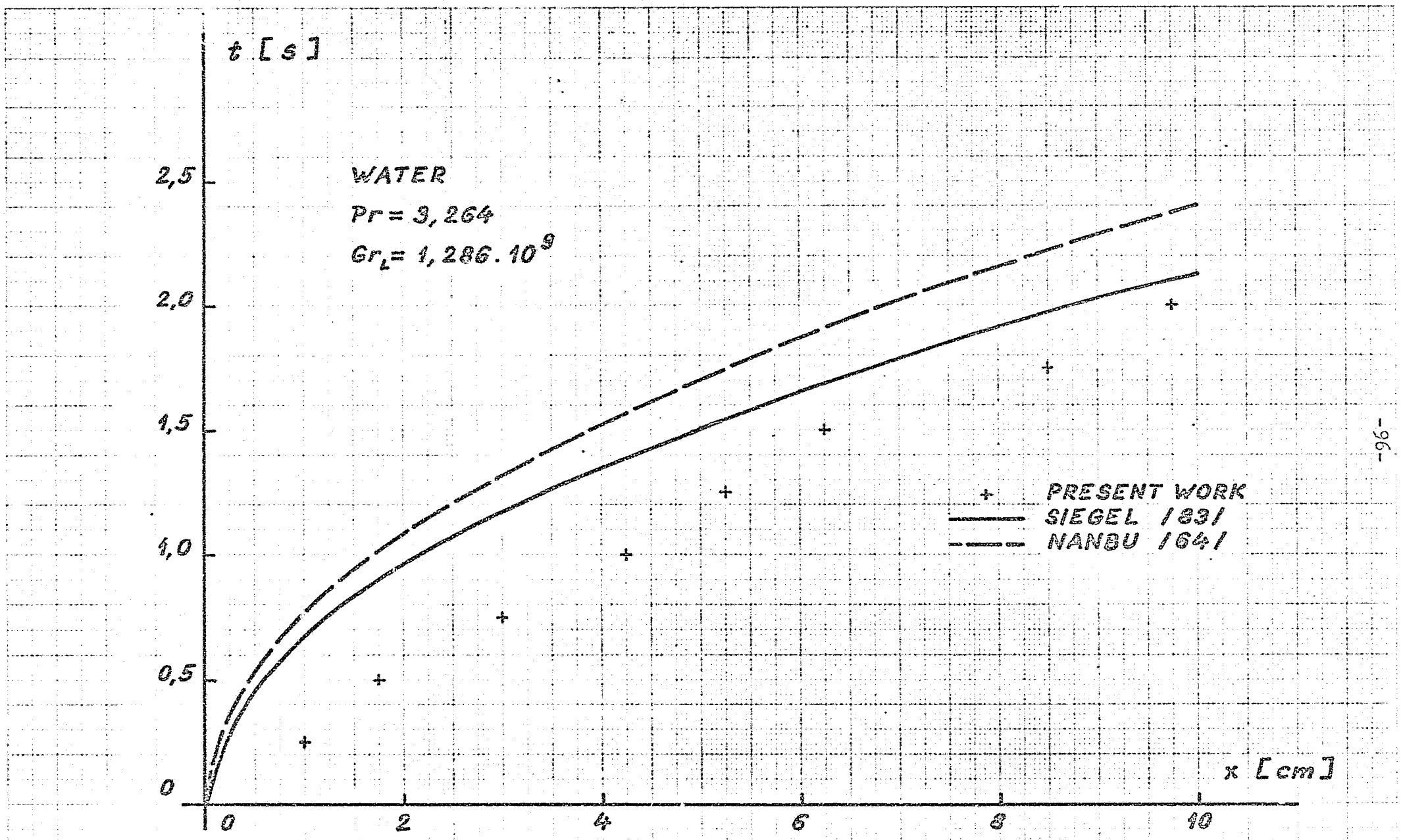

FIG. 43. PROPAGATION OF THE LEADING-EDGE DISTURBANCE IN WATER

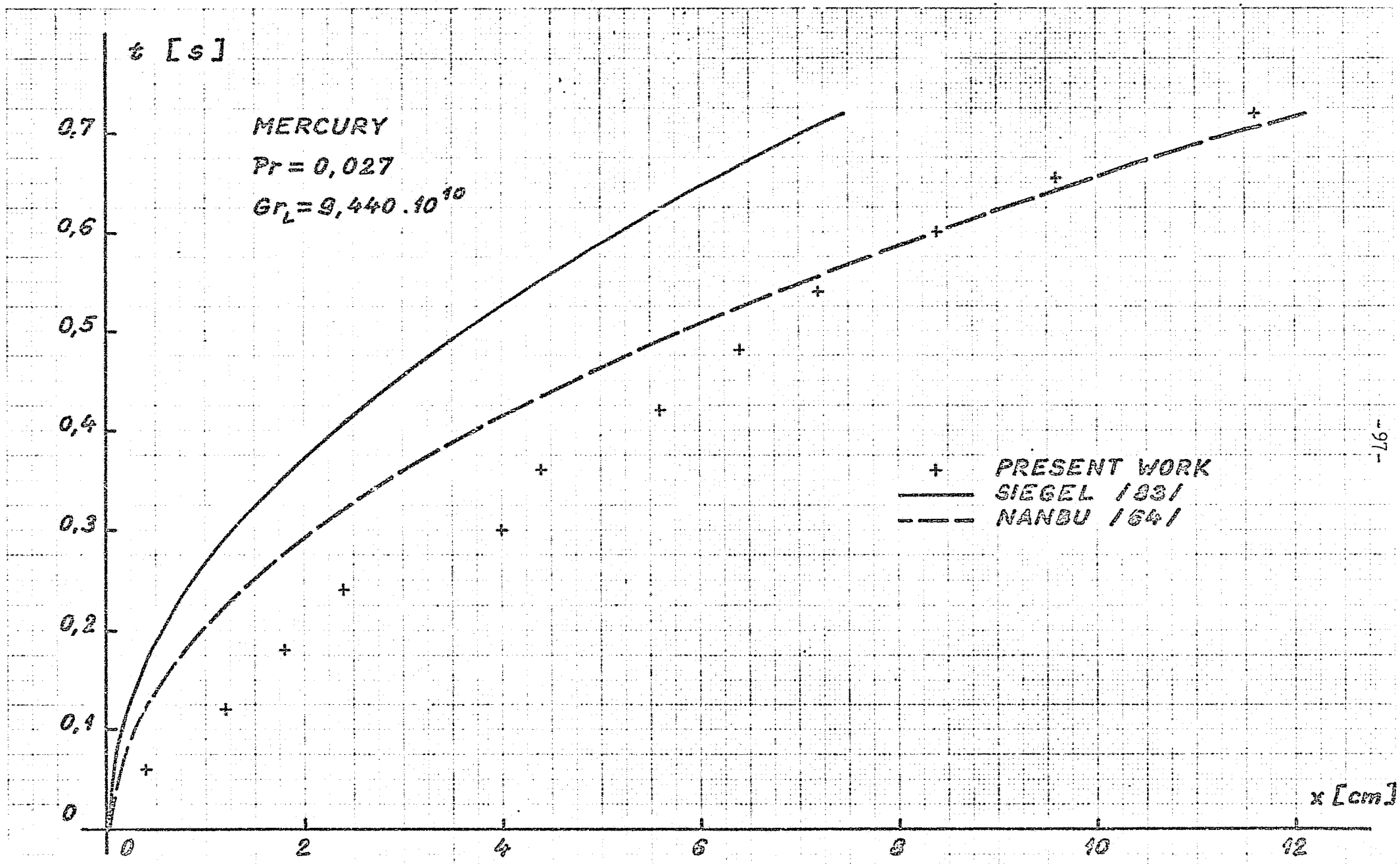

FIG. 44. PROPAGATION OF THE LEADING-EDGE DISTURBANCE IN MERCURY

so that the convective terms and eddy diffusivity in equation (54) can be neglected. This assumption leads to an equation of one--dimensional unsteady heat conduction

$$\frac{\partial T}{\partial t} = \alpha \frac{\partial^2 T}{\partial y^2} \qquad (100)$$

which describes, together with initial and boundary conditions appropriate to our problem, unsteady heat conduction into a half-infinite space. It is not easy to solve this problem (see e.g. Gröber et al. /123/ or Carslaw & Jaeger /106/), but it has an analytical solution, which is in our case

$$T(y,t) = T_f + (T_w - T_f)\, erfc \frac{y}{2\sqrt{\alpha t}} \qquad (101)$$

It is possible to express temperature gradient at the wall analytically from the equation (101) and to obtain, in the end, an equation for heat transfer coefficient as a function of time. This equation is

$$Nu_L(t) = \frac{L}{\sqrt{\pi \alpha t}} \qquad (102)$$

and it can be used for approximate prediction of the initial stage of the free convection transient. The equation (102) shows, that heat transfer rate at the start of the transient is infinite.

Curves calculated from the equation (102) have been shown in Figs. 14, 27, and 40. The agreement is quite good, but only for a very short initial period. A comparison of the analytical prediction with our results is presented here also in the form of tables. At the same time, the results of the main and control finite-difference calculations are also compared. Table 1 gives the results for air, Table 2 for water, and Table 3 for mercury. In all three cases, the same observations can be made. The analytically predicted values are at the beginning only slightly lower than the finite-difference solution, but with advancing time the difference is increasing. This behaviour is obviously a result of the ensuing fluid flow, which enhances the heat transfer rate. The results of the main and control finite-difference calculations are almost identical, which means that discretization errors are practically negligible.

TABLE 1. PURE CONDUCTION IN AIR

t	Nu_L		
[s]	$\Delta t = 0{,}0025\,s$	$\Delta t = 0{,}005\,s$	Equat. (102)
0,1	287,126	283,903	278,830
0,2	203,492	202,456	197,163
0,3	170,469	169,864	160,983
0,4	153,410	152,928	139,415
0,5	143,862	143,402	124,697
0,6	137,830	137,463	113,832
0,7	133,507	133,087	105,388
0,8	131,038	130,587	98,581
0,9	129,865	129,417	92,943
1,0	129,598	129,180	88,174

TABLE 2. PURE CONDUCTION IN WATER

t	Nu_L		
[s]	$\Delta t = 0{,}005$ s	$\Delta t = 0{,}010$ s	Equat. (102)
0,25	306,254	303,200	284,913
0,50	222,230	221,243	201,464
0,75	196,094	195,505	164,495
1,00	187,897	187,470	142,457
1,25	187,172	186,850	127,417
1,50	189,022	188,682	116,315
1,75	192,105	191,728	107,687
2,00	195,394	195,070	100,732

TABLE 3. PURE CONDUCTION IN MERCURY

t	Nu_L		
[s]	$\Delta t = 0{,}0015$ s	$\Delta t = 0{,}0025$ s	Equat. (102)
0,06	134,852	134,026	133,940
0,12	97,812	97,519	94,710
0,18	82,570	82,411	77,330
0,24	74,920	74,840	66,970
0,30	70,620	70,575	59,900
0,36	67,617	67,558	54,681
0,42	65,702	65,629	50,624
0,48	64,590	64,501	47,355
0,54	64,044	63,941	44,647
0,60	63,926	63,809	42,355

7.4 Temperature Profiles

We shall compare here the temperature profiles, resulting from our finite-difference calculations at the end of the transient, with steady state temperature profiles measured by various research workers. In all cases, the calculated profiles at the upper end of the plate are being compared. There are no pertinent data for mercury, so that comparisons for air and water only will be made here.

Some research workers approximated their experimental results by nondimensional correlations, which are convenient for comparison purposes and will be used also here.

Coutanceau /8/ made measurements of natural convection in air for temperatures and plate length very similar to our calculated example. He approximated the measured profiles of mean temperatures by general formulae, which can be used for construction of temperature profiles under different conditions. The formulae are quite complicated and will not be repeated here. In Fig. 45, the empirical profile of Coutanceau is compared with our finite--difference results. Coutanceau claimed two parts of the profile, both linear in semi-logarithmic coordinates. These 'linear' parts cannot be recognised in our results, but otherwise the agreement is quite good.

Fujii et al. /23/ give formulae for mean temperature profiles in air, which are based on the measurements of Cheesewright /6/. The formulae are

$$\vartheta = 1 - \xi \qquad \text{for} \quad \xi < 0,2 \qquad (103)$$

and

$$\vartheta = \frac{0,415}{\sqrt{\xi^{1,5} + 0,18}} \qquad \text{for} \quad \xi > 0,2 \qquad (104)$$

Fig. 46 shows this approximation together with our results. The agreement in the inner part of the boundary layer is good, but in the outer part our temperatures are considerably lower than the predicted curve. One reason for this discrepancy is obviously the asymptotic character of the equation (104). It is also possible, that our turbulence model does not formulate the physical processes in that zone well enough.

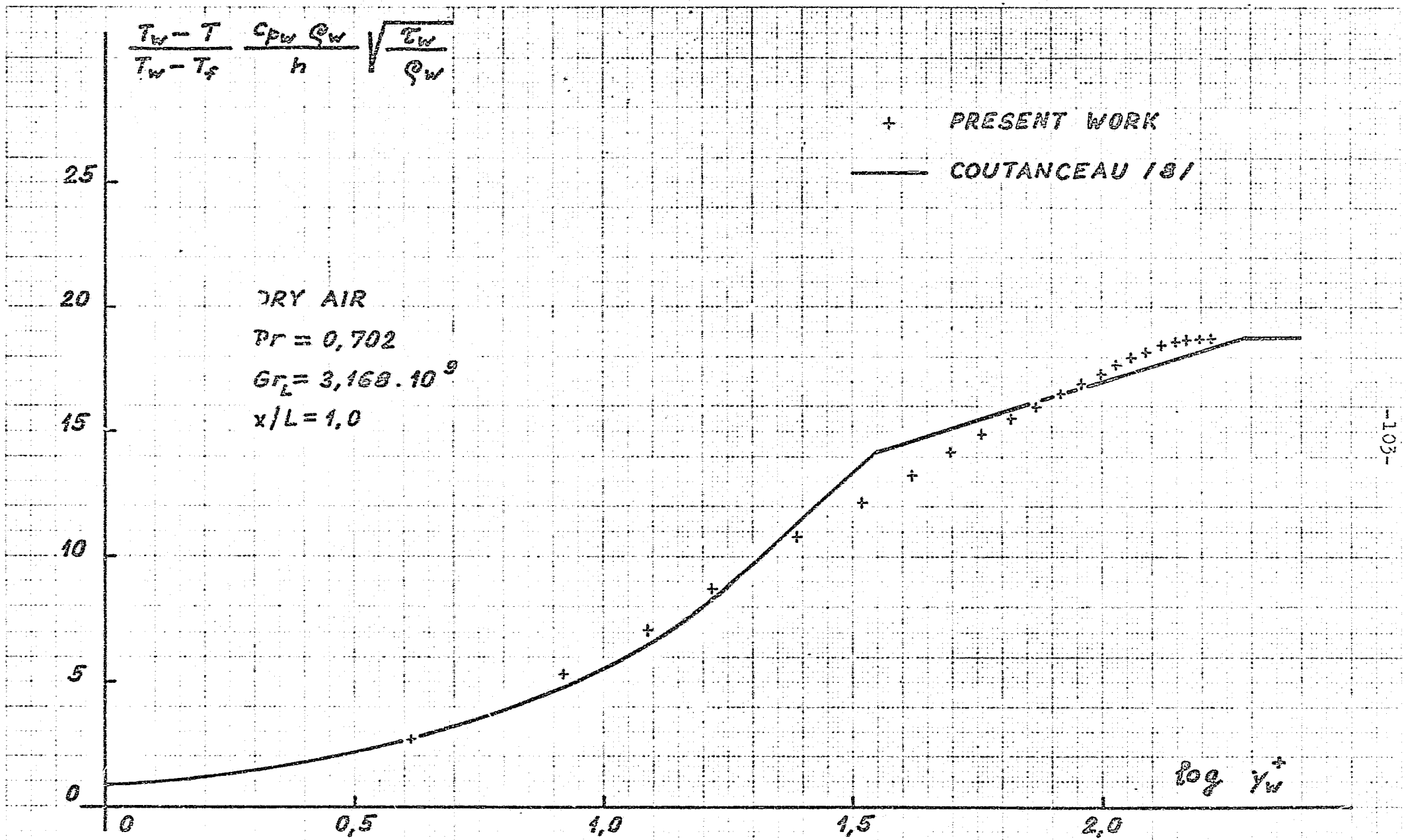

FIG. 45. TEMPERATURE PROFILE IN AIR COMPARED WITH COUTANCEAU /8/

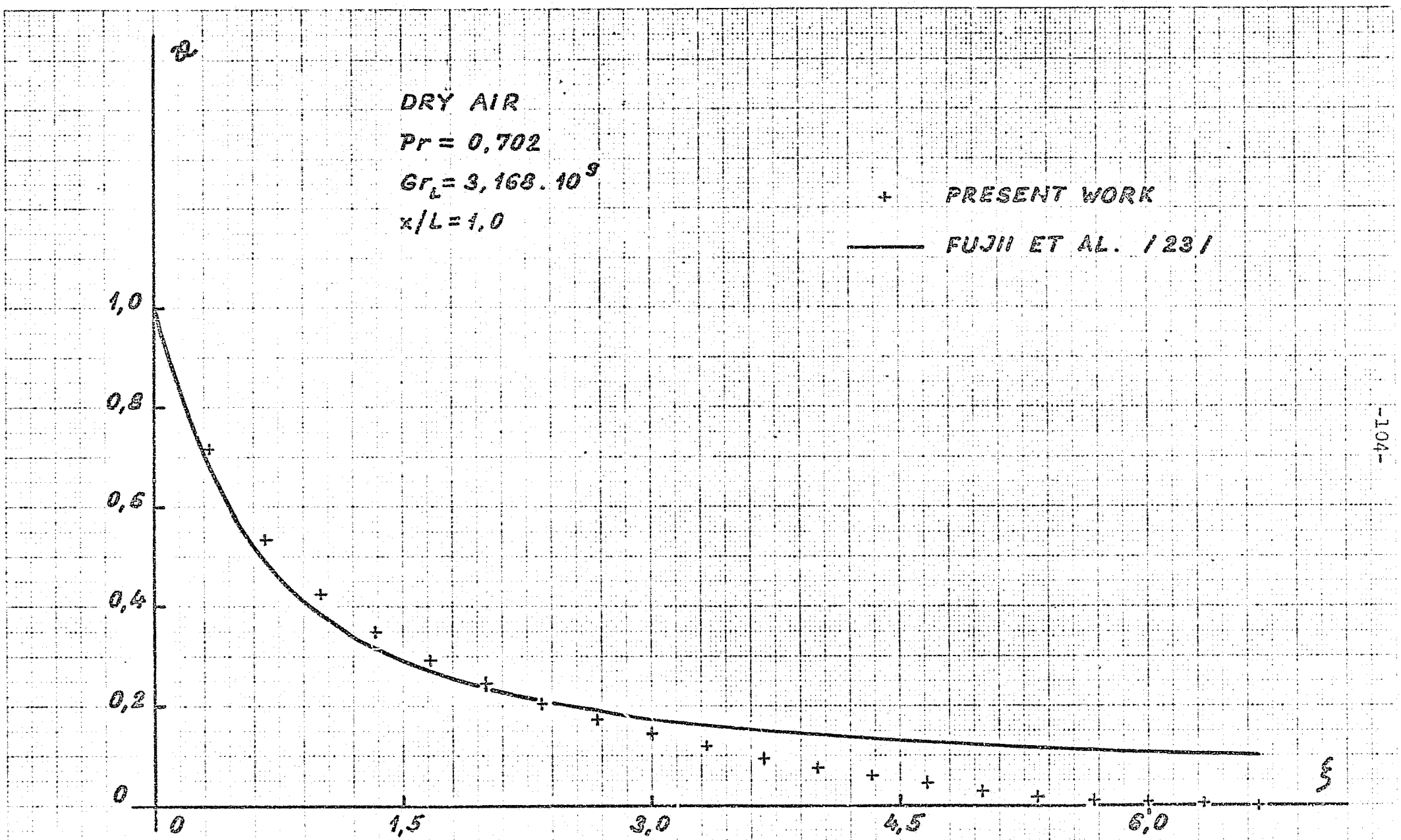

FIG. 46. TEMPERATURE PROFILE IN AIR COMPARED WITH FUJII ET AL. /23/

Fujii et al. /23/ approximated also their own measurements in water by

$$\vartheta = 1 - \xi \qquad \text{for} \quad \xi < 0,5 \qquad (105)$$

and

$$\vartheta = \frac{0,25}{\sqrt{\xi - 0,25}} \qquad \text{for} \quad \xi > 0,5 \qquad (106)$$

Fig. 47 displays this approximation together with our results. The agreement is again reasonable, and similar observations as in the preceding case can also be made here.

It can be said, that in all three comparisons our calculated temperature profiles agree well with the experimental results of other workers, and especially the good agreement in the inner part of the boundary layer is important from the heat transfer point of view. Moreover, the formulae of Fujii et al. /23/ are called by themselves 'simple and rough representations', and in this sense also the agreement in the outer part of the boundary layer is certainly adequate.

7.5 Velocity Profiles

Predicted steady state profiles of the vertical velocity component will be compared here with the available experimental data of other research workers. As in the case of temperature, the calculated profiles at the upper end of the plate are being compared. The measurement of velocities is more difficult than measurement of temperatures and this is the main reason, why the data on velocity profiles are relatively scarce.

Coutanceau measured in his abovementioned study /8/ also mean velocities in air by means of a Pitot microtube. The formulae for construction of velocity profiles again are quite complicated and will not be repeated here. Fig. 48 shows Coutanceau's approximation together with our results. The agreement is quite reasonable. However, as in the case of temperature profiles, the two parts linear in semi-logarithmic coordinates are hardly displayed by our results.

Vliet & Liu /92/ presented a nondimensional formula for the outer part of the velocity profiles measured by them in water.

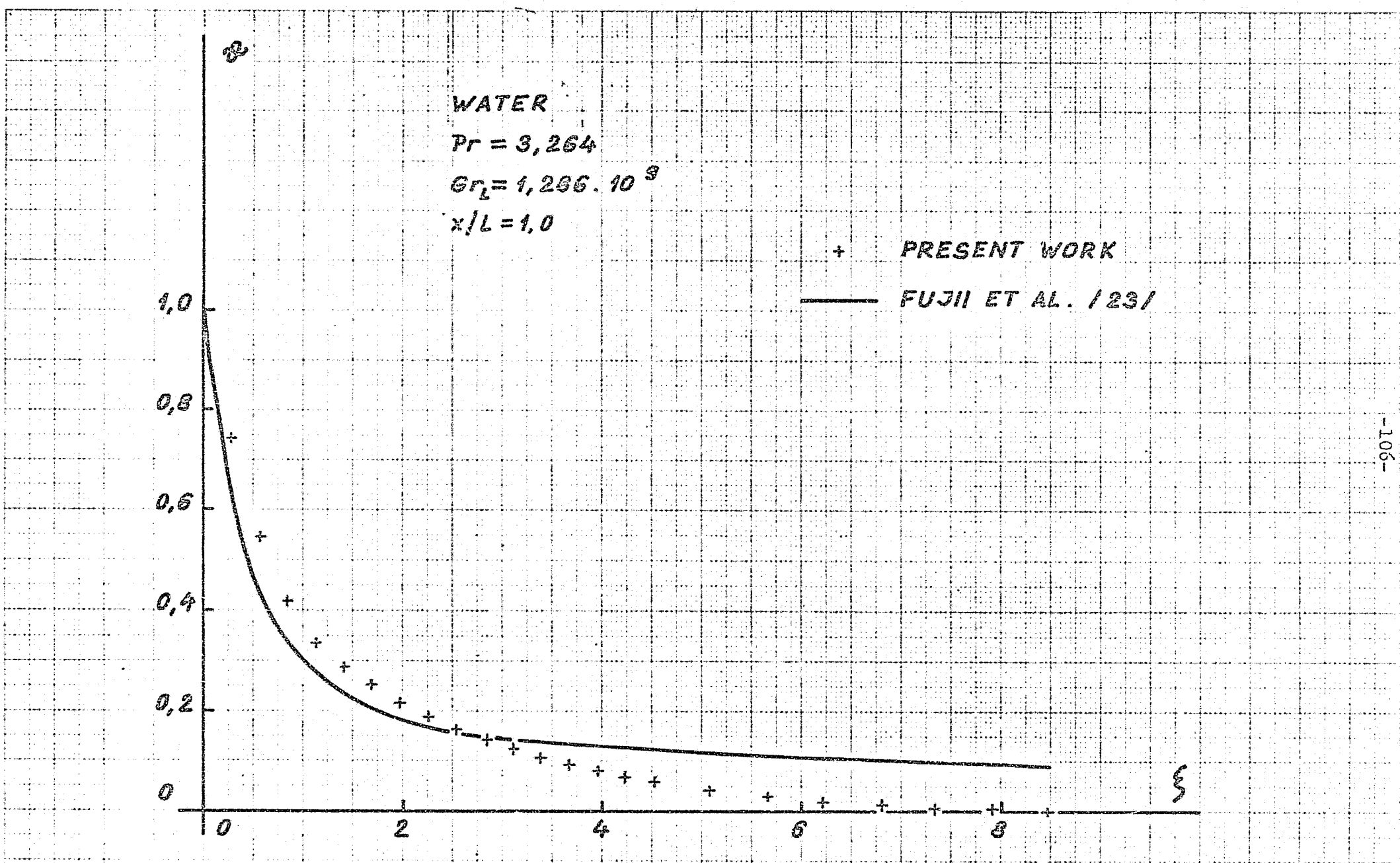

FIG. 47. TEMPERATURE PROFILE IN WATER COMPARED WITH FUJII ET AL. /23/

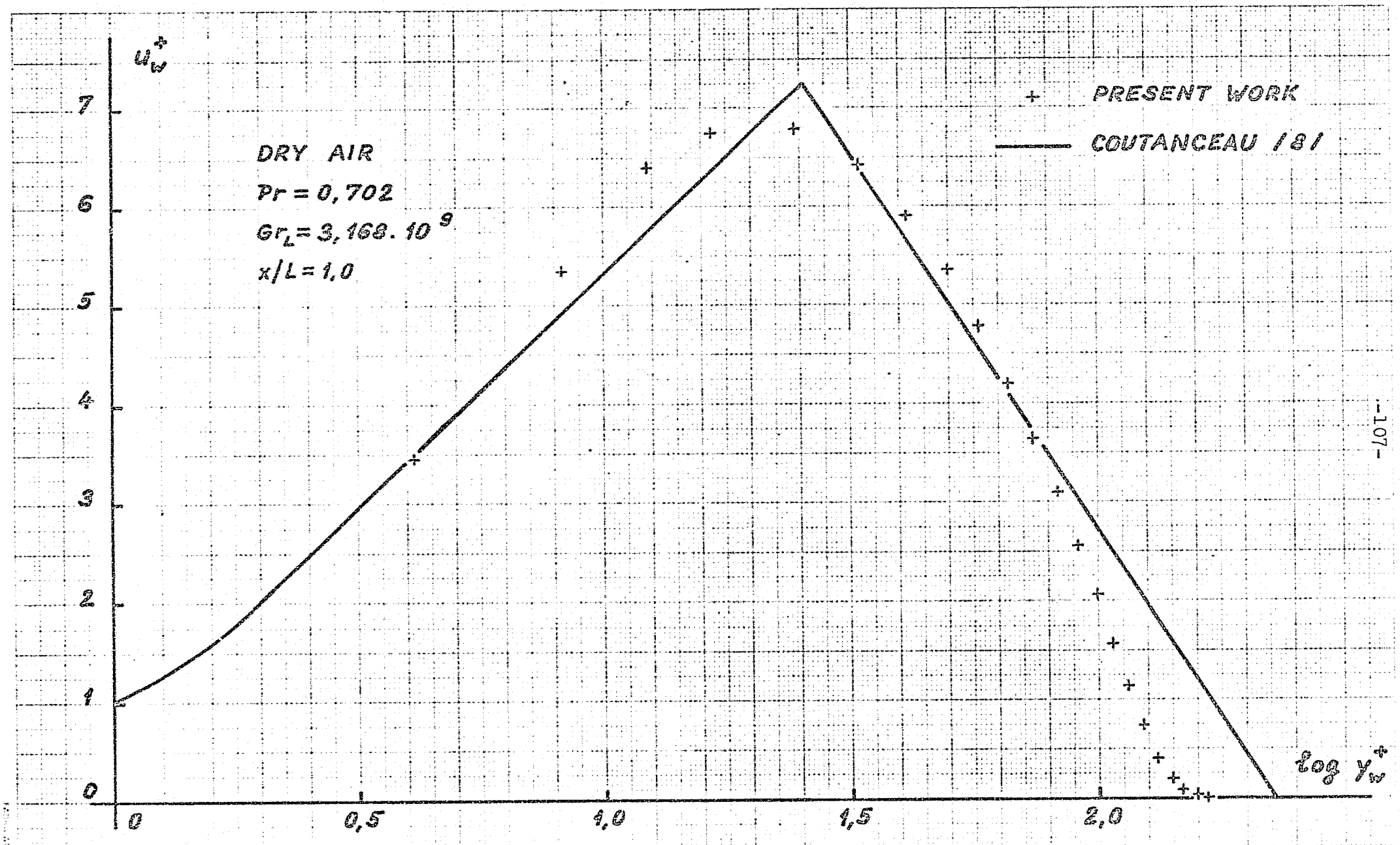

FIG. 48. VELOCITY PROFILE IN AIR COMPARED WITH COUTANCEAU /81/

Their formula is

$$\frac{u}{u_{max}} = 1,61 \left(\frac{y}{4,1\delta}\right)^{\frac{1}{10}} \left(1 - \frac{y}{4,1\delta}\right)^{4} \quad \text{for } \frac{y}{\delta} > 0,15 \qquad (107)$$

with

$$\delta = \int_0^{\infty} \frac{u}{u_{max}} dy \qquad (108)$$

Fig. 49 shows this approximation together with our results. The agreement is not very good. This is not surprising, as the measurements of Vliet & Liu were made for a uniform wall heat flux and a perfect agreement of their velocity profiles with our isothermal plate results cannot be expected. The comparison was only made due to the lack of more suitable data.

There are no published data about velocity profiles in mercury, and for this simple reason the peculiar velocity profiles resulting from our calculations cannot be verified at the present time.

7.6 Heat Transfer Coefficients

The rate of heat transfer between the plate and the adjacent fluid is given by the overall heat transfer coefficient, which is usually expressed in a nondimensional form as the overall Nusselt number

$$Nu_L = \frac{\bar{h} L}{k} \qquad (109)$$

The steady state Nusselt numbers, obtained at the end of our calculated transients, will be compared here with values calculated from various empirical or theoretical formulae, available from the literature. The multiplicity of these formulae and the considerable disagreement among their results show quite clearly, that all investigations of turbulent natural convection are a difficult undertaking.

The formulae for both air and water are identical and our results are compared in Table 4 with the predictions according to different authors. All empirical correlations are given in the form

$$Nu_L = a \left(Pr\, Gr_L\right)^{\frac{1}{3}} \qquad (110)$$

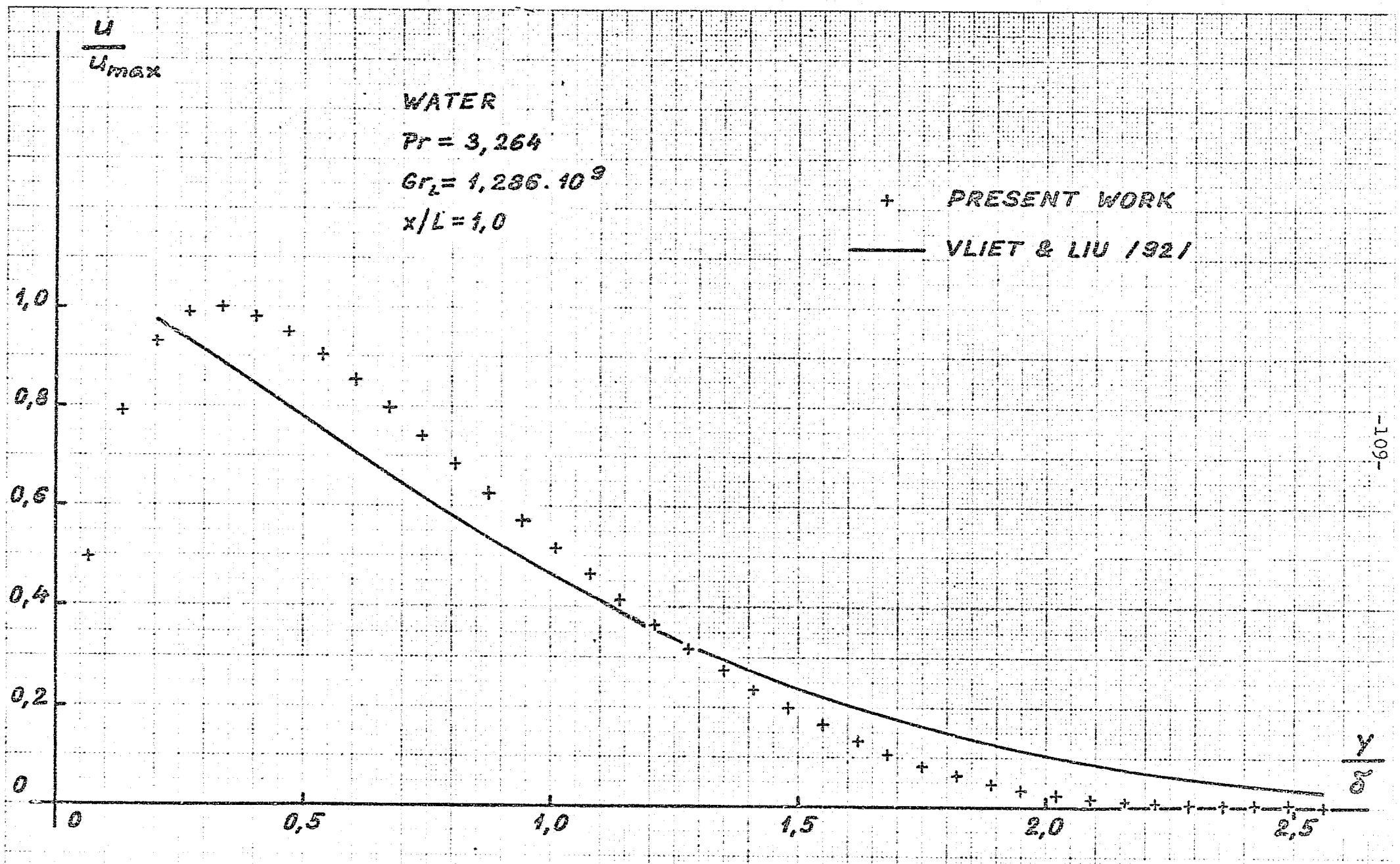

FIG. 49. VELOCITY PROFILE IN WATER COMPARED WITH VLIET & LIU /92/

TABLE 4. OVERALL NUSSELT NUMBERS IN AIR AND WATER

	AIR		WATER	
AUTHOR AND FORMULA	Nu_L	± %	Nu_L	± %
PRESENT WORK				
FINITE DIFFERENCES	141,661	0	199,671	0
EQUATION (96)	130,940	− 7,57	183,134	− 8,28
KUTATELADZE & BORISHANSKII /140/ $0,135\ (Gr_L Pr)^{\frac{1}{3}}$	176,191	+ 24,38	217,735	+ 9,05
McADAMS /145/ $0,129\ (Gr_L Pr)^{\frac{1}{3}}$	168,360	+ 18,85	208,057	+ 4,20
SAUNDERS /74/ $0,110\ (Gr_L Pr)^{\frac{1}{3}}$	143,564	+ 1,34	177,414	− 11,15
BAYLEY /2/ $0,100\ (Gr_L Pr)^{\frac{1}{3}}$	130,512	− 7,87	161,285	− 19,22
KATO ET AL. /46/ $0,138\ Gr_L^{0,36}\ (Pr^{0,175} - 0,55)$	141,616	− 0,03	178,502	− 10,60
ECKERT & JACKSON /11/ $0,0246\ Gr_L^{\frac{2}{5}} Pr^{\frac{7}{15}} (1 + 0,494\ Pr^{\frac{2}{3}})^{-\frac{2}{5}}$	115,410	− 18,53	140,117	− 29,83

and the coefficients resulting from our calculations are $a = 0{,}10854$ for air and $a = 0{,}12380$ for water. These values are in between the coefficients given by other authors, and our predictions seem to be quite reasonable. In fact, the coefficient in the case of air is almost equal to the value obtained by Saunders /74/, who made his measurements in air.

It is probable, that the influence of the Prandtl number is not so simple as assumed in the equation (110), and this could be the reason for the difference between our own coefficients for air and water. There are two theoretical formulae, both obtained from an integral analysis, and in both cases the dependence on the Prandtl number is more complicated.

Our results are in good agreement with the formula of Kato et al. /46/, although that formula is valid for $Ra_L > 10^{10}$. In the case of air, the prediction of Kato et al. is practically equal to the result of our calculations. The formula of Eckert & Jackson /11/ gives Nusselt numbers substantially lower than our results. However, certain assumptions made in the derivation of that formula are questionable and the theory is regarded today as more or less outdated.

It is also possible to derive formulae for the overall Nusselt number from the least-squares correlations for local Nusselt numbers, which are

for air

$$Nu_x = 0{,}09653 \cdot Gr_x^{0{,}32912} \qquad (111)$$

for water

$$Nu_x = 0{,}16708 \cdot Gr_x^{0{,}33378} \qquad (112)$$

and for mercury

$$Nu_x = 0{,}08106 \cdot Gr_x^{0{,}25323} \qquad (113)$$

If we assume, that the exponent of the Prandtl number is the same as the exponent of the Grashof number, we obtain in the case of air

$$Nu_L = 0{,}10985 \; (Pr\, Gr_L)^{0{,}32912} \qquad (114)$$

and in the case of water

$$Nu_L = 0,11243 \; (Pr\, Gr_L)^{0,33378} \qquad (115)$$

These results indicate that the one-third power correlation is correct. Although our few results are hardly a sufficient foundation for some far-reaching conclusions, it seems to be reasonable to recommend the formula

$$Nu_L \doteq 0,11 \; (Pr\, Gr_L)^{\frac{1}{3}} \qquad (116)$$

for prediction of steady state overall Nusselt numbers in gases and in liquids with a Prandtl number similar to that of water. The one-third power means that the heat transfer coefficient becomes independent on the reference dimension. For design calculations of unsteady natural convection, the coefficient should be diminished to $a \doteq 0,10$. In this way, also the 'overshoot' is covered by the formula and there remains a safety margin in the steady state.

It was also attempted to correlate nondimensionally histories of the overall Nusselt number for both air and water. For this purpose, the coefficient a was plotted as a function of a nondimensional time previously used by Hellums & Churchill /41,42/, viz.

$$\frac{Nu_L}{\sqrt[3]{Ra_L}} = \phi\left(t\sqrt{\frac{g\,\beta\,\Delta T}{L}}\right) \qquad (117)$$

The air and water histories are shown in Fig. 50, and in these nondimensional coordinates the curves are quite similar. They cannot be identical, as can be seen from the equation (98) or (99) giving the time, when steady state is attained. If steady state be reached at the same nondimensional time in the cases of fluids with different Prandtl numbers, it follows from the equation (98) that the coordinates

$$\frac{Nu_L}{\sqrt[3]{Ra_L}} = \phi\left(\frac{t\sqrt{\frac{g\,\beta\,\Delta T}{L}}}{1,80\sqrt{1,5+Pr}}\right) \qquad (118)$$

should be used. On the other hand, the requirement of identical curves during the initial pure conduction regime can be satisfied only with the coordinates

$$\frac{Nu_L}{\sqrt[3]{Ra_L}} = \phi\left[t\left(\frac{\beta\,\Delta T\, g\,\sqrt{\alpha}}{\nu}\right)^{\frac{2}{3}}\right] \qquad (119)$$

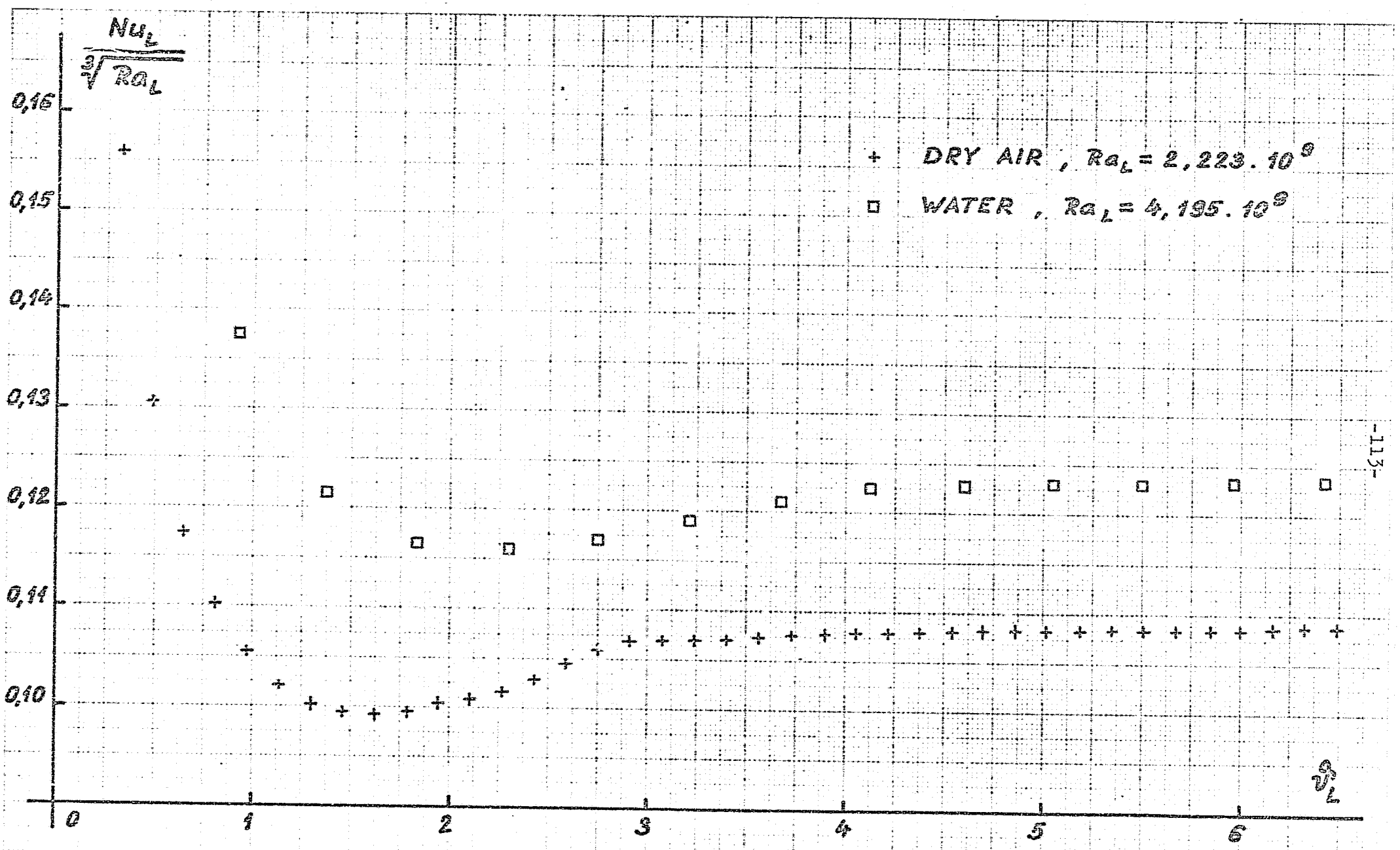

FIG. 50 . NONDIMENSIONAL TRANSIENT HEAT TRANSFER IN AIR AND WATER

It is evident, that the requirements of equations (118) and (119) are incompatible and the histories cannot be expressed by a curve identical for both air and water (or generally fluids with different Prandtl numbers).

The overall Nusselt number resulting from our calculation with mercury is compared in Table 5 with the predictions of other workers. The correlations are less abundant here, and strictly speaking only two formulae are available for comparison. The agreement with the empirical formula for liquid metals given by Heřmanský /126/ is quite good. Bayley /2/ gives a theoretical correlation for mercury at boiling temperature ($Pr = 0,01$) only, and it is

$$Nu_L = 0,68 \cdot Gr_L^{0,25} \qquad (120)$$

In Table 5, the influence of the Prandtl number was assumed to be of the form

$$Nu_L = a\,(Pr^2 Gr_L)^{0,25} \qquad (121)$$

and the Bayley's correlation was correspondingly adjusted. The agreement with this correlation is also reasonable.

The empirical correlation of Kutateladze /139/ predicts a much lower Nusselt number, but it is valid for $Pr^2 Gr_L < 10^4$ only. On the other hand, the theoretical correlation of Kato et al. /46/ predicts a considerably higher Nusselt number, but it is valid for $Ra_L > 10^{10}$. Our result is in between and therefore these discrepancies establish, at least indirectly, the validity of our result.

If a correlation of the form (121) is assumed, the coefficient corresponding to our result is $a = 0,73325$. We can also derive a formula for the overall Nusselt number from the least-squares approximation of local Nusselt numbers (113) in a similar way as it has been done for air and water. This time, we obtain

$$Nu_L = 0,66757\,(Pr^2 Gr_L)^{0,25323} \qquad (122)$$

It can be concluded, that our results indicate that the formula

$$Nu_L \doteq 0,7\,(Pr^2 Gr_L)^{0,25} \qquad (123)$$

TABLE 5. OVERALL NUSSELT NUMBERS IN MERCURY

AUTHOR AND FORMULA	Nu_L	± %
PRESENT WORK FINITE DIFFERENCES EQUATION (96)	 66,5002 64,1753	 0 - 3,50
HEŘMANSKÝ /126/ $0,16\,[Pr^2 Gr_L/(1+Pr)]^{\frac{1}{3}}$	64,6239	-2,82
BAYLEY /2/ $0,80\,(Pr^2 Gr_L)^{0,25}$	72,5543	+9,10
KUTATELADZE /139/ $0,53\,(Pr^2 Gr_L)^{0,25}$	48,0672	-27,72
KATO ET AL. /46/ $0,183\,Gr_L^{0,32} Pr^{0,55}$	81,2187	+22,13

can be used for prediction of steady state overall Nusselt number in liquid metals. This particular form means that the heat transfer coefficient does not depend on the fluid kinematic viscosity.

8. CONCLUSIONS

Finally, our method and the obtained results will be critically reviewed, and some suggestions for further work will also be given.

8.1 Evaluation of the Present Work

There are no publications concerning the problem of unsteady turbulent free convection and in this sense the work described in this dissertation was a venture into terra incognita. Moreover, the first solution of the corresponding steady state problem only appeared in November 1974 /60/, when the development of the present computer programme had already been finished.

The problem of unsteady turbulent free convection over a vertical flat plate was formulated mathematically by a system of simultaneous nonlinear partial differential equations, incorporating a phenomenological turbulence model. The system is of a parabolic nature and was solved by an explicit finite-difference method.

A computer programme was written and calculations were made for air, water, and mercury. Each transient consists of three stages: the initial conduction regime, an intermediate stage, and the steady state. The results concerning the first and third stages were compared with published data of other research workers. The agreement was reasonable and no significant discrepancies were discovered.

In all cases calculated, heat transfer coefficient goes through a temporary minimum, which is called an 'overshoot'. The existence of such an 'overshoot' is very important from the design engineer's point of view. However, the transient is extremely fast and the 'overshoot' is not significant in comparison with the final steady state value of the heat transfer coefficient.

The main drawback of the calculations presented in this dissertation is the fact, that they were made for relatively low Rayleigh numbers. Although most authors prescribe turbulent correlations for our Rayleigh numbers, this region is now usually called transitional-turbulent, i.e. a region which is no longer laminar but not fully turbulent yet.

The economic point of view is especially important here, as our computing times are already for the relatively low Rayleigh

numbers very long. If higher plates were considered, the computing times would increase rapidly due to the increased number of grid points because of both a longer plate and a thicker boundary layer, due to a shorter permissible time step because of higher values of of velocities and effective viscosity at the upper end of the plate, and also due to a longer time required to attain steady state.

If computers were available that had speeds an order of magnitude greater than they have at this writing, it would be easily possible to make with the present method calculations of fully turbulent natural convection transients in acceptable computing times. However, with the present-day machines such calculations can hardly be contemplated.

8.2 Suggestions for Further Work

The solvability of turbulent free convection by a phenomenological turbulence model had not been established before the present work, and for this reason the formulation was kept as simple as possible. There is a considerable scope for refinements and some of them will be mentioned below.

The physical model can be refined by using variable properties instead of the present Boussinesq approximation. In this way the results would certainly be improved and calculations could be made in a region of great changes of the values of the properties, e.g. near the critical state.

The presently used turbulence model was chosen as one of the simplest available, and a more sophisticated model (e.g. Hanjalić & Launder /124/) could be employed. The same applies to the law of the wall. Instead of the constant turbulent Prandtl number, a suitable formula for variable turbulent Prandtl number could be used.

Furthermore, the assumption of turbulence starting from the leading edge should be abandonded and a suitable criterion for transition from the laminar to turbulent part of the boundary layer incorporated into the physical model.

The numerical method should be investigated with the goal of an improved efficiency. Implicit methods are inherently more stable than the presently employed explicit one, and they permit longer time steps. On the other hand, the calculations for one time step are more time-consuming. It is therefore uncertain, if an implicit

method improves economy in our case, but this possibility should be investigated.

Unfortunately, all the abovementioned improvements would not only substantially complicate the computer programme, but the refinements in the physical model would also increase the computing times and thereby worsen the economy.

The calculations presented in this dissertation were made for simple initial and boundary conditions. More complicated situations, such as thermally stratified fluids, nonisothermal wall or mixed convection could also be investigated with the present method.

It has been shown by Gebhart /24/, that the thermal capacity of the wall has a decisive influence on the transient. Therefore, the next big step in the treatment of unsteady turbulent free convection should be an attempt to solve the boundary layer equations simultaneously with the temperature field in the plate, which is coupled with the boundary layer through the common heat flux at the plate surface. To mention just one difficulty, the heat conduction equation is elliptic in both x - and y-directions, while the boundary layer equations themselves are parabolic in the x-direction. It is probably impossible to solve this problem with the present-day computers.

It could also be interesting to make some measurements of the complete transient. Quite generally, all measurements of natural convection are very sensitive to any disturbances in the surrounding fluid and must be done under carefully controlled conditions. Thus far, optical interferometric methods have been exclusively employed for all measurements of temperature profiles in natural convection transients. The Mach-Zehnder interferometer, used for this purpose at the Heat Transfer Laboratory of the University of Minnesota, has been described by Goldstein /121/ and is a standard example of this type of equipment.

No results concerning the development of velocity profiles in natural convection transients, either laminar or turbulent, have been reported. This is not surprising, as the results would be completely irrelevant from the engineering point of view. Moreover, it is very difficult to imagine a suitable measurement technique for such an undertaking.

Although experimental data covering the whole transient would be very useful for comparison with our theoretical results, such

experiments are certainly not necessary for the verification of our method. The results of our calculations for the initial period of the transient agree almost perfectly with the analytical solution for pure conduction, and the final values agree also quite well with published experimental data for steady state turbulent free convection. The correctness of both the initial and final stage gives credence to the results for the intermediate stage as well.

Appendix A. COMPUTER PROGRAMME

A computer programme, based on the numerical algorithm described in Chapter 5, was written, successfully compiled and employed for calculations. A short description of the programme and its complete listing are given in this Appendix.

A.1 Programme Description

The programme was written in FORTRAN IV, and the G-level compiler was used for the compilation. The programme was run on the IBM 370/145 computer of the University of the Witwatersrand. However, it should be possible to run the programme on any other (big enough) machine, if all options of the G-compiler were available. The present version requires approximately 230 K of core storage space, but this value can be easily adjusted by the DIMENSION statements. Moreover, a temporary workfile on a DASD (direct access storage device, usually a disk) is employed for storage of some intermediate results. There is also a plotter subroutine, which would have to be changed eventually, should the programme be transferred to some other installation.

The more important symbols used in the programme are defined in the following Section. The programme consists of the MAIN programme and seven subprogrammes fulfilling the following tasks:

BLOCK DATA - initialisation of permanent arrays defined by DATA statements;

PISA - printing of the velocity, temperature, and effective viscosity fields;

GRAF - plotting of the velocity, temperature, and effective viscosity profiles;

PLCH - numerical integration according to equation (93) (used for the calculation of the overall Nusselt number);

MEZI - interpolation between the grid points by Lagrange polynomials (used in the plotted curves);

LONUS - iterative solution of a system of two nonlinear algebraic equations (used in the least-squares approximation of the local Nusselt numbers);

STELAM - initialisation of temperature, velocity, and effective viscosity fields by means of the Eckert & Jackson /11/ correlations (can be used for the calculations of steady state).

A.2 Symbols Used in the Programme

The meaning of the more important symbols, used in the computer programme, is given in the following Table A-1, which should be consulted together with the Nomenclature.

TABLE A-1. COMPUTER PROGRAMME SYMBOLS

A	=	A	PRLAM	=	Pr
APRO1	=	a	PRTUR	=	Pr_t
APRO2	=	b	R	=	ω
B	=	B	RDYN	=	μ
BETA	=	β	RLAM	=	ν
CP	=	c_p	RO	=	ϱ
CST	=	t	T	=	T
DELC	=	Δt	TAU	=	τ_w
DELX	=	Δx	TF	=	T_f
DELY	=	Δy	TW	=	T_w
DNU	=	Nu_x	U	=	u
DNUL	=	Nu_L	V	=	v
FO	=	ϑ_x	VOD	=	k
GRVT	=	g	XCB	=	x
I	=	i	XNU	=	Gr_x
IMZ	=	i_{max}	XNUL	=	Gr_L
J	=	j	Y	=	y
JMZ	=	j_{max}	YDELR	=	y^+_{eim}

A.3 Programme Listing

A complete FORTRAN listing of the computer programme is presented on the following pages 123 - 138. However, JCL (job control language) cards, which are specific for an installation, are not included in the listing.

```
      C     NACO
      C     UNSTEADY TURBULENT FREE CONVECTION OVER A VERTICAL FLAT PLATE
      C     JAROSLAV RENAR
      C     UNIVERSITY OF THE WITWATERSRAND,JOHANNESBURG,R.S.A.
      C
0001        DEFINE FILE 8(72,61,U,IFL)
      C
0002        COMMON /CMN1/LIN,MEDA,IKROKY,M,CST,KLI,KLJ,JAK,KROKY
0003        COMMON /CMN2/PRLAM,XNJL,TIME,XCBK,BGRX
0004        COMMON /CMN4/TEK,TURB
0005        COMMON /CMN5/XCB,Y,U,V,T,R,CER
0006        COMMON /CMN6/XNU,CNU,DNU
      C
0007        LOGICAL LYD,LPLOT,LST
0008        LOGICAL LAK,LEV
      C
0009        DIMENSION T(161,61),U(161,61),V(161,61),R(161,61)
0010        DIMENSION TS(61),TN(61),US(61),UN(61),RS(61),RN(61),Y(61),DCB(61)
0011        DIMENSION YGR(61),KROKY(61),CER(61)
0012        DIMENSION XCB(161),XNU(161),CNU(161),CONU(161)
0013        DIMENSION TAU(161),DNU(161),JDEL(161),CFO(16')
0014        DIMENSION KPS(49)
0015        DIMENSION MGR(8),JMZGR(8),TIME(8)
0016        DIMENSION AGR(3),BGR(3),IGR(3)
0017        DIMENSION TEK(2,3),TURB(3),JAK(4)
      C
0018        EQUIVALENCE (TF,DTT),(ROYN,ALCGR,DUU),(AI,AJ,DUUM),
     1              (CGR,TAUUU),(XER,DRR),
     2              (BETA,DCXU),(DELTA,DCYV),(XCBI,YDEL,RIJL)
0019        EQUIVALENCE (PS(1),YGR(1))
0020        EQUIVALENCE (IMZ3,IFLFIN)
0021        EQUIVALENCE (TF,AGR(1))
      C
0022        DATA GRVT/980.665/
0023        DATA AGR/2*0.0,1.0/
      C
0024        PROPER(X,A0,A1,A2,A3,A4,A5)=A0+X*(A1+X*(A2+X*(A3+X*(A4+X*A5))))
      C
0025        KAR=5
0026        LIN=6
0027        KOS=8
      C
0028        NRUN=0
0029      1 READ (KAR,1001,END=13)IMZ,JMZ,MEZ,KPSM,KLI,MEDA
0030        KLJ=1
0031        READ (KAR,1001)KAMPA
0032        WRITE (LIN,2001)
0033        IF (MEDA.EQ.3)READ (KAR,1004)(TEK(I,3),I=1,2)
0034        WRITE (LIN,2002)(TEK(I,MEDA),I=1,2)
0035        NRUN=NRUN+1
0036        IF (KPSM.NE.49)GO TO 24
0037        READ (KAR,1001)KPSTAR,KPSTEP
0038        DO 27 I=1,49
0039       27 KPS(I)=KPSTAR+KPSTEP*(I-1)
0040        GO TO 25
0041       24 READ (KAR,1001)(KPS(I),I=1,KPSM)
0042       25 READ (KAR,1003)LPLOT
0043        IF (.NOT.LPLOT)GO TO 49
```

```
0044              READ (KAR,1001)IGRM,MGRM
0045              READ (KAR,1001)(IGR(I),I=1,IGRM)
0046              READ (KAR,1001)(MGR(I),I=1,MGRM)
0047              READ (KAR,1002)BGRX,(BGR(I),I=1,3)
0048           49 IMZ1=IMZ-1
0049              IMZ3=IMZ-3
0050              JMZ1=JMZ-1
0051              JMZ2=JMZ-2
0052              READ (KAR,1002)DELX,DELY,DELC
0053              HAPLCH=DELX/22.5
0054              READ (KAR,1002)UPS,VPS,TPS,RPS
0055              JAK(1)=ALOG10(ABS(UPS))+0.1
0056              JAK(2)=ALOG10(ABS(VPS))+0.1
0057              JAK(3)=ALOG10(ABS(TPS))+0.1
0058              JAK(4)=ALOG10(ABS(RPS))+0.1
0059              DO 28 I=1,4
0060           28 JAK(I)=-JAK(I)
0061              CMAX=DELC*FLOAT(MEZ)
0062              ZDELY=1./DELY
0063              ZDELY2=0.5*ZDELY
0064              ZDELY6=ZDELY/6.
0065              READ (KAR,1002)PRTUR,A,B,YDELR
0066              LYD=YDELR.EQ.0.0
0067              READ (KAR,1002)TW,TF
0068              TW11=-11.+TW
0069              TFPT=TF+0.1
0070              TQ=0.5*(TW+TF)
0071              PRINT (LIN,2003)TW,TF,TQ
0072              WRITE (LIN,2004)
0073              GO TO (35,21,36),MEOA
0074           35 BETA=1./(273.16+TQ)
0075              RLAM=PROPER(TQ, 0.1329190E+01, 0.8701713E-02, 0.1058708E-04,
                 1                -0.6733529E-08, 0.1087031E-10,-0.2048712E-13)
                 2                *0.1E+00
0076              CP=PROPER(TQ, 0.1006253E+01, 0.1492203E-04, 0.3047016E-06,
                 1               0.1941328E-08,-0.1014805E-10, 0.1576442E-13)
                 2               *0.1E+08
0077              RO=PROPER(TQ, 0.1292283E+01,-0.4725332E-02, 0.1689556E-04,
                 1              -0.5331271E-07, 0.1184000E-09,-0.1248237E-12)
                 2              *0.1E-02
0078              VOD=PROPER(TQ, 0.2414441E+01, 0.7986858E-02,-0.4491811E-05,
                 1               0.1143821E-07,-0.6061998E-10, 0.1228035E-12)
                 2              *0.1E+04
0079              GO TO 37
0080           21 BETA=PROPER(TQ,-0.5975000E-01, 0.1657302E-01,-0.1976530E-03,
                 1               0.1839307E-05,-0.8085664E-08, 0.9615385E-11)
                 2              *0.1E-02
0081              RLAM=PROPER(TQ, 0.1763000E+01,-0.5560162E-01, 0.1134461E-02,
                 1              -0.1448397E-04, 0.1023601E-06,-0.3012821E-09)
                 2              *0.1E-01
0082              CP=PROPER(TQ, 0.4213925E+01,-0.2959161E-02, 0.9098470E-04,
                 1             -0.1357474E-05, 0.1074738E-07,-0.3301282E-10)
                 2             *0.1E+08
0083              RO=PROPER(TQ, 0.9998000E+00, 0.6833228E-04,-0.8494755E-05,
                 1              0.6331555E-07,-0.3321678E-09, 0.6410256E-12)
                 2              *0.1E+01
0084              VOD=PROPER(TQ, 0.5905833E+00, 0.3300612E-02,-0.6698572E-04,
                 1               0.1248397E-05,-0.1254371E-07, 0.4807692E-10)
```

```
                2                *0.1E+06
0085              GO TO 37
0086           36 READ (KAR,1002)BETA,RLAM,CP,RO,VOD
0087           37 RPS=RPS/RLAM
0088              WRITE (LIN,2005)CP
0089              WRITE (LIN,2006)RO
0090              WRITE (LIN,2007)RLAM
0091              RLAM3=-3.*RLAM
0092              READ (KAR,1002)HTGEXP,CKROKY
0093              IKROKY=-(ALOG10(CKROKY)+0.1)
                C
0094              RDYN=RO*RLAM
0095              WRITE (LIN,2009)RDYN
0096              WRITE (LIN,2009)VOD
0097              WRITE (LIN,2010)BETA
0098              RE2=RDYN*ZDELY2
0099              PRLAM=RDYN*CP/VOD
0100              WRITE (LIN,2011)PRLAM
0101              DELTA=TW-TF
0102              HGRCGR=BETA*DELTA*GRVT
0103              CGR=HGRCGR/RLAM**2
0104              ALCGR=ALOG(CGR)
0105              CONU1=-ZDELY6/DELTA
0106              CDCFO=SQRT(HGRCGR)
0107              XNU(1)=0.0
0108              CFC(1)=0.0
0109              DO 17 I=2,IMZ
0110              AI=I-1
0111              XCBI=AI*DELX
0112              XCB(I)=XCBI
0113              CFC(I)=CDCFO/SQRT(XCBI)
0114              XNU(I)=CGR*XCBI**3
0115              CNU(I)=ALCGR+3.*ALOG(XCBI)
0116           17 CONU(I)=CONU1*XCBI
0117              XNUL=XNU(IMZ)
0118              WRITE (LIN,2012)XNUL
0119              WRITE (LIN,2013)
0120              WRITE (LIN,2014)(TURB(I),I=1,3)
0121              WRITE (LIN,2015)YDELR
0122              WRITE (LIN,2016)A,B
0123              WRITE (LIN,2017)PRTUR
0124              WRITE (LIN,2018)DELX,DELY,DELC
                C
0125              DCX=DELC/DELX
0126              DCY=DELC/DELY
0127              DCY2=DCY/DELY
0128              DCY2K1=DCY2*RLAM*(1./PRLAM-1./PRTUR)
0129              DCY2K2=DCY2/PRTUR
0130              DCGB=DELC*GRVT*BETA
0131              DYX=DELY/DELX
0132              HGR=DELC*B
0133              CR=0.015376/RLAM
0134              Y(1)=0.0
0135              KROKY(1)=0
0136              DO 16 J=2,JMZ
0137              AJ=J-1
0138              Y(J)=DELY*AJ
0139              KROKY(J)=CKROKY*Y(J)+0.1
```

```
0140            CER(J)=CR*Y(J)
0141         16 DCB(J)=HOR/Y(J)**2
0142            DCA=A*DCY
0143            HORYD=YDELR*RLAM*SQRT(RO)
0144            JDEL(1)=0
      C
0145            DO 2 I=1,IMZ
0146            U(I,1)=0.0
0147            V(I,1)=0.0
0148            R(I,1)=RLAM
0149            T(I,1)=TH
0150            TAU(I)=0.0
0151            U(I,JMZ)=0.0
0152            V(I,JMZ)=0.0
0153            R(I,JMZ)=RLAM
0154          2 T(I,JMZ)=TF
      C
0155            DO 3 J=2,JMZI
0156            U(1,J)=0.0
0157            V(1,J)=0.0
0158            R(1,J)=RLAM
0159          3 T(1,J)=TF
      C
0160            CST=0.0
0161            M=0
      C
0162            LST=.FALSE.
0163            GO TO (29,30),KAMPA
0164         30 CALL STELAM(RLAM,CGR,TF,DELTA,DELY,DYX,IMZ,JMZ,JMZI)
0165            DO 42 I=2,IMZ
0166            TAU(I)=RO2*(4.*U(I,2)-U(I,3))
0167         42 JDEL(I)=0
0168            LST=.TRUE.
0169            GO TO 43
0170         44 LST=.FALSE.
0171            GO TO 45
0172         29 CONTINUE
      C
0173            DO 4 I=2,IMZ
0174            DO 4 J=2,JMZ1
0175            U(I,J)=0.0
0176            V(I,J)=0.0
0177            R(I,J)=RLAM
0178          4 T(I,J)=TF
      C
0179         45 IPISA=1
0180            MGRN=1
0181            IFL=1
0182            FIND (KOS'IFL)
      C
0183          5 CST=CST+DELC
0184            M=M+1
      C
0185            DO 7 J=2,JMZI
0186            TS(J)=TF
0187            US(J)=0.0
0188          7 RS(J)=RLAM
      C
```

```
0189              I=1
0190            6 IM1=I
0191              I=I+1
0192              TAUOD=SQRT(TAU(I))
0193              IF (TAUOD)32,22,32
0194           32 YDEL=HORYD/TAUOD
0195              JDEL(I)=0.5+YDEL/DELY
0196              JDELI=JDEL(I)
0197              GO TO 23
0198           22 JDEL(I)=0
0199              JDELI=0
                C
0200           23 J=1
0201              TIJ=TW
0202              UIJ=0.0
0203              RIJ=RLAM
0204              JP1=2
0205              TIJP1=T(I,2)
0206              UIJP1=U(I,2)
0207              RIJP1=R(I,2)
0208              RP=0.5*(RIJ+RIJP1)
0209              DTT=TIJP1-TIJ
0210              DDT=(DCY2K1+DCY2K2*RP)*DTT
0211              DUU=UIJP1-UIJ
0212              DDU=DCY2*RP*DUU
0213            8 JM1=J
0214              TIJM1=TIJ
0215              UIJM1=UIJ
0216              RIJM1=RIJ
0217              J=JP1
0218              TIJ=TIJP1
0219              UIJ=UIJP1
0220              RIJ=RIJP1
0221              JP1=JP1+1
0222              TIJP1=T(I,JP1)
0223              UIJP1=U(I,JP1)
0224              RIJP1=R(I,JP1)
0225              DCXU=DCX*UIJ
0226              DCYV=DCY*V(I,J)
0227              RP=0.5*(RIJ+RIJP1)
0228              DTT=TIJP1-TIJ
0229              DDTM=DDT
0230              DDT=(DCY2K1+DCY2K2*RP)*DTT
0231              DUUM=DUU
0232              DUU=UIJP1-UIJ
0233              DDUM=DDU
0234              DDU=DCY2*RP*DUU
                C
0235              IF (JM1-JDELI)31,34,18
0236           31 XER=CER(J)*UIJ
0237              EPSR=XER*(1.-EXP(-XER))
0238              RN(J)=RLAM*(1.+EPSR)
0239              GO TO 15
0240           34 DDR=0.5*(RIJM1+RIJ)*(RIJ-RIJM1)
0241           18 RIJL=RIJ-RLAM
0242              DRP=RIJP1-RIJ
0243              DDRM=DDR
0244              DDR=DCY2*RP*DRR
```

```
0245            RN(J)=RIJ-DCXU*(RIJ-R(IM1,J))-DCYV*DRR+DDR-DDRM+
               1      DCA*RIJL*ABS(DUUM)-DCB(J)*RIJ*RIJL
0246          15 TN(J)=TIJ-DCXU*(TIJ-T(IM1,J))-DCYV*DTT+DDT-DDTM
0247            UN(J)=UIJ-DCXU*(UIJ-U(IM1,J))-DCYV*DUU+DDU-DDUM+
               1      DCGB*(TIJ-TF)
0248            V(I,J)=V(I,JM1)-DYX*(UN(J)-US(J))
0249            IF (J-JMZ1)8,108,108
0250          108 TAU(I)=RD2*(4.*UN(2)-UN(3))
              C
0251            DO 9 J=2,JMZ1
0252            T(IM1,J)=TS(J)
0253            TS(J)=TN(J)
0254            R(IM1,J)=RS(J)
0255            RS(J)=RN(J)
0256            U(IM1,J)=US(J)
0257          9 US(J)=UN(J)
              C
0258            V(I,JMZ)=V(I,JMZ1)
0259            IF (I-IMZ)6,106,106
0260          106 CONTINUE
              C
0261            DO 10 J=2,JMZ1
0262            T(IMZ,J)=TN(J)
0263            U(IMZ,J)=UN(J)
0264            R(IMZ,J)=RN(J)
0265          10 V(1,J)=V(1,J-1)-DYX*U(2,J)
0266            V(1,JMZ)=V(1,JMZ1)
              C
0267            IF (M.NE.KPS(IPISA))GO TO 14
0268          43 WRITE (LIN,2001)
0269            CALL PISA(UPS,1,U,IMZ,JMZ)
0270            WRITE (LIN,2001)
0271            CALL PISA(VPS,2,V,IMZ,JMZ)
0272            WRITE (LIN,2001)
0273            CALL PISA(TPS,3,T,IMZ,JMZ)
0274            IF (LYD)GO TO 39
0275            WRITE (LIN,2001)
0276            CALL PISA(RPS,4,R,IMZ,JMZ)
0277          39 WRITE (LIN,2001)
0278            WRITE (LIN,2019)CST,M,(TEK(J,MEDA),J=1,2),PRLAM,HTGEXP,XNUL
0279            DNU(1)=0.0
0280            DO 20 I=2,IMZ
0281          20 DNU(I)=CONU(I)*(TWL1+18.*T(I,2)-9.*T(I,3)+2.*T(I,4))
0282            I=IMZ
0283          38 FO=CST*CFO(I)
0284            IF (I.EQ.1)GO TO 47
0285            HTG=DNU(I)/XNU(I)**HTGEXP
0286            GO TO 48
0287          47 HTG=0.C
0288          48 WRITE (LIN,2021)I,XCB(I),JDEL(I),TAU(I),FO,XNU(I),DNU(I),HTG
0289            I=I-KLI
0290            IF (I)51,51,38
0291          51 DNUL=PLCH(IMZ,IMZ3,HAPLCH,DNU)
0292            WRITE (LIN,2022)XNUL,DNUL
0293            WRITE (LIN,2023)
0294            CALL LONUS(IMZ,2,APRO1,APRO2,&46)
0295            WRITE (LIN,2025)APRO1,APRO2
0296          46 IF (LST)GO TO 44
```

```
0297              IPISA=IPISA+1
                C
0298              IF (.NOT.LPLOT)GO TO 14
0299              IF (M.NE.MGR(MGRN))GO TO 14
0300              JMZGR(MGRN)=JMZ
0301              TIME(MGRN)=CST
0302              DO 19 K=1,IGRM
0303              IGRK=IGR(K)
0304              WRITE (KOS'IFL)(T(IGRK,J),J=1,JMZ)
0305              WRITE (KOS'IFL)(U(IGRK,J),J=1,JMZ)
0306              DO 40 J=1,JMZ
0307           40 YGR(J)=R(IGRK,J)/RLAM
0308           19 WRITE (KOS'IFL)(YGR(J),J=1,JMZ)
0309              MGRN=MGRN+1
                C
0310           14 COR=R(IMZ,JMZ2)/RLAM
0311              IF (U(IMZ,JMZ2).LT.0.1.AND.T(IMZ,JMZ2).LT.CMPT.AND.
                 1    COR.LT.1.01)GO TO 11
0312              DO 26 K=1,KLJ
0313              JMZ2=JMZ1
0314              JMZ1=JMZ
0315              JMZ=JMZ+1
0316              IF (JMZ.GT.61)GO TO 33
0317              Y(JMZ)=DELY*FLOAT(JMZ1)
0318              KROKY(JMZ)=CKROKY*Y(JMZ)+0.1
0319              DCB(JMZ)=HOR/Y(JMZ)**2
0320              DO 12 I=1,IMZ
0321              T(I,JMZ)=TF
0322              U(I,JMZ)=0.0
0323              V(I,JMZ)=V(I,JMZ1)
0324           12 R(I,JMZ)=RLAM
0325           26 CONTINUE
0326              IF (JMZ.EQ.41)KLJ=2
0327           11 IF (M.LT.MEZ)GO TO 5
0328              IF (CST.LT.CMAX)GO TO 5
                C
0329           33 IF (NRUN.NE.1.OR..NOT.LPLOT)GO TO 1
0330              WRITE (LIN,2024)
0331              WRITE (LIN,2020)(IGR(I),I=1,IGRM),(MGR(J),J=1,MGRM)
0332              IFLFIN=3*MGRM*IGRM+1
0333              IFLSTP=3*IGRM-1
0334              CALL MEZI(JMZ,JMZ1,DELY,Y)
0335              DO 41 K=1,IGRM
0336              IGRK=IGR(K)
0337              XCBK=XCB(IGRK)
0338              IFLK=3*(K-1)
0339              IGRAS=ALOG10(XNU(IGRK))+0.00001
0340              GRAS=XNU(IGRK)/10.**IGRAS
0341              DO 41 I=1,3
0342              IF (I.EQ.3.AND.LYD)GO TO 41
0343              IFL=I+IFLK
0344              LEV=IFL.NE.1
0345              FIND (KOS'IFL)
0346              CALL GRAF(I,AGR(I),BGR(I),LEV,GRAS,IGRAS)
0347              LEV=I.EQ.3.AND.K.EQ.IGRM
0348              DO 41 M=1,MGRM
0349              LAK=M.NE.MGRM
0350              JMZ=JMZGR(M)
```

```
0351              READ (KOS'IFL)(YGR(J),J=1,JMZ)
0352              IFL=IFL+IFLSTP
0353              IF (IFL.LT.IFLFIN)FIND (KOS'IFL)
0354              CALL CARA(M,JMZ,YGR,LAK,LEV)
0355           41 CONTINUE
               C
0356              GO TO 1
0357           13 STOP 1
               C
0358            1001 FORMAT (16I5)
0359            1002 FORMAT (5E15.6)
0360            1003 FORMAT (16L5)
0361            1004 FORMAT (20A4)
               C
0362            2001 FORMAT (1H1////1X,62H UNSTEADY TURBULENT FREE-CONVECTION OVER A VE
                    1RTICAL FLAT PLATE/2X,61(1H*)//)
0363            2002 FORMAT (1HO,8H FLUID :,12X,2A4/2X,5(1H-)/)
0364            2003 FORMAT (1HO,15H TEMPERATURES :/2X,12(1H-)/1X,5H WALL,33X,F5.1,
                    1        6H  DEGC/1X,6H FLUID,32X,F5.1,6H  DEGC/1X,5H MEAN,33X,
                    2        F5.1,6H  DEGC/)
0365            2004 FORMAT (1HO,19H FLUID PROPERTIES :/2X,16(1H-)/)
0366            2005 FORMAT (1X,14H SPECIFIC HEAT,26X,E13.7,12H  ERG/G*DEGC)
0367            2006 FORMAT (1X,8H DENSITY,32X,E13.7,9H  G/CM**3)
0368            2007 FORMAT (1X,20H KINEMATIC VISCOSITY,20X,E13.7,9H  CM**2/S)
0369            2008 FORMAT (1X,18H DYNAMIC VISCOSITY,22X,E13.7,13H  DYN*S/CM**2)
0370            2009 FORMAT (1X,21H THERMAL CONDUCTIVITY,19X,E13.7,15H  ERG/CM*S*DEGC)
0371            2010 FORMAT (1X,33H VOLUMETRIC EXPANSION COEFFICIENT,7X,E13.7,
                    1        8H  1/DEGC)
0372            2011 FORMAT (1HO,15H PRANDTL NUMBER,23X,F11.7)
0373            2012 FORMAT (1HO,15H GRASHOF NUMBER,25X,E13.7/)
0374            2013 FORMAT (1HO,19H TURBULENCE MODEL :/2X,16(1H-)/)
0375            2014 FORMAT (1X,18H LAW OF THE WALL :,7X,3A4)
0376            2015 FORMAT (1HO,24H INNER REGION LIMIT  YM+,14X,F7.3)
0377            2016 FORMAT (1HO,26H NEE-KOVASZNAY CONSTANT  A,12X,F7.3/1X,
                    1        26H NEE-KOVASZNAY CONSTANT  B,12X,F7.3)
0378            2017 FORMAT (1HO,25H TURBULENT PRANDTL NUMBER,13X,F7.3/)
0379            2018 FORMAT (1HO,21H FINITE DIFFERENCES :/2X,18(1H-)//1X,
                    1        19H DELTA X (VERTICAL),21X,F5.3,4H  CM/1X,
                    2        21H DELTA Y (HORIZONTAL),19X,F5.3,4H  CM//1X,
                    3        10H TIME STEP,30X,F6.4,3H  S)
0380            2019 FORMAT (1X,20H LOCAL HEAT TRANSFER,87X,5H TIME,9X,F5.2,3H  S/
                    1        108X,10H TIME STEP,I6/109X,2A4/1X,3H  I,3X,2H X,4X,
                    2        6H INNER,11X,14H WALL FRICTION,1X,13H NONDIM. TIME,2X,
                    3        11H GRASHOF(X),4X,11H NUSSELT(X),4X,7H NU(X)/,11X,
                    4        10H PRANDTL =,F12.5/6X,5H (CM),2X,12H REGION J(X),4X,
                    5        12H (DYN/CM**2),49X,8H GR(X)**,F6.4,4X,10H GRASHOF =,5X,
                    6        E10.4/)
0381            2020 FORMAT (5X,18I7)
0382            2021 FORMAT (1X,I3,F7.1,9X,I2,7X,5E15.7)
0383            2022 FORMAT (1HO,59X,11H GRASHOF(L),4X,11H NUSSELT(L)/1X,
                    1        24H OVERALL HEAT TRANSFER :,34X,2E15.7)
0384            2023 FORMAT (1HO,30H LEAST SQUARES APPROXIMATION :)
0385            2024 FORMAT (1H1////5X,22H PLOTTER DIAGNOSTICS ://)
0386            2025 FORMAT (1X,7H NU(X)=,E14.7,8H*GR(X)**,E14.7)
               C
0387              END
```

```
0001            BLOCK DATA
                C
0002            COMMON /CMN3/A(4,4,3)
0003            COMMON /CMN4/TEK(2,3),TURB(3),OSA(9,3),TEPISA(19,4)
                C
0004            DATA A/ 0.6720, 0.5040,-0.2240, 0.0480,
                1       0.4160, 0.8320,-0.3120, 0.0640,
                2       0.2240, 1.0080,-0.2880, 0.0560,
                3       0.0880, 1.0560,-0.1760, 0.0320,
                4      -0.0480, 0.8640, 0.2160,-0.0320,
                5      -0.0640, 0.6720, 0.4480,-0.0560,
                6      -0.0560, 0.4480, 0.6720,-0.0640,
                7      -0.0320, 0.2160, 0.8640,-0.0480,
                8       0.0320,-0.1760, 1.0560, 0.0880,
                9       0.0560,-0.2880, 1.0080, 0.2240,
                A       0.0640,-0.3120, 0.8320, 0.4160,
                B       0.0480,-0.2240, 0.5040, 0.6720/
0005            DATA TURB/4HDEIS,4HSLER,4H    /
0006            DATA TEK/4HDRY ,4HAIR ,4HRATE,4HR   ,4H    ,4H    /
0007            DATA TEPISA/4HVERT,4HICAL,4H VEL,4HOCIT,4HY FI,4HELD ,4H    ,
                1           4HU - ,4HVERT,4HICAL,4H VEL,4HOCIT,4HY CO,4HMPON,
                2           4HENT ,4H    ,4HCM/S,4H    ,4H   U,
                3           4HHORI,4HZONT,4HAL V,4HELOC,4HITY ,4HFIEL,4HD   ,
                4           4HV - ,4HHORI,4HZONT,4HAL V,4HELOC,4HITY ,4HCOMP,
                5           4HONEN,4HT  -,4HCM/S,4H    ,4H   V,
                6           4HTEMP,4HERAT,4HURE ,4HFIEL,4HD   ,4H    ,4H    ,
                7           4HT - ,4HTEMP,4HERAT,4HURE ,4H    ,4H    ,4H    ,
                8           4H    ,4H    ,4HDEGC,4H    ,4H   T,
                9           4HEFFE,4HCTIV,4HE VI,4HSCOS,4HITY ,4HFIEL,4HD   ,
                A           4HR - ,4HRATI,4HO EF,4HFECT,4HIVE ,4HV./K,4HINEM,
                B           4HATIC,4H V. ,4HMOND,4HIM. ,4H   R/
0008            DATA OSA/4H    ,4H  T ,4H- TE,4HMPER,4HATUR,4HE  (,4HDEGC,4H)   ,
                1        4H    ,
                2        4H   U,4H - V,4HERTI,4HCAL ,4HVELO,4HCITY,4H  (C,4HM/S),
                3        4H    ,
                4        4H R -,4H RAT,4HIO E,4HFFEC,4HT./K,4HINEM,4H. VI,4HSCOS,
                5        4HITY /
                C
0009            END
```

```
0001            SUBROUTINE PISA(COFY,IH,X,IMZ,JMZ)
                C
0002            COMMON /CMN1/LIN,MEDA,IKROKY,M,CST,KLI,KLJ,JAK(4),KROKY(61)
0003            COMMON /CMN2/PRLAM,XNUL
0004            COMMON /CMN4/TEK(2,3),TURB(3),OSA(9,3),TEPISA(19,4)
0005            COMMON /CMN5/XCB(161)
0006            DIMENSION X(161,61),IPS(61)
                C
0007            COFR=COFY
0008            WRITE (LIN,2101)(TEPISA(I,IH),I=1,7),CST,M,(TEK(J,MEDA),J=1,2),
               1                 PRLAM
0009            WRITE (LIN,2102)(TEPISA(I,IH),I=8,16),JAK(IH),
               1                (TEPISA(J,IH),J=17,18),XNUL,IKROKY
0010            WRITE (LIN,2103)(KROKY(J),J=1,JMZ,KLJ)
0011            WRITE (LIN,2104)(J,J=1,JMZ,KLJ)
0012            WRITE (LIN,2105)TEPISA(19,IH)
0013            I=IMZ
0014          101 CONTINUE
0015            DO 102 J=1,JMZ,KLJ
0016            Y=COFR*X(I,J)
0017          102 IPS(J)=Y+0.5
0018            WRITE (LIN,2106)I,XCB(I),(IPS(J),J=1,JMZ,KLJ)
0019            I=I-KLI
0020            IF (I)103,103,101
                C
0021          103 RETURN
                C
0022          2101 FORMAT (2X,7A4,78X,5H TIME,9X,F5.2,3H  S/108X,10H TIME STEP,
                  1        I6/109X,2A4/1X,13H DIMENSIONS :,94X,10H PRANDTL =,F12.5)
0023          2102 FORMAT (2X,9A4,4H10**,I2,2X,2A4,54X,10H GRASHOF =,5X,E10.4/1X,
                  1        28H X - DISTANCE ALONG THE WALL,16X,3H CM/1X,
                  2        27H Y - DISTANCE FROM THE WALL,10X,4H10**,I2,1X,3H CM/)
0024          2103 FORMAT (7X,3H Y ,41I3)
0025          2104 FORMAT (7X,3H J ,41I3)
0026          2105 FORMAT (2X,5H I  X,2X,A4)
0027          2106 FORMAT (1X,I3,F5.1,1X,41I3)
                C
0028            END
```

```
0001            SUBROUTINE GRAF(IH,FIRSTV,DELTAV,LEV,GRAS,IGRAS)
                C
0002            COMMON /CMN1/LIN,MEDA
0003            COMMON /CMN2/PRLAM,XNUL,TIME(8),XCBIGR,BGRX
0004            COMMON /CMN4/TEK(2,3),TURB(3),OSA(9,3)
0005            DIMENSION IBUF(1000)
0006            DIMENSION YIN(61),X(303),Y(303)
0007            DIMENSION OSAB(9)
0008            DIMENSION TEXT(2)
0009            LOGICAL LAK,LEV
                C
0010            IF (LEV)GO TO 3
0011            CALL PLOTS(IBUF,4000)
0012            XST=1.0
0013            YST=7.0
0014            DO 2 I=1,2
0015          2 TEXT(I)=TEK(I,MEDA)
0016            GO TO 4
0017          3 XST=31.7
0018            YST=0.0
0019          4 CALL PLOT(XST,YST,-3)
0020            CALL PLOT(-2.4,-3.0,3)
0021            CALL PLOT(-2.4,18.0,2)
0022            CALL PLOT(27.3,18.0,2)
0023            CALL PLOT(27.3,-3.0,2)
0024            CALL PLOT(-2.4,-3.0,2)
0025            CALL AXIS(0.,0.,33H Y - DISTANCE FROM THE WALL  (CM),-33,
               1        25.,0.,0.0,BGRX,10.)
0026            DO 6 J=1,9
0027          6 OSAB(J)=OSA(J,IH)
0028            CALL AXIS(0.,0.,OSAB,36,15.,90.,FIRSTV,DELTAV,10.)
0029            CALL SYMBOL(0.0,15.5,0.4,TEXT,0.,8)
0030            CALL SYMBOL(4.2,15.5,0.4,5HPR = ,0.,5)
0031            CALL NUMBER(5.9,15.5,0.4,PRLAM,0.,5)
0032            CALL SYMBOL(9.7,15.5,0.4,8HGR(X) = ,0.,8)
0033            CALL NUMBER(12.4,15.5,0.4,GRAS,0.,5)
0034            CALL SYMBOL(15.2,15.5,0.4,3H*10,0.,3)
0035            AGRAS=IGRAS
0036            CALL NUMBER(16.2,15.9,0.25,AGRAS,0.,0)
0037            CALL SYMBOL(18.0,15.5,0.4,12HSTATION X = ,0.,12)
0038            CALL NUMBER(22.3,15.5,0.4,XCBIGR,0.,2)
0039            CALL SYMBOL(24.4,15.5,0.4,2HCM,0.,2)
0040            CRITER=0.01*DELTAV
0041            RETURN
                C
0042            ENTRY CARA(M,JMZ,YIN,LAK,LEV)
                C
0043            CALL BODY(CRITER,FIRSTV,JMZ,YIN,X,Y,KMZ)
0044            KMZ1=KMZ+1
0045            KMZ2=KMZ+2
0046            X(KMZ1)=0.0
0047            X(KMZ2)=BGRX
0048            Y(KMZ1)=FIRSTV
0049            Y(KMZ2)=DELTAV
0050            N=M-1
0051            CALL LINE(X,Y,KMZ,1,5,N)
0052            IF (LAK)RETURN
                C
```

```
0053              CALL SYMBOL(21.7,13.7,0.5,9HTIME  (S),0.,9)
0054              YST=13.7
0055              DO 5 J=1,M
0056              N=J-1
0057              YST=YST-0.9
0058              YSS=YST+0.2
0059              CALL SYMBOL(21.8,YSS,0.3,N,0.,-1)
0060            5 CALL NUMBER(24.0,YST,0.3,TIME(J),0.,2)
0061              IF (LEV)CALL PLOTT(31.7)
0062              RETURN
                C
0063              END
```

```
0001                  FUNCTION PLCH(IMZ,KMZ,HAPLCH,Y)
                    C
0002                  COMMON /CMN5/X(161)
0003                  DIMENSION Y(161)
0004                  DIMENSION COEF(4)
                    C
0005                  DATA COEF/32.,12.,32.,14./
                    C
0006                  SUMA=-7.*Y(IMZ)/X(IMZ)
0007                  DO 1 K=2,KMZ,4
0008                  K1=K-1
0009                  DO 1 N=1,4
0010                  KN1=K1+N
0011                1 SUMA=SUMA+COEF(N)*Y(KN1)/X(KN1)
0012                  PLCH=SUMA*HAPLCH
                    C
0013                  RETURN
0014                  END
```

```
0001            SUBROUTINE MEZI(JMZ,JMZ1,DELY,XIN)
                C
0002            COMMON /CMN3/A(4,4,3)
0003            DIMENSION XIN(61),YIN(61),Z(301),X(303),Y(303)
0004            DIMENSION LN(3)
0005            DIMENSION DZ(4)
                C
0006            LN(1)=0
0007            DX=0.2*DELY
0008            KMZ=1+5*JMZ1
0009            DO 7 I=1,4
0010          7 DZ(I)=DX*FLOAT(I)
                C
0011            DO 1 J=1,JMZ1
0012            ZL=XIN(J)
0013            JL=1+5*(J-1)
0014            Z(JL)=ZL
0015            DO 1 I=1,4
0016            K=JL+I
0017          1 Z(K)=ZL+DZ(I)
0018            Z(KMZ)=XIN(JMZ)
0019            RETURN
                C
0020            ENTRY BODY(CRIT,CMPRSN,JMZ,YIN,X,Y,KMZ)
                C
0021          6 IF (JMZ.LE.4)GO TO 5
0022            ROZD=YIN(JMZ)-CMPRSN
0023            IF (ABS(ROZD).GT.CRIT)GO TO 5
0024            JMZ=JMZ-1
0025            GO TO 6
                C
0026          5 JMZ1=JMZ-1
0027            KMZ=1+5*JMZ1
0028            LN(3)=JMZ-4
                C
0029            DO 2 I=1,KMZ
0030          2 X(I)=Z(I)
                C
0031            DO 3 J=1,JMZ1
0032            LN(2)=J-2
0033            YL=YIN(J)
0034            JL=1+5*(J-1)
0035            Y(JL)=YL
0036            M=2
0037            IF (J.EQ.1)M=1
0038            IF (J.EQ.JMZ1)M=3
0039            NULA=LN(M)
0040            DO 3 I=1,4
0041            K=JL+I
0042            SUM=0.0
0043            DO 4 N=1,4
0044          4 SUM=SUM+A(N,I,M)*YIN(NULA+N)
0045          3 Y(K)=SUM
0046            Y(KMZ)=YIN(JMZ)
                C
0047            RETURN
0048            END
```

```
0001            SUBROUTINE LONUS(N,IDOL,AN,BN,*)
                C
0002            COMMON /CMN1/LIN
0003            COMMON /CMN6/X(161),CB(161),P(161)
0004            DIMENSION S(6)
0005            EQUIVALENCE (CA,F),(CC,G),(CD,FG),(CE,FD),(CF,ZM),
               1            (GD,S(1))
0006            DATA MEZ,CRIT/100,0.0001/
                C
0007            BN=0.1
0008            M=0
0009          3 BS=BN
0010            DO 5 I=1,6
0011          5 S(I)=0.0
                C
0012            DO 4 I=IDOL,N
0013            CA=X(I)**BS
0014            CC=CA*CA
0015            CD=CA*P(I)
0016            CE=CD*CB(I)
0017            CF=CC*CB(I)
0018            S(1)=S(1)+CD
0019            S(2)=S(2)+CC
0020            S(3)=S(3)+CE
0021            S(4)=S(4)+CF
0022            S(5)=S(5)+CE*CB(I)
0023          4 S(6)=S(6)+CF*CB(I)
                C
0024            F=S(1)/S(2)
0025            G=S(3)/S(4)
0026            FD=(S(3)*S(2)-2.*S(1)*S(4))/(S(2)*S(2))
0027            GD=(S(5)*S(4)-2.*S(3)*S(6))/(S(4)*S(4))
0028            IF (FD.EQ.GD)GO TO 1
0029            FG=F-G
0030            ZM=FG/(FD-GD)
0031            BN=BS-ZM
                C
0032            M=M+1
0033            IF (M-MEZ)7,1,1
0034          1 WRITE (LIN,2202)
0035            RETURN 1
0036          7 IF (ABS(FG).GT.CRIT.OR.ABS(ZM).GT.CRIT)GO TO 3
0037            AN=0.5*(F+S)
                C
0038            RETURN
                C
0039         2202 FORMAT (1HO,23H CONVERGENCE DIFFICULTY)
                C
0040            END
```

```
0001            SUBROUTINE STELAM(RLAM,CGR,TF,DELTA,DELY,DYX,IMZ,JMZ,JMZ1)
                C
0002            COMMON /CMNZ/PRLAM
0003            COMMON /CMN5/XCB(161),Y(61),U(161,61),V(161,61),T(161,61),
               1             R(161,61),CER(61)
                C
0004            CC=PRLAM+0.9524
0005            CUMX=5.17*RLAM*SQRT(CGR/CC)
0006            CDLX=3.93*(CC/CGR)**0.25/SQRT(PRLAM)
                C
0007            DO 102 I=2,IMZ
0008            UMX=CUMX*SQRT(XCB(I))
0009            DLX=CDLX*XCB(I)**0.25
0010            JDEL=0.5+DLX/DELY
                C
0011            IF (JDEL-2)103,104,110
0012          110 IF (JDEL.GT.JMZ1)JDEL=JMZ1
0013          104 JDEL1=JDEL+1
                C
0014            DO 105 J=2,JDEL
0015            YD=Y(J)/DLX
0016            YD2=(1.-YD)**2
0017            T(I,J)=TF+DELTA*YD2
0018            U(I,J)=UMX*YD*YD2
0019            XER=CER(J)*U(I,J)
0020            EPSR=XER*(1.-EXP(-XER))
0021          105 R(I,J)=RLAM*(1.+EPSR)
                C
0022            IF (JDEL-JMZ1)106,102,102
0023          103 JDEL1=2
0024          106 CONTINUE
                C
0025            DO 107 J=JDEL1,JMZ1
0026            T(I,J)=TF
0027            U(I,J)=0.0
0028          107 R(I,J)=RLAM
                C
0029          102 CONTINUE
                C
0030            DO 108 I=2,IMZ
0031            DO 108 J=2,JMZ
0032          108 V(I,J)=V(I,J-1)-DYX*(U(I,J)-U(I-1,J))
0033            DO 109 J=2,JMZ
0034          109 V(1,J)=V(2,J)
                C
0035            RETURN
                C
0036            END
```

Appendix B. COMPUTER PRINTOUT

It is not feasible to print out each time step of the calculations, as the resulting printout would be voluminous indeed. Moreover, the I/O (input/output) operations consume a considerable amount of computer time. For these reasons, the calculated values were printed out always after a certain number of time steps. However, the complete printouts cannot be presented here, as they are still too voluminous: the main calculation printouts contain 201 pages in the case of air, 161 pages in the case of water and 151 pages in the case of mercury.

Therefore, only the title page and three characteristic time steps of each main calculation were chosen for presentation in this Appendix. The characteristic time steps are:

1) the time step in the middle between the start of the transient and the time, when minimum Nu_L is obtained;
2) the time step, when Nu_L goes through its minimum;
3) the last time step in the calculation, when practically steady state is reached.

B.1 Dry Air

The title page of the main calculation and the calculated values at t = 0,5 , 1,0 , 4,0 s are presented on the following pages 140 - 155.

UNSTEADY TURBULENT FREE CONVECTION OVER A VERTICAL FLAT PLATE
****

FLUID : DRY AIR

TEMPERATURES :

WALL	90.0	DEGC
FLUID	20.0	DEGC
MEAN	55.0	DEGC

FLUID PROPERTIES :

SPECIFIC HEAT	0.1009237E 08	ERG/G*DEGC
DENSITY	0.1075648E-02	G/CM**3
KINEMATIC VISCOSITY	0.1833758E 00	CM**2/S
DYNAMIC VISCOSITY	0.1977367E-03	GYR*S/CM**2
THERMAL CONDUCTIVITY	0.2941347E 04	ERG/CM*S*DEGC
VOLUMETRIC EXPANSION COEFFICIENT	0.3047295E-02	1/DEGC
PRANDTL NUMBER	0.7017862	
GRASHOF NUMBER	0.2107736E 10	

TURBULENCE MODEL :

LAW OF THE WALL : DEISSLER

INNER REGION LIMIT YM+ 15.000

VAN-DRIVAZNAY CONSTANT A 0.100
VAN-DRIVAZNAY CONSTANT B 1.000

TURBULENT PRANDTL NUMBER 0.800

FINITE DIFFERENCES :

DELTA X (VERTICAL)	0.500	CM
DELTA Y (HORIZONTAL)	0.100	CM
TIME STEP	0.0025	S

UNSTEADY TURBULENT FREE CONVECTION OVER A VERTICAL FLAT PLATE
********** ******** ********** ********************************

VERTICAL VELOCITY FIELD

TIME 0.50 S
TIME STEP 200
DRY AIR
PRANDTL = 0.70179
GRASHOF = 0.3168E 10

DIMENSIONS :
U - VERTICAL VELOCITY COMPONENT 10**-1 CM/S
X - DISTANCE ALONG THE WALL CM
Y - DISTANCE FROM THE WALL 10**-2 CM

	Y	0 10 20 30 40 50 60 70 80 90	100	110	120	130	140	150	160	170	180	190
	J	1 2 3 4 5 6 7 8 9	10	11	12	13	14	15	16	17	18	19	20
I	X	U											
161	80.0	0 15 72 82 46 22 41 94 157 118	83	55	34	21	12	7	3	2	1	0	0	0
157	78.0	0 15 72 82 46 22 41 94 157 118	83	55	34	21	12	7	3	2	1	0	0	0
153	76.0	0 15 72 82 46 22 41 94 157 118	83	55	34	21	12	7	3	2	1	0	0	0
149	74.0	0 15 72 82 46 22 41 94 157 118	83	55	34	21	12	7	3	2	1	0	0	0
145	72.0	0 15 72 82 46 22 41 94 157 118	83	55	34	21	12	7	3	2	1	0	0	0
141	70.0	0 15 72 82 46 22 41 94 157 118	83	55	34	21	12	7	3	2	1	0	0	0
137	68.0	0 15 72 82 46 22 41 94 157 118	83	55	34	21	12	7	3	2	1	0	0	0
133	66.0	0 15 72 82 46 22 41 94 157 118	83	55	34	21	12	7	3	2	1	0	0	0
129	64.0	0 15 72 82 46 22 41 94 157 118	83	55	34	21	12	7	3	2	1	0	0	0
125	62.0	0 15 72 82 46 22 41 94 157 118	83	55	34	21	12	7	3	2	1	0	0	0
121	60.0	0 15 72 82 46 22 41 94 157 118	83	55	34	21	12	7	3	2	1	0	0	0
117	58.0	0 15 72 82 46 22 41 94 157 118	83	55	34	21	12	7	3	2	1	0	0	0
113	56.0	0 15 72 82 46 22 41 94 157 118	83	55	34	21	12	7	3	2	1	0	0	0
109	54.0	0 15 72 82 46 22 41 94 157 118	83	55	34	21	12	7	3	2	1	0	0	0
105	52.0	0 15 72 82 46 22 41 94 157 118	83	55	34	21	12	7	3	2	1	0	0	0
101	50.0	0 15 72 82 46 22 41 94 157 118	83	55	34	21	12	7	3	2	1	0	0	0
97	48.0	0 15 72 82 46 22 41 94 157 118	83	55	34	21	12	7	3	2	1	0	0	0
93	46.0	0 15 72 82 46 22 41 94 157 118	83	55	34	21	12	7	3	2	1	0	0	0
89	44.0	0 15 72 82 46 22 41 94 157 118	83	55	34	21	12	7	3	2	1	0	0	0
85	42.0	0 15 72 82 46 22 41 94 157 118	83	55	34	21	12	7	3	2	1	0	0	0
81	40.0	0 15 72 82 46 22 41 94 157 118	83	55	34	21	12	7	3	2	1	0	0	0
77	38.0	0 15 72 82 46 22 41 94 157 118	83	55	34	21	12	7	3	2	1	0	0	0
73	36.0	0 15 72 82 46 22 41 94 157 118	83	55	34	21	12	7	3	2	1	0	0	0
69	34.0	0 15 72 82 46 22 41 94 157 118	83	55	34	21	12	7	3	2	1	0	0	0
65	32.0	0 15 72 82 46 22 41 94 157 118	83	55	34	21	12	7	3	2	1	0	0	0
61	30.0	0 15 72 82 46 22 41 94 157 118	83	55	34	21	12	7	3	2	1	0	0	0
57	28.0	0 15 72 82 46 22 41 94 157 118	83	55	34	21	12	7	3	2	1	0	0	0
53	26.0	0 15 72 82 46 22 41 94 157 118	83	55	34	21	12	7	3	2	1	0	0	0
49	24.0	0 15 72 82 46 22 41 94 157 118	83	55	34	21	12	7	3	2	1	0	0	0
45	22.0	0 15 72 82 46 22 41 94 157 118	83	55	34	21	12	7	3	2	1	0	0	0
41	20.0	0 15 72 82 46 22 41 94 157 118	83	55	34	21	12	7	3	2	1	0	0	0
37	18.0	0 15 72 82 46 22 41 94 157 118	83	55	34	21	12	7	3	2	1	0	0	0
33	16.0	0 15 72 82 46 22 41 94 157 118	83	55	34	21	12	7	3	2	1	0	0	0
29	14.0	0 15 72 82 46 22 41 94 157 118	83	55	34	21	12	7	3	2	1	0	0	0
25	12.0	0 15 72 82 46 22 31 94 155 114	82	54	34	20	12	6	3	2	1	0	0	0
21	10.0	0 15 72 82 32 21 83 148 109	75	50	31	19	11	6	3	1	1	0	0	0
17	8.0	0 14 95 82 21 21 59 123	99	61	40	25	14	8	4	2	1	0	0	0
13	6.0	0 13 81 73 01 95 124	92	65	42	27	17	10	5	3	1	1	0	0
9	4.0	0 11 51 40 15 82 112	84	60	40	26	16	9	5	3	2	1	0	0
5	2.0	0 6 35 34 32 61 91	87	60	40	26	16	10	6	3	2	1	0	0
1	0.0	0 0 0 0 0 0 0 0 0	0	0	0	0	0	0	0	0	0	0	0	0

UNSTEADY TURBULENT FREE CONVECTION OVER A VERTICAL FLAT PLATE
****

HORIZONTAL VELOCITY FIELD

TIME 0.50. S
TIME STEP 200
DRY AIR
PRANDTL = 0.70179
GRASHOF = 0.3168E 10

DIMENSIONS :
V - HORIZONTAL VELOCITY COMPONENT -1C**-1 CM/S
X - DISTANCE ALONG THE WALL CM
Y - DISTANCE FROM THE WALL 1C**-2 CM

	Y	C	10	2C	3C	4C	5C	6C	7C	8C	9C	1C0	11C	12C	13C	14C	15C	16C	17C	18C	19C	20C
	J	1	2	3	4	5	6	7	8	9	10	11	12	13	14	15	16	17	18	19	20	
I	X	V																				
161	80.0	0	0	0	0	0	0	0	0	0	0	0	0	0	0	0	0	0	0	0	0	0
157	78.0	0	0	0	0	0	0	0	0	0	0	0	0	0	0	0	0	0	0	0	0	0
153	76.0	0	0	0	0	0	0	0	0	0	0	0	0	0	0	0	0	0	0	0	0	0
149	74.0	0	0	0	0	0	0	0	0	0	0	0	0	0	0	0	0	0	0	0	0	0
145	72.0	0	0	0	0	0	0	0	0	0	0	0	0	0	0	0	0	0	0	0	0	0
141	70.0	0	0	0	0	0	0	0	0	0	0	0	0	0	0	0	0	0	0	0	0	0
137	68.0	0	0	0	0	0	0	0	0	0	0	0	0	0	0	0	0	0	0	0	0	0
133	66.0	0	0	0	0	0	0	0	0	0	0	0	0	0	0	0	0	0	0	0	0	0
129	64.0	0	0	0	0	0	0	0	0	0	0	0	0	0	0	0	0	0	0	0	0	0
125	62.0	0	0	0	0	0	0	0	0	0	0	0	0	0	0	0	0	0	0	0	0	0
121	60.0	0	0	0	0	0	0	0	0	0	0	0	0	0	0	0	0	0	0	0	0	0
117	58.0	0	0	0	0	0	0	0	0	0	0	0	0	0	0	0	0	0	0	0	0	0
113	56.0	0	0	0	0	0	0	0	0	0	0	0	0	0	0	0	0	0	0	0	0	0
109	54.0	0	0	0	0	0	0	0	0	0	0	0	0	0	0	0	0	0	0	0	0	0
105	52.0	0	0	0	0	0	0	0	0	0	0	0	0	0	0	0	0	0	0	0	0	0
101	50.0	0	0	0	0	0	0	0	0	0	0	0	0	0	0	0	0	0	0	0	0	0
97	48.0	0	0	0	0	0	0	0	0	0	0	0	0	0	0	0	0	0	0	0	0	0
93	46.0	0	0	0	0	0	0	0	0	0	0	0	0	0	0	0	0	0	0	0	0	0
89	44.0	0	0	0	0	0	0	0	0	0	0	0	0	0	0	0	0	0	0	0	0	0
85	42.0	0	0	0	0	0	0	0	0	0	0	0	0	0	0	0	0	0	0	0	0	0
81	40.0	0	0	0	0	0	0	0	0	0	0	0	0	0	0	0	0	0	0	0	0	0
77	38.0	0	0	0	0	0	0	0	0	0	0	0	0	0	0	0	0	0	0	0	0	0
73	36.0	0	0	0	0	0	0	0	0	0	0	0	0	0	0	0	0	0	0	0	0	0
69	34.0	0	0	0	0	0	0	0	0	0	0	0	0	0	0	0	0	0	0	0	0	0
65	32.0	0	0	0	0	0	0	0	0	0	0	0	0	0	0	0	0	0	0	0	0	0
61	30.0	0	0	0	0	0	0	0	0	0	0	0	0	0	0	0	0	0	0	0	0	0
57	28.0	0	0	0	0	0	0	0	0	0	0	0	0	0	0	0	0	0	0	0	0	0
53	26.0	0	0	0	0	0	0	0	0	0	0	0	0	0	0	0	0	0	0	0	0	0
49	24.0	0	0	0	0	0	0	0	0	0	0	0	0	0	0	0	0	0	0	0	0	0
45	22.0	0	0	0	0	0	0	0	0	0	0	0	0	0	0	0	0	0	0	0	0	0
41	20.0	0	0	0	0	0	0	0	0	0	0	0	0	0	0	0	0	0	0	0	0	0
37	18.0	0	0	0	0	0	0	0	0	0	0	0	0	0	0	0	0	0	0	0	0	0
33	16.0	0	0	0	0	0	0	0	0	0	0	0	0	0	0	0	0	0	0	0	0	0
29	14.0	0	0	0	0	0	0	0	0	0	0	0	0	0	0	0	0	0	0	0	0	0
25	12.0	0	0	0	0	1	1	1	1	1	1	2	2	2	2	2	2	2	2	2	2	2
21	10.0	0	0	1	1	2	3	4	5	5	6	6	6	6	6	6	6	6	6	6	6	6
17	8.0	0	1	2	3	5	6	8	9	10	10	11	11	11	11	11	11	11	11	11	11	11
13	6.0	0	1	2	4	6	8	10	11	12	13	13	13	13	13	13	13	13	14	14	14	14
9	4.0	0	1	3	5	8	10	12	13	14	14	15	15	15	15	15	15	15	15	15	15	15
5	2.0	0	2	4	7	11	14	16	17	18	19	19	19	18	19	19	19	19	19	19	19	19
1	0.0	0	3	14	19	22	24	25	25	25	26	26	26	26	26	26	26	26	26	26	26	26

UNSTEADY TURBULENT FREE CONVECTION OVER A VERTICAL FLAT PLATE
****

TEMPERATURE FIELD

DIMENSIONS :
T - TEMPERATURE 10**-1 DEGC
X - DISTANCE ALONG THE WALL CM
Y - DISTANCE FROM THE WALL 10**-2 CM

TIME 0.50 S
TIME STEP 200
DRY AIR
PRANDTL = 0.70179
GRASHOF = 0.3168E 10

```
      Y   0 10 20 30 40 50 60 70 80 90100110120130140150160170180190
      J   1  2  3  4  5  6  7  8  9 10 11 12 13 14 15 16 17 18 19 20
  I   X     T
161 80.0 900784678584507441333333292246224022521520820520220120120020
157 78.0 900784678584507441333333292246224022521520820520220120120020
153 76.0 900784678584507441333333292246224022521520820520220120120020
149 74.0 900784678584507441333333292246224022521520820520220120120020
145 72.0 900784678584507441333333292246224022521520820520220120120020
141 70.0 900784678584507441333333292246224022521520820520220120120020
137 68.0 900784678584507441333333292246224022521520820520220120120020
133 66.0 900784678584507441333333292246224022521520820520220120120020
129 64.0 900784678584507441333333292246224022521520820520220120120020
125 62.0 900784678584507441333333292246224022521520820520220120120020
121 60.0 900784678584507441333333292246224022521520820520220120120020
117 58.0 900784678584507441333333292246224022521520820520220120120020
113 56.0 900784678584507441333333292246224022521520820520220120120020
109 54.0 900784678584507441333333292246224022521520820520220120120020
105 52.0 900784678584507441333333292246224022521520820520220120120020
101 50.0 900784678584507441333333292246224022521520820520220120120020
 97 48.0 900784678584507441333333292246224022521520820520220120120020
 93 46.0 900784678584507441333333292246224022521520820520220120120020
 89 44.0 900784678584507441333333292246224022521520820520220120120020
 85 42.0 900784678584507441333333292246224022521520820520220120120020
 81 40.0 900784678584507441333333292246224022521520820520220120120020
 77 38.0 900784678584507441333333292246224022521520820520220120120020
 73 36.0 900784678584507441333333292246224022521520820520220120120020
 69 34.0 900784678584507441333333292246224022521520820520220120120020
 65 32.0 900784678584507441333333292246224022521520820520220120120020
 61 30.0 900784678584507441333333292246224022521520820520220120120020
 57 28.0 900784678584507441333333292246224022521520820520220120120020
 53 26.0 900784678584507441333333292246224022521520820520220120120020
 49 24.0 900784678584507441333333292246224022521520820520220120120020
 45 22.0 900784678584507441333333292246224022521520820520220120120020
 41 20.0 900784678584507441333333292246224022521520820520220120120020
 37 18.0 900784678584507441333333292246224022521520820520220120120020
 33 16.0 900784678584507441333333292246224022521520820520220120120020
 29 14.0 900784678584507441333333292246224022521520820520220120120020
 25 12.0 900784678584507441333333292246224022521520820520220120120020
 21 10.0 900784678584507441333333292246224022521520820520220120120020
 17  8.0 900784678584507441333333292246224022521520820520220120120020
 13  6.0 900784678584507441333333292246224022521520820520220120120020
  9  4.0 900784678584507441333333292246224022521520820520220120120020
  5  2.0 900784678584507441333333292246224022521520820520220120120020
  1  0.0 900784678584507441333333292246224022521520820520220120120020
```

UNSTEADY TURBULENT FREE CONVECTION OVER A VERTICAL FLAT PLATE
****

EFFECTIVE VISCOSITY FIELD

DIMENSIONS :
R - RATIO EFFECTIVE V./KINEMATIC V. 10**-2 NONDIM.
X - DISTANCE ALONG THE WALL   CM
Y - DISTANCE FROM THE WALL   10**-2 CM

```
      Y    0 10 20 30 40 50 60 70 80 90100110120130140150160170180190
      J    1  2  3  4  5  6  7  8  9 10 11 12 13 14 15 16 17 18 19 20
  I   X      R
161  80.0 100100100100100100100100100100100100100100100100100100100100
157  78.0 100100100100100100100100100100100100100100100100100100100100
153  76.0 100100100100100100100100100100100100100100100100100100100100
149  74.0 100100100100100100100100100100100100100100100100100100100100
145  72.0 100100100100100100100100100100100100100100100100100100100100
141  70.0 100100100100100100100100100100100100100100100100100100100100
137  68.0 100100100100100100100100100100100100100100100100100100100100
133  66.0 100100100100100100100100100100100100100100100100100100100100
129  64.0 100100100100100100100100100100100100100100100100100100100100
125  62.0 100100100100100100100100100100100100100100100100100100100100
121  60.0 100100100100100100100100100100100100100100100100100100100100
117  58.0 100100100100100100100100100100100100100100100100100100100100
113  56.0 100100100100100100100100100100100100100100100100100100100100
109  54.0 100100100100100100100100100100100100100100100100100100100100
105  52.0 100100100100100100100100100100100100100100100100100100100100
101  50.0 100100100100100100100100100100100100100100100100100100100100
 97  48.0 100100100100100100100100100100100100100100100100100100100100
 93  46.0 100100100100100100100100100100100100100100100100100100100100
 89  44.0 100100100100100100100100100100100100100100100100100100100100
 85  42.0 100100100100100100100100100100100100100100100100100100100100
 81  40.0 100100100100100100100100100100100100100100100100100100100100
 77  38.0 100100100100100100100100100100100100100100100100100100100100
 73  36.0 100100100100100100100100100100100100100100100100100100100100
 69  34.0 100100100100100100100100100100100100100100100100100100100100
 65  32.0 100100100100100100100100100100100100100100100100100100100100
 61  30.0 100100100100100100100100100100100100100100100100100100100100
 57  28.0 100100100100100100100100100100100100100100100100100100100100
 53  26.0 100100100100100100100100100100100100100100100100100100100100
 49  24.0 100100100100100100100100100100100100100100100100100100100100
 45  22.0 100100100100100100100100100100100100100100100100100100100100
 41  20.0 100100100100100100100100100100100100100100100100100100100100
 37  18.0 100100100100100100100100100100100100100100100100100100100100
 33  16.0 100100100100100100100100100100100100100100100100100100100100
 29  14.0 100100100100100100100100100100100100100100100100100100100100
 25  12.0 100100100100100100100100100100100100100100100100100100100100
 21  10.0 100100100100100100100100100100100100100100100100100100100100
 17   8.0 100100100100100100100100100100100100100100100100100100100100
 13   6.0 100100100100100100100100100100100100100100100100100100100100
  9   4.0 100100100100100100100100100100100100100100100100100100100100
  5   2.0 100100100100100100100100100100100100100100100100100100100100
  1   0.0 100100100100100100100100100100100100100100100100100100100100
```

TIME   0.50 S
TIME STEP   200
DRY AIR
PRANDTL =   0.70179
GRASHOF =   0.3168E 10

UNSTEADY TURBULENT FREE CONVECTION OVER A VERTICAL FLAT PLATE
****

LOCAL HEAT TRANSFER

TIME 0.50, S
TIME STEP 200
DRY AIR
PRANDTL = 0.70179
GRASHOF = 0.3168E 10

I	X (CM)	INTER. REGION J(X)	WALL FRICTION (DYN/CM**2)	NONDIM. TIME	GRASHOF(X)	NUSSELT(X)	NU(X)/ GR(X)**0.3333
161	80.0	5	0.3966447E-01	0.8085205E 00	0.3167736E 10	0.1349762E 03	0.9190619E-01
157	78.0	5	0.3966447E-01	0.8188206E 00	0.2936044E 10	0.1316019E 03	0.9190643E-01
153	76.0	5	0.3966447E-01	0.8295242E 00	0.2715938E 10	0.1282275E 03	0.9190637E-01
149	74.0	5	0.3966447E-01	0.8408593E 00	0.2507114E 10	0.1248531E 03	0.9190637E-01
145	72.0	5	0.3966447E-01	0.8528555E 00	0.2309273E 10	0.1214787E 03	0.9190637E-01
141	70.0	5	0.3966447E-01	0.8656447E 00	0.2122136E 10	0.1181042E 03	0.9190656E-01
137	68.0	5	0.3966447E-01	0.8792637E 00	0.1945306E 10	0.1147298E 02	0.9190643E-01
133	66.0	5	0.3966447E-01	0.8937514E 00	0.1778773E 10	0.1113555E 03	0.9190631E-01
129	64.0	5	0.3966447E-01	0.9091531E 00	0.1621871E 10	0.1079811E 03	0.9190631E-01
125	62.0	5	0.3966447E-01	0.9254176E 00	0.1474533E 10	0.1046064E 03	0.9190637E-01
121	60.0	5	0.3966446E-01	0.9426591E 00	0.1336337E 10	0.1012330E 03	0.9190714E-01
117	58.0	5	0.3966442E-01	0.9608922E 00	0.1207155E 10	0.9785802E 02	0.9190637E-01
113	56.0	5	0.3966442E-01	0.9802308E 00	0.1086553E 10	0.9449296E 02	0.9190571E-01
109	54.0	5	0.3966441E-01	0.9997999E 00	0.9742272E 09	0.9113925E 02	0.9190679E-01
105	52.0	5	0.3966440E-01	0.1020864E 01	0.8699135E 09	0.8778145E 02	0.9190673E-01
101	50.0	5	0.3966439E-01	0.1042736E 01	0.7732723E 09	0.8436066E 02	0.9190696E-01
97	48.0	5	0.3966439E-01	0.1064705E 01	0.6842307E 09	0.8092436E 02	0.9190720E-01
93	46.0	5	0.3966439E-01	0.1086824E 01	0.6022162E 09	0.7761207E 02	0.9190708E-01
89	44.0	5	0.3966437E-01	0.1109110E 01	0.5270331E 09	0.7423715E 02	0.9190667E-01
85	42.0	5	0.3966437E-01	0.1131564E 01	0.4583311E 09	0.7086282E 02	0.9190696E-01
81	40.0	5	0.3966434E-01	0.1154209E 01	0.3959670E 09	0.6748972E 02	0.9190732E-01
77	38.0	5	0.3966432E-01	0.1177124E 01	0.3394921E 09	0.6411450E 02	0.9190726E-01
73	36.0	5	0.3966426E-01	0.1200271E 01	0.2885997E 09	0.6074026E 02	0.9190732E-01
69	34.0	5	0.3966421E-01	0.1223713E 01	0.2431732E 09	0.5736574E 02	0.9190750E-01
65	32.0	5	0.3966417E-01	0.1247542E 01	0.2027351E 09	0.5399142E 02	0.9190762E-01
61	30.0	5	0.3966411E-01	0.1271803E 01	0.1670436E 09	0.5061758E 02	0.9190787E-01
57	28.0	5	0.3966436E-01	0.1296449E 01	0.1358167E 09	0.4724326E 02	0.9190947E-01
53	26.0	5	0.3966393E-01	0.1321839E 01	0.1087424E 09	0.4386880E 02	0.9190947E-01
49	24.0	5	0.3966331E-01	0.1347615E 01	0.8552836E 08	0.4049440E 02	0.9190977E-01
45	22.0	5	0.3966378E-01	0.1374173E 02	0.6557901E 08	0.2712000E 02	0.9190995E-01
41	20.0	5	0.3966337E-01	0.1401741E 01	0.4943587E 08	0.3374502E 02	0.9191109E-01
37	18.0	5	0.3966336E-01	0.1430511E 01	0.3608264E 08	0.3037174E 02	0.9191281E-01
33	16.0	5	0.3966332E-01	0.1460706E 01	0.2534189E 08	0.2699741E 02	0.9191370E-01
29	14.0	5	0.3966329E-01	0.1492734E 01	0.1697797E 08	0.2362478E 02	0.9192145E-01
25	12.0	5	0.3966473E-01	0.2087590E 01	0.1069111E 08	0.2030022E 02	0.9215019E-01
21	10.0	5	0.3966536E-01	0.2236941E 01	0.6186984E 07	0.1729504E 02	0.9421021E-01
17	8.0	5	0.3822390E-01	0.2556766E 01	0.3167736E 07	0.1491095E 02	0.1015292E 00
13	6.0	5	0.3531136E-01	0.2922209E 01	0.1336338E 07	0.1253656E 02	0.1137352E 00
9	4.0	5	0.3039532E-01	0.3615813E 01	0.3959670E 06	0.9536393E 01	0.1296678E 00
5	2.0	6	0.2390170E-01	0.5113934E 01	0.4949588E 05	0.6034554E 01	0.1643579E 00
1	0.0	0	0.0	0.0	0.0	0.0	0.0

GRASHOF(L)	NUSSELT(L)
0.3167736E 10	0.8775575E 02

EVERAGE HEAT TRANSFER :

LEAST SQUARES APPROXIMATION :
NU(X)= 0.5[illegible]E-01*X(X)** 0.3333E 00

UNSTEADY TURBULENT FREE CONVECTION OVER A VERTICAL FLAT PLATE
****

VERTICAL VELOCITY FIELD

TIME 1.00 S
TIME STEP 400
DRY AIR
PRANDTL = 0.70179
GRASHOF = 0.3168E 10

DIMENSIONS :
U - VERTICAL VELOCITY COMPONENT 10**-1 CM/S
X - DISTANCE ALONG THE WALL CM
Y - DISTANCE FROM THE WALL 10**-2 CM

I	X	Y J	0 1	10 2	20 3	30 4	40 5	50 6	60 7	70 8	80 9	90 10	100 11	110 12	120 13	130 14	140 15	150 16	160 17	170 18	180 19	190 20	200 21	210 22	220 23	230 24	240 25	250 26	260 27
161	80.0		0																										
157	78.0		0																										
153	76.0		0																										
149	74.0		0																										
145	72.0		0																										
141	70.0		0																										
137	68.0		0																										
133	66.0		0																										
129	64.0		0																										
125	62.0		0																										
121	60.0		0																										
117	58.0		0																										
113	56.0		0																										
109	54.0		0																										
105	52.0		0																										
101	50.0		0																										
97	48.0		0																										
93	46.0		0																										
89	44.0		0																										
85	42.0		0																										
81	40.0		0																										
77	38.0		0																										
73	36.0		0																										
69	34.0		0																										
65	32.0		0																										
61	30.0		0																										
57	28.0		0																										
53	26.0		0																										
49	24.0		0																										
45	22.0		0																										
41	20.0		0																										
37	18.0		0																										
33	16.0		0																										
29	14.0		0																										
25	12.0		0																										
21	10.0		0																										
17	8.0		0																										
13	6.0		0																										
9	4.0		0																										
5	2.0		0																										
1	0.0		0	0	0	0	0	0	0	0	0	0	0	0	0	0	0	0	0	0	0	0	0	0	0	0	0	0	0

UNSTEADY TURBULENT FREE CONVECTION OVER A VERTICAL FLAT PLATE
****

HORIZONTAL VELOCITY FIELD

TIME 1.00 S
TIME STEP 400
DRY AIR
PRANDTL = 0.70179
GRASHOF = 0.3168E 10

DIMENSIONS :
V - HORIZONTAL VELOCITY COMPONENT -10**-1 CM/S
X - DISTANCE ALONG THE WALL CM
Y - DISTANCE FROM THE WALL 10**-2 CM

	Y	0	10	20	30	40	50	60	70	80	90	100	110	120	130	140	150	160	170	180	190	200	210	220	230	240	250	260
	J	1	2	3	4	5	6	7	8	9	10	11	12	13	14	15	16	17	18	19	20	21	22	23	24	25	26	27
I	X	V																										
161	80.0	0	0	0	0	0	0	0	0	0	0	0	0	0	0	0	0	0	0	0	0	0	0	0	0	0	0	0
157	76.0	0	0	0	0	0	0	0	0	0	0	0	0	0	0	0	0	0	0	0	0	0	0	0	0	0	0	0
153	72.0	0	0	0	0	0	0	0	0	0	0	0	0	0	0	0	0	0	0	0	0	0	0	0	0	0	0	0
149	68.0	0	0	0	0	0	0	0	0	0	0	0	0	0	0	0	0	0	0	0	0	0	0	0	0	0	0	0
145	64.0	0	0	0	0	0	0	0	0	0	0	0	0	0	0	0	0	0	0	0	0	0	0	0	0	0	0	0
141	60.0	0	0	0	0	0	0	0	0	0	0	0	0	0	0	0	0	0	0	0	0	0	0	0	0	0	0	0
137	56.0	0	0	0	0	0	0	0	0	0	0	0	0	0	0	0	0	0	0	0	0	0	0	0	0	0	0	0
133	52.0	0	0	0	0	0	0	0	0	0	0	0	0	0	0	0	0	0	0	0	0	0	0	0	0	0	0	0
129	48.0	0	0	0	0	0	0	0	0	0	0	0	0	0	0	0	0	0	0	0	0	0	0	0	0	0	0	0
125	44.0	0	0	0	0	0	0	0	0	0	0	0	0	0	0	0	0	0	0	0	0	0	0	0	0	0	0	0
121	40.0	0	0	0	0	0	0	0	0	0	0	0	0	0	0	0	0	0	0	0	0	0	0	0	0	0	0	0
117	36.0	0	0	0	0	0	0	0	0	0	0	0	0	0	0	0	0	0	0	0	0	0	0	0	0	0	0	0
113	32.0	0	0	0	0	0	0	0	0	0	0	0	0	0	0	0	0	0	0	0	0	0	0	0	0	0	0	0
109	28.0	0	0	0	0	0	0	0	0	0	0	0	0	0	0	0	0	0	0	0	0	0	0	0	0	0	0	0
105	24.0	0	0	0	0	0	0	0	0	0	0	0	0	0	0	0	0	0	0	0	0	0	0	0	0	0	0	0
101	20.0	0	0	0	0	0	0	0	0	0	0	0	0	0	0	0	0	0	0	0	0	0	0	0	0	0	0	0
97	16.0	0	0	0	0	0	0	0	0	0	0	0	0	0	0	0	0	0	0	0	0	0	0	0	0	0	0	0
93	12.0	0	0	0	0	0	0	0	0	0	0	0	0	0	0	0	0	0	0	0	0	0	0	0	0	0	0	0
89	8.0	0	0	0	0	0	0	0	0	0	0	0	0	0	0	0	0	0	0	0	0	0	0	0	0	0	0	0
85	4.0	0	0	0	0	0	0	0	0	0	0	0	0	0	0	0	0	0	0	0	0	0	0	0	0	0	0	0
81	0.0	0	0	0	0	0	0	0	0	0	0	0	0	0	0	0	0	0	0	0	0	0	0	0	0	0	0	0
77	38.0	0	0	0	0	0	0	0	0	0	1	1	1	1	1	1	1	1	1	1	1	1	1	1	1	1	1	1
73	36.0	0	0	0	0	0	0	1	1	1	2	2	2	2	3	3	3	3	3	3	3	3	3	3	3	3	3	3
69	34.0	0	0	0	0	1	1	2	2	3	4	4	5	5	6	6	6	6	7	7	7	7	7	7	7	7	7	7
65	32.0	0	0	0	1	1	2	3	4	5	6	7	8	9	9	10	10	10	10	10	10	10	11	11	11	11	11	11
61	30.0	0	0	1	1	2	3	4	5	7	8	9	10	11	11	12	12	12	13	13	13	13	13	13	13	13	13	13
57	28.0	0	0	1	2	3	4	5	6	7	9	10	11	11	12	12	13	13	13	13	13	13	13	13	13	13	13	13
53	26.0	0	0	1	2	3	4	5	6	7	8	9	10	11	11	12	12	12	12	12	12	12	12	12	12	12	12	12
49	24.0	0	0	1	2	3	4	5	6	7	8	9	10	10	11	11	11	11	11	11	12	12	12	12	12	12	12	12
45	22.0	0	0	1	2	3	4	5	6	7	8	9	9	10	10	10	11	11	11	11	11	11	11	11	11	11	11	11
41	20.0	0	0	1	2	3	4	5	6	7	8	9	9	10	10	10	11	11	11	11	11	11	11	11	11	11	11	11
37	18.0	0	0	1	2	3	4	5	6	7	8	9	10	10	10	11	11	11	11	11	11	11	11	11	11	11	11	11
33	16.0	0	0	1	2	3	4	6	7	8	9	9	10	10	11	11	11	11	11	11	11	11	11	11	11	11	11	11
29	14.0	0	0	1	2	4	5	6	7	8	9	10	10	11	11	12	12	12	12	12	12	12	12	12	12	12	12	12
25	12.0	0	1	1	3	4	5	7	8	9	10	10	11	11	12	12	12	12	12	12	12	12	12	12	12	12	12	12
21	10.0	0	1	2	3	4	6	7	9	10	11	11	12	12	12	13	13	13	13	13	13	13	13	13	13	13	13	13
17	8.0	0	1	2	3	5	7	8	10	11	12	12	13	13	13	13	13	14	14	14	14	14	14	14	14	14	14	14
13	6.0	0	1	2	4	6	8	10	11	12	13	13	14	14	14	14	14	15	15	15	15	15	15	15	15	15	15	15
9	4.0	0	1	3	6	8	10	12	14	14	15	15	16	16	16	16	16	16	16	16	16	16	16	16	16	16	16	16
5	2.0	0	2	6	9	12	14	16	17	18	19	19	19	19	19	19	19	19	19	19	19	19	19	19	19	19	19	19
1	0.0	0	3	14	19	22	24	25	25	26	26	26	26	26	26	26	26	26	26	26	26	26	26	26	26	26	26	26

UNSTEADY TURBULENT FREE CONVECTION OVER A VERTICAL FLAT PLATE
****

TEMPERATURE FIELD

TIME 1.00 S
TIME STEP 400
DRY AIR
PRANDTL = 0.70179
GRASHOF = 0.3168E 10

DIMENSIONS :
T - TEMPERATURE 10**-1 DEGC
X - DISTANCE ALONG THE WALL CM
Y - DISTANCE FROM THE WALL 10**-2 CM

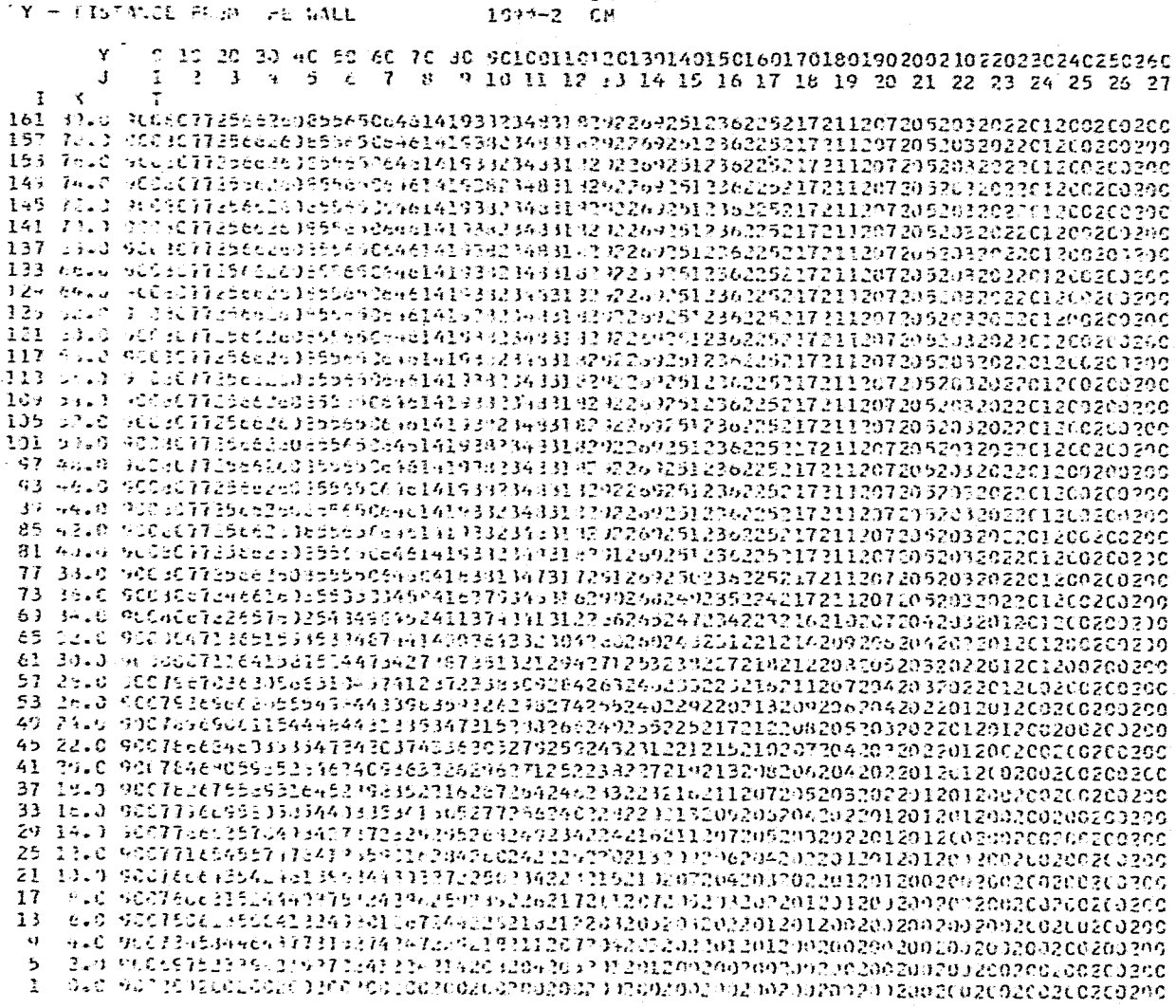

UNSTEADY TURBULENT FREE CONVECTION OVER A VERTICAL FLAT PLATE
****

EFFECTIVE VISCOSITY FIELD

TIME 1.00 S
TIME STEP 400
DRY AIR
PRANDTL = 0.70179
GRASHOF = 0.3168E 10

DIMENSIONS :
P - RATIO EFFECTIVE V./KINEMATIC V. 10**-2 NONDIM.
X - DISTANCE ALONG THE WALL CM
Y - DISTANCE FROM THE WALL 10**-2 CM

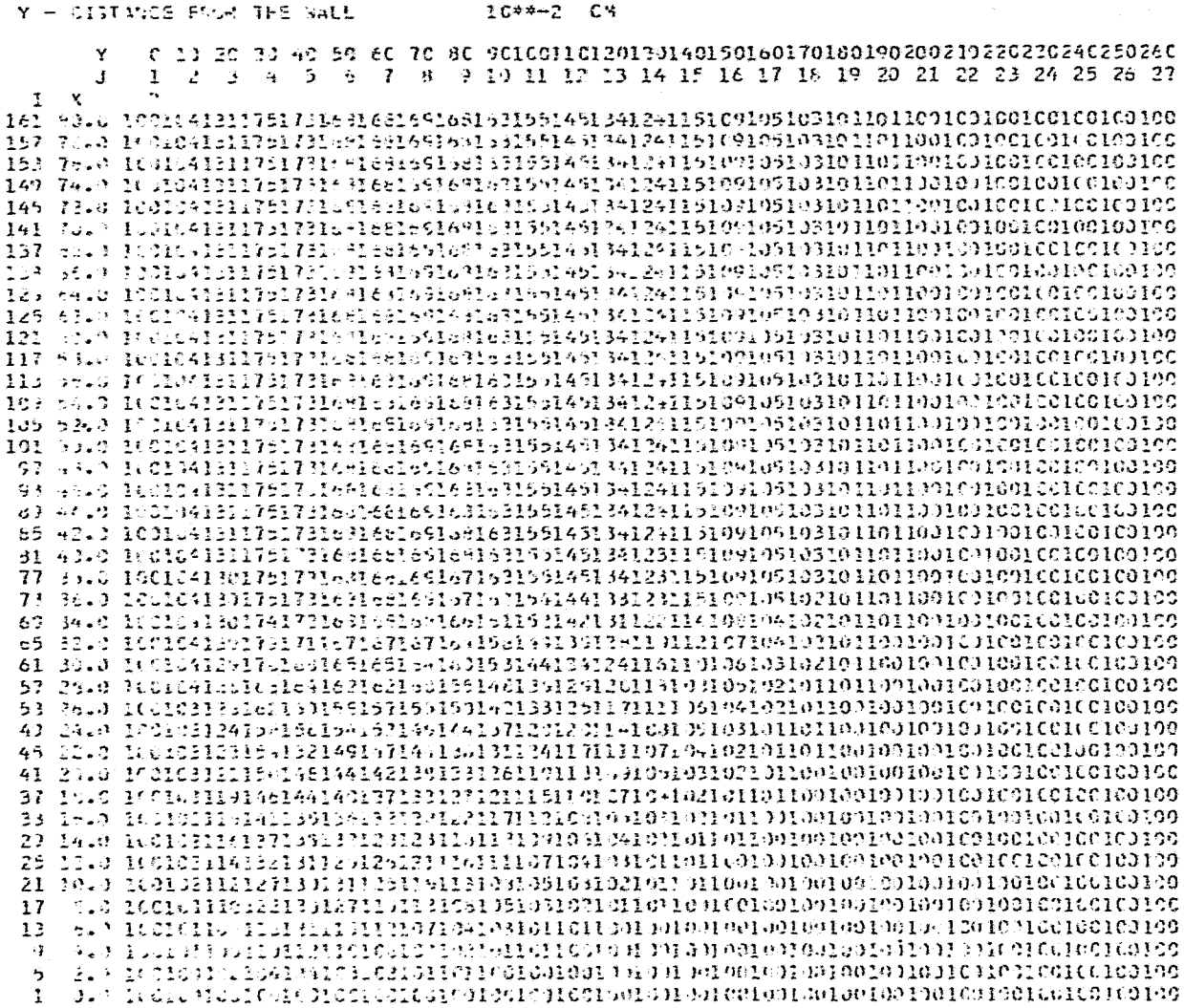

Author Remar Jaroslav
Name of thesis Numerical Solution of unsteady turbulent free convection over a vertical flat plate 1975

PUBLISHER:
University of the Witwatersrand, Johannesburg
©2013

LEGAL NOTICES:

Copyright Notice: All materials on the University of the Witwatersrand, Johannesburg Library website are protected by South African copyright law and may not be distributed, transmitted, displayed, or otherwise published in any format, without the prior written permission of the copyright owner.

Disclaimer and Terms of Use: Provided that you maintain all copyright and other notices contained therein, you may download material (one machine readable copy and one print copy per page) for your personal and/or educational non-commercial use only.

The University of the Witwatersrand, Johannesburg, is not responsible for any errors or omissions and excludes any and all liability for any errors in or omissions from the information on the Library website.